Extensive and Intelligent Exploitation of Renewable Energies at Sewage Treatment Plants

Von der Fakultät für Ingenieurwissenschaften
Abteilung Elektrotechnik und Informationstechnik
der Universität Duisburg-Essen

zur Erlangung des akademischen Grades

Doktors der Ingenieurwissenshaften (Dr.-Ing.)

genehmigte Dissertation

von

Ngoc-Hung Truong
aus
Binh Dinh, Vietnam

Gutachter: Prof. Dr.-Ing. habil. Gerhard Krost
Gutachter: Prof. Dr.-Ing. Holger Hirsch
Tag der mündlichen Prüfung: 06.04.2016

ABSTRACT

The work deals with comprehensive energy harvest in large wastewater treatment plants in order to make them utmost independent from external energy supply at reasonable energy cost. Thus, the complete system investigated makes not only use of biogas from sludge digester in a small combustion engine driven combined heat and power (CHP) unit which is state of the art at many places already; rather solar thermal sludge drying and subsequent incineration for a small scale steam power plant is included with usage of waste heat from CHP and steam unit for support of sludge drying. Furthermore, wind and solar based power harvest on the ground of the plant is integrated, including a hydrogen energy storage path for compensation of fluctuations, as well as small hydro generation at the clear water output. The thesis illustrates the composition and global power streams of such innovative kind of plant, describes the optimal sizing of particular plant components by use of a meta-heuristic approach, and presents several results of simulative plant operation over a full year for two examples with different conditions (Germany and Vietnam), in particular highlighting the mutual dependencies of plant devices, altogether proving that reasonable performance at vast energy independence and equitable cost can be achieved.

KURZFASSUNG

Die Arbeit befasst sich mit der umfassenden Ausnutzung erneuerbarer Energien in großen Kläranlagen, um ein Höchstmaß an Unabhängigkeit von der externen Energieversorgung unter angemessenen Energiekosten zu erreichen. So nutzt das untersuchte System nicht nur Biogas aus der Klärschlamm–Faulung in einem Blockheizkraftwerk (was vielerorts bereits –Stand der Technik ist), sondern auch eine solarthermische Schlammtrocknung mit anschließender Verbrennung für ein kleines Dampfkraftwerk bei gleichzeitiger Verwendung der Abwärme aus Blockheizkraftwerk und Dampfeinheit zur Unterstützung der Schlammtrocknung. Darüber hinaus wird Wind- und Solarenergie auf dem Gelände der Anlage genutzt, ergänzt durch einen Wasserstoff-Energiespeicherpfad zur Kompensation der Fluktuationen, sowie ein Kleinwasserkraftwerk am Ausfluss des geklärten Wassers. Die Dissertation erläutert die Konfiguration einer solchen innovativen Anlage, veranschaulicht die globalen Energieströme, beschreibt die optimale Dimensionierung der Anlagenkomponenten durch die Verwendung von Meta-Heuristik und stellt Ergebnisse eines simulierten Betriebes über ein ganzes Jahr für zwei Beispiele mit unterschiedlichen Bedingungen (Deutschland und Vietnam) vor; insbesondere werden die wechselseitigen Abhängigkeiten der Anlagenkomponenten untersucht und gezeigt, dass durch eine solche Lösung eine weitgehende Energieunabhängigkeit unter vertretbaren Kosten erreicht werden kann.

ACKNOWLEDGMENT

This dissertation is the product of my research activities carried out at the Institute of Electrical Power System (Elektrische Anlagen und Netze - EAN) at the University of Duisburg-Essen. I would like to express my sincere and profound gratitude to my supervisor, ***Prof. Dr.-Ing. habil. Gerhard Krost***.

He gave me an opportunity to conduct unique research in a highly challenging and interesting area. His thorough and in-depth technical skills help develop my research skills dramatically.

I gratefully acknowledge all those members of the Institute of Electrical Power Systems, University of Duisburg-Essen, for their invaluable assistance and kindness, which made my study both worthwhile and rewarding. I especially want to thank ***Prof. Dr.-Ing. habil. Istvan Erlich***, the head of the Institute of Electrical Power Systems.

Moreover, my heartful appreciation goes to my co-supervisor ***Prof. Dr.-Ing. Holger Hirsch*** from department of power transmission and storage, the University of Duisburg-Essen.

I would like to thank the Vietnam International Education Development (VIED) and Quy Nhon vocational training colleges for sponsoring my Ph.D. study at the Institute of Electrical Power System, University of Duisburg-Essen, Germany.

Last, but not least, my gratitude goes to my wife, sons, mother and father, friends. Without their encouragements and continuous support this Ph.D. study could not have come to a satisfactory conclusion.

Duisburg, April 2016

Truong, Ngoc-Hung

List of Contents

LIST OF FIGURES

LIST OF TABLES

List of Abbreviations

AF	Asymmetry Factor
ANFIS	Adaptive Neural Fuzzy System
C#	C shape
CH_4	Methane gas
CHP	Combined Heat and Power
COD	Chemical Oxygen Demand
DE	Germany
DSR	Dry Substance Ratio
el	electrical
GK	Size class (Größenklasse)
h	Enthalpy
H_2	Hydrogen gas
IDE	Integration Development Environment
MVMO	Mean-Variance Mapping Optimization
OPC	OLE (Object Linking and Embedding) Processing Control
PE	Person Equivalents
PLC	Program Logic Controller
PV	Photovoltaic
PWM	Pulse Width Modulation
RS	Recommendation Standard
RTU	Remote Terminal Unit
SCADA	Supervisory Control And Data Acquisition
TCP/IP	Transmission Control Protocol / Internet Protocol
th	thermal
VN	Vietnam
WT	Wind Turbine
WWTP	Wastewater Treatment Plant
X	Steam fraction
x_i	Optimization variables

1. INTRODUCTION

1.1 Motivation

Even if electricity consumption of waste water treatment plants in industrialized countries such as Germany is with 4.4 TWh [1] below 1% of total national electricity demand, it may come up to respectable 30% when focusing on the public/municipal sector. Furthermore, the treatment of infectious sewage sludge poses a problem, in particular in very densely populated regions. Disposal is expensive and environmentally questionable, and co-incineration of wet sludge, e.g. in proximately located thermal power plants, is inefficient and requires additional energy input for transportation. Therefore, local energetic exploitation of the organic sewage contents to the greatest possible extent is a reasonable solution from the perspectives of both economy and ecology.

Anaerobic digestion of sewage sludge is a well-established technique to stabilize the sludge and procure biogas with a relatively high content of methane (CH_4), which can be converted to electricity and heat by way of a combustion engine based Combined Heat and Power (CHP) unit. Less common is the energetic use of the sludge output from the digester: this can be de-watered and dried; having a contents of dry substance of, e.g., 80% it procures a heating value similar to that of lignite, thus allowing for effective incineration in a conventional boiler driving a steam turbine/generator set, altogether located on site of the sewage plant. The large polluting mass stream of sludge is at the same time diminished to a marginal output of inert ashes. Drying of sludge can fundamentally be achieved by use of waste heat from both biogas driven combustion engine and steam turbine condenser.

Waste water plants are usually located in some distance to populated regions and have rather large expanses. This makes them eminently eligible for additional harvest of renewable energy by, e.g., a wind turbine and/or collection of solar irradiation; the latter in particular in order to support the sludge drying process. Special glass houses and ploughing systems for this purpose are commercially available. On the other hand, natural fluctuation of renewable sources calls for employment of energy storage. While the solar fluctuations can be intercepted by an appropriate size/surface of the glass house for sludge drying, electricity can be independently stored in form of hydrogen gas yielded from electrolysis; for the re-conversion of hydrogen to electricity the combustion engine driven generator set originally provided for biogas exploitation can be jointly used, as long as the composition of gases does not exceed a given limit.

The demanding task in designing such kind of plant is firstly to achieve a sound balance of electricity demand/generation and secondly to prudently dispose (waste-) heat streams from electricity generation, which can be deployed for maintaining the necessary temperature level of the digester during all seasons, as well as for drying the wet sludge before incineration; altogether with the aim of making the wastewater cleaning process utmost independent of external energy supply.

1.2 Thesis Organization

Chapter 1 describes the motivation and goals of this work; chapter 2 gives a rough survey of wastewater systems and treatment; chapter 3 describes the various possibilities of energy harvest in wastewater plants and discusses energy storage needed for the compensation of fluctuating wind and solar based power generation; chapter 4 deals with modeling the energetic components of wastewater plants, and chapter 5 with the simulation of plant operation. Aspects of practical implementation are covered in chapter 6; chapter 7 describes the optimization of component rating aiming in energetic independency of the plant at reasonable cost. In chapter 8 plant design and performance for examples of Germany and Vietnam are investigated, and at the end some conclusions are drawn in chapter 9.

2. WASTEWATER SYSTEMS AND TREATMENT

2.1 Sewage systems

Wastewater typically origins from the following sources:

- Industrial processes
- Households and small business
- Rainwater

Large industries mostly have their own specialized wastewater clarification and are therefore regarded outside the scope of this work. In contrast, the wastewaters from households, small business as well as rain water are mostly treated in municipal wastewater plants, and this is the area where this work focuses on.

The wastewater is collected and transported in pipe systems for which two approaches are being applied [2, 3]:

- Separate sewer systems, keeping wastewater and rainwater separated, Figure 2.1a;
- Combined sewer systems treating wastewater and rainwater altogether, Figure 2.1b.

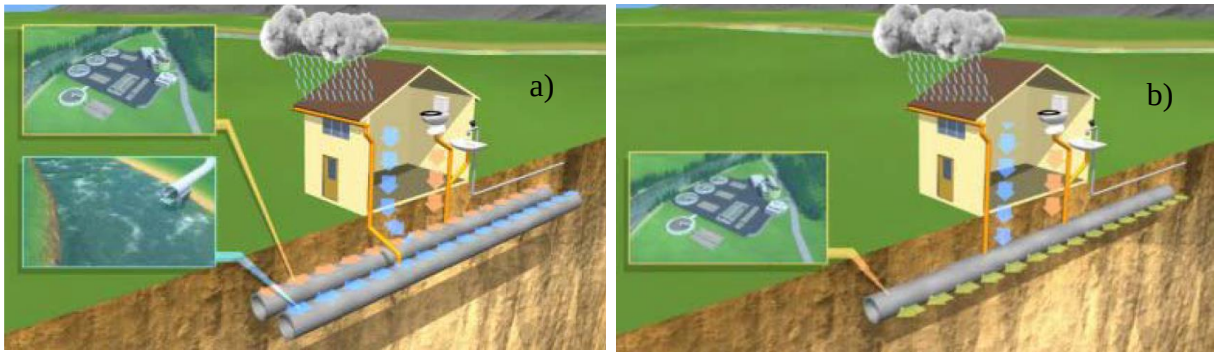

Figure 2.1: Sewer systems: a) separate; b) combined [4]

While the wastewater stream from households and small business typically follows a moderate daily time-dependency, which is widely smoothed by current times in the pipe system, the rainwater occurrence may be very heavy and punctual, in particular in case of strong showers or thunderstorms. Therefore, retention basins for the rainwater are usually foreseen which widely smooth out these peaks.

Furthermore, the organic contents of both waste and rainwater are different; this is relevant for energy exploitation which will be shown later. Rather, the inertness of the complete sewer system leads to widely constant streams with relatively barely varying organic contents.

The tubes of the sewage system finally lead up to the wastewater clarification plant, the function of which will roughly be explained in the following.

2.2 Wastewater clarification

In the clarification process the following stages are consequently passed by the water [2], Figure 2.2:

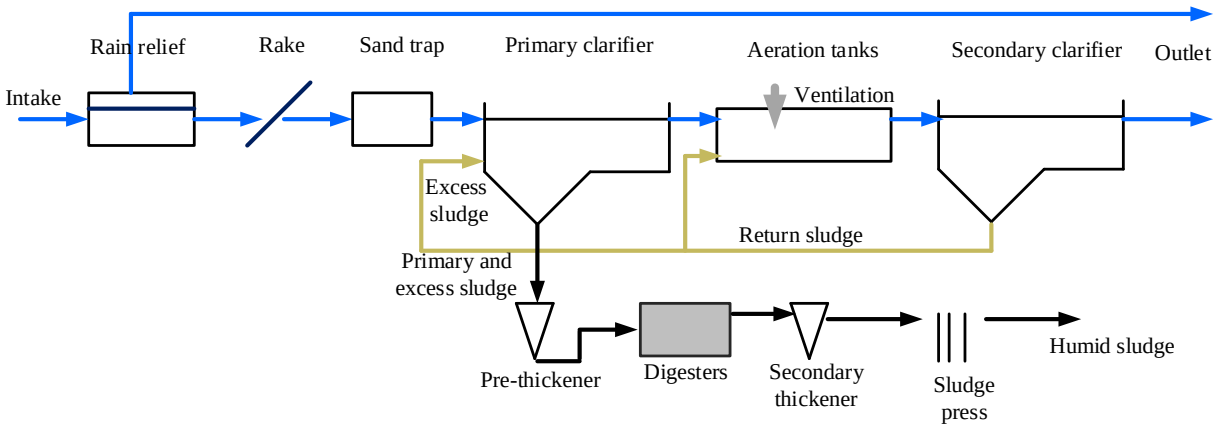

Figure 2.2: Schematic of wastewater treatment process [2]

2.2.1 Expurgation system

Rakes or sieves remove coarse impurities such as hygiene items, pieces of wood or rough waste in order to avoid congestion of pumps and pipes.

2.2.2 Sand and grease trap

In a sedimentation basin sand, gravel and stones settle to the bottom, floating particles such as fats accumulate on the surface and can be removed there.

2.2.3 Primary clarifier

The flow of the waste water slowly passes the primary clarification basin which will settle any undissolved substances as sludge on the bottom; this sludge then is subject to further processing, see section 2.3.

2.2.4 Aeration basin / oxygen

Next, the mechanically pretreated wastewater passes the aeration basin. Micro-organisms (especially bacteria) convert the wastewater contents to mostly carbon-dioxide and biomass. Since oxygen is needed for the bacteria, compressed air is blown into the basin. Phosphorus compounds are also reduced, which otherwise the water would over fertilize.

2.2.5 Secondary clarifier

In the secondary clarification basin, the mud enriched with microorganisms settles to the bottom and is re-directed back into the cleaning cycle in order to maintain the concentration of micro-organisms.

2.2.6 Water outlet

The purified water with good quality is directed into a nearby river or stream. If height difference allows, a micro hydro plant can produce some electricity, see examples in chapter 8.

2.3 Sludge treatment

The sewage sludge resulting from the clarification process requires special treating since it has a high water contents (> 98%) und is biologically unstable.

2.3.1 Thickener

Mostly by further sedimentation, the sludge is concentrated to a typical value of typically 95% water contents.

2.3.2 Digestion

2.3.2.1 Aerobic digestion

Aerobic digestion (a subset of the activated sludge process) is a bacterial process occurring in the presence of oxygen. Under aerobic condition, bacteria rapidly consume organic matter and convert it into carbon dioxide. There is a relatively high electricity demand of this process caused by the blowers, pumps and motors needed to add oxygen to the process. Therefore, **an**aerobic digestion is more frequently applied in wastewater plants as described in the following.

2.3.2.2 Anaerobic digestion

Anaerobic digestion is a bacterial process that is carried out in the absence of oxygen. The process can either be thermophilic digestion, in which sludge is fermented in tanks at a temperature of 55°C, or mesophilic, at a temperature of around 37…38°C. Though allowing shorter retention time (and thus smaller tanks), thermophilic digestion is more expensive in terms of energy consumption for heating the sludge [5]; therefore, mesophilic digestion is mostly preferred and regarded further in this work.

Anaerobic digestion takes place in four steps, Figure 2.3a:

- *hydrolysis*: complex organic matter is decomposed into simple soluble organic molecules using water to split the chemical bonds between the substances;
- *fermentation or acidogenesis* is the chemical decomposition of carbohydrates by enzymes, bacteria, yeasts, or molds in absence of oxygen;
- the fermentation products are converted into acetate, hydrogen and carbon dioxide by what are known as *acetagenic* bacteria;
- methane gas is formed from acetate as well as hydrogen and carbon dioxide by *methanogenic* bacteria.

a)

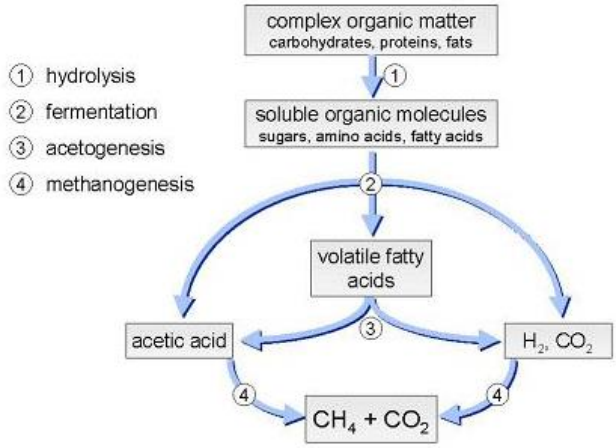

b)

Figure 2.3: a) Path of anaerobic digestion [6], b) Photo of digesters [7]

The sludge remains in the digester for typically 25 days [8] at temperature of 37… 38°C. In practice, most digesters are in egg-shaped form, see photo in Figure 2.3b. As Figure 2.3a shows, a gas that is mainly composed of methane and carbon dioxide, also referred to as biogas, is produced. The amount of gas produced varies with the amount of organic waste fed to the digester and temperature. Energy is needed to heat up the sludge and maintain the desired temperature constant independent of the ambient temperature.

According to [9] the typical biogas production has methane (CH_4) contents of approximately 65%; the biogas comprises ca. 6.5 kWh/m^3 at atmospheric pressure.

The energy of the biogas can simply be used for heating up the sludge, or for combustion in a combined heat and power unit as it will be considered later in this work.

2.3.3 Dewatering

Filter presses are normally used in order to reduce the volume of sludge output before deposition or further treatment [10]. The remaining water content is still in the range of typically ca. 70…75% [11].

2.3.4 Further sludge processing

For the stabilized and dewatered sludge, the following possibilities for further treatment exist:

- Fertilization in agriculture; this allows only for treatment of smaller quantities and is limited by law in many countries due to the heavy metal contents of the sludge.

- Disposal, which requires firm detachment of storage sites in order to avoid ground water contamination.

- Co-incineration in a nearby plant; this requires further energy for transportation, while the energy harvest is marginal in consequence of the high water contents of sludge.

- Thermo-solar sludge drying on site of the wastewater plant and subsequent incineration in a small local steam power unit. This most interesting possibility will further be investigated in this work.

2.4 Properties of wastewater

2.4.1 Quantities

In order to reasonably determine the size of a wastewater plant – as well as for the additive energetic components which will later be investigated in this work – the input sewage stream gives a right measure. Usually for wastewater plant dimensioning the value of "Person Equivalents" (PE) is being used. This value results from the number of inhabitants who are depolluted by the sewage plant under regard, plus an additive equivalent number given by size and type of small business being depolluted by the same plant [12], and also includes an average share of rainwater.

Based on this PE value, in German cities the wastewater production was calculated with ca. 150…200 liters per PE and per day in the past, but it is steadily decreasing since several years (due to the water saving policy) and is now tending to about 120 liters per PE and per day [13]. As another example, for Vietnam this value is very similar [14]. In the following, a value of 130 liters per PE and per day is assumed.

2.4.2 Energetic contents

As already stated before, the wastewater contains a certain quantity of organic substances which can be transposed to an energy contents by use of the "Chemical Oxygen Demand" (COD) required for complete oxidation (under ideal conditions) of all dry substance being contained in the sewage

[15]; as an average, a COD of 0.12 kg / (PE·d) is a generally and internationally accepted value [16]. Given the equivalence of 1 kg COD to 3.49 kWh [17], the energetic equivalence of a sewage stream (or a sludge stream) can be calculated as a flow of chemical power:

$$P_{chem} = 0.4188 \text{ kWh/(PE·d)} = 17.45 \text{ W/PE} \quad (2.1)$$

Passing through the processes of wastewater and sludge treatment as described above, the PE related COD values and chemical power flows according to Table 2.1 are found [18].

Table 2.1: Flow of chemical power in wastewater plant

	COD [g/(PE·d)]	P_{chem} [W/PE]
Wastewater input	120	17.45
Sewage output (= digester input)	67	9.743
Digester output (sludge)	30	4.363
Digester output (biogas)	37	5.380

2.5 Energy demand of wastewater plants

2.5.1 Electricity

The relative electrical energy demand of wastewater treatment plants varies by size. Five size categories for division of assets are distinguished in the literature [19]:

- GK1: 0 – 999 PE
- GK2: 1000 – 5000 PE
- GK3: 5001 – 10,000 PE
- GK4: 10,101 – 100,000 PE and
- GK5: > 100,000 PE.

Increasing urbanization all over the world will lead in future to a majority of sewage plants of type GK5. Therefore, and since the highest urgency for wastewater treatment is given for densely populated regions, this work will focus on this plant category in particular.

Many electric devices such as pumps, conveyors, compressors etcetera compose the electric load of a wastewater plant. Uniformly the literature declares the compressors for the ventilation of the aeration basin as the major electric load [20, 21, 22, 23, 24, 25]. Table 2.2 gives a survey in more detail with example numbers from [25]. Since many of the consumers – especially the predominant aeration basin ventilation – are continuously in operation, the electric consumption of a larger wastewater plant can be seen to be rather constant at 3.2 W/PE on average, see Table 2.2. This is in rather good agreement with the literature reference of 22 W/(m^3·d) given in [26] for a wastewater production of 145 liters/(PE·d), which is moderately above the value of 120 liters/(PE·d) as given in [27], see section 2.4.1. The calculations made in this work will be based on 22 W/(m^3·d).

Table 2.2: Electric loads in wastewater plants [25]

	kWh/(PE·yr)	Normal range [Appendix A2.1]	Aver. power (W/PE)
1-Intake	**4**	**2.5 … 6.0**	
1.1-Intake pumping station	2.5	1.5 … 3.5	
1.2-Rake	0.75	0.2 … 1	
1.3-Sand and grease trap	0.75	0.5 … 1	
2-Biological waste water treatment	**21.25**	**14.5 … 33**	
2.1-Ventilation	14	11.5 … 22	
2.2-Stirrer	3	1.5 … 4.5	
2.3-Return sludge pump	2.5	1… 4.5	
2.4-Sundries	1.25	0.5 … 2	
2.5-Filter	0.5	0.5… 1	
3-Infrastructure	**2.75**	**1… 4.5**	
3.1-Heating	1.25	0… 2.5	
3.2-Others	1.5	1… 2	
Total	**28**	**20… 50**	**3.2**

2.5.2 Thermal demand

Heat demand in a wastewater plant is given mainly by the digestion process and – to a minor and mostly negligible part – the heating of the control and administration building.

The demand of the anaerobic digestion results from

- warming up the incoming sludge (<2% of input sewage) from original (ambient) temperature to the desired 37…38°C;
- compensating the heat losses of the digester vessel(s).

For the calculation of the PE related heat power demand as a function of ambient temperature, the following equations can be used:

$$P_{thwarmup}/\mathrm{PE} = 2\% \cdot 0.12\ \mathrm{m^3/(PE \cdot d)} \cdot \rho_{\mathrm{H2O}} \cdot c_{\mathrm{H2O}} \cdot (37.5°\mathrm{C} - T_{ambient}) \qquad (2.2)$$

with the assumption that the heat capacity c of liquid sludge is that of water;

$$P_{loss}/\mathrm{PE} \approx u \cdot 6\pi \cdot [2\% \cdot 0.12\ \mathrm{m^3/(PE \cdot d)} \cdot 25\ \mathrm{d} \cdot 1/2\pi]^{2/3} \cdot (37.5°\mathrm{C} - T_{ambient}) \qquad (2.3)$$

for a cylindrical digestion tank with minimal surface shape (height = diameter);

u: heat transition factor (depending on digester hull material), $(\mathrm{W/(m^2 \cdot K)})$;

$T_{ambient}$: ambient temperature in °C;

25 d: rest time of sludge in digester.

Equation (2.3) is an approximation for a cylindrical digestion tank; most digesters are in typical egg-shaped form (see photo in Figure 2.3 b) which leads to slightly lower losses; thus, equation (2.3) can be regarded as a conservative estimation.

3. ENERGY HARVEST IN WASTEWATER PLANTS

As it was shown in section 2.4.2, wastewater contains a quantity of energy in form of organic substances; in the following, ways for exploitation of parts of this energy will be shown. Furthermore, the typical locations of wastewater plants distant from residential areas favor them as sites for wind power generation, and usually large terrains of these plants also allow for solar energy harvest. Finally, the almost steady clear water output is eligible for small hydro generation if the height difference between plant and river/stream admits.

3.1 Use of biogas

According to Table 2.1 in section 2.4.2, about 31% of the original COD contents of wastewater can be converted to biogas by anaerobic digestion [26], resulting in ca. 5.38 W/PE. The approximately 20 liters of biogas per person and per day produced typically consist of ca. 65% methane (CH_4); the rest is mainly carbon-dioxide (CO_2) [26, 27, 28]. The typical calorific value of such biogas is about 6.5 kWh/m^3 at normal pressure and is thus appropriate for energetic use in a combustion engine after passing a slight gas cleaning process by, e.g., an active coal filter.

For the combustion itself small combustion engine driven Combined Heat and Power (CHP) units are on the market, providing efficiencies in the range of ca. 35…45% (electricity output) and ca. 45…55% (thermal output), in total often at or above 90%, see Figure 3.1 as an example [29]. While the electricity is usually fed into the local grid and contributes to cover the electricity demand of the sewage plant, the heat can be used for sludge heating (see section 2.5.2) and warming of local buildings.

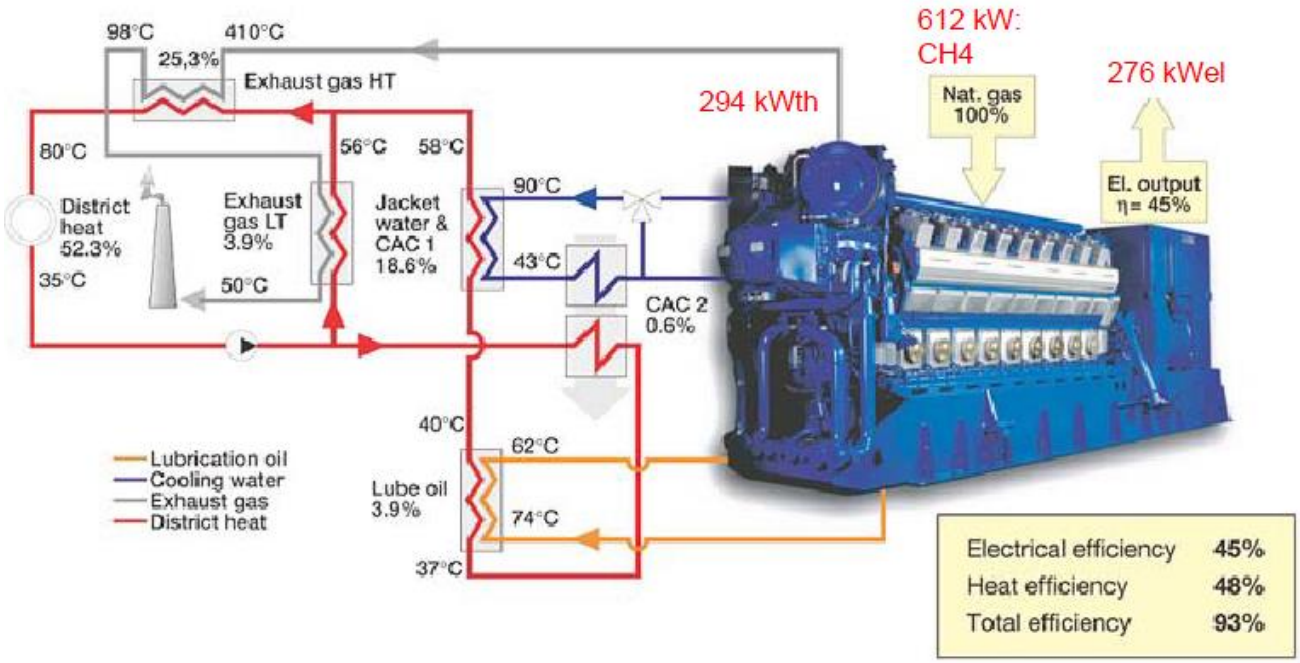

Figure 3.1: Combined Heat and Power (CHP) unit [29]

3.2 Thermal exploitation of sludge

While the use of biogas is nowadays fairly customary in modern wastewater plants, thermal treatment of sludge is found rather rarely in practice; sometimes incineration is applied in order to get rid of the infectious sludge and avoid disposal, with energy use only as a side aspect. On the other hand, the COD contents of digester sludge output is still about 25% of plant input COD (see Table 2.1), providing a chemical power stream of more than 4.3 W/PE; however, the sludge humidity at digester output is above 95%, and after dewatering it is still in the range of 70 …75%, see section 2.3.3. This results in a very low calorific value unsuitable for effective incineration. There are two possibilities for enhancement of the calorific value as roughly described in the following.

3.2.1 Mixing coal as an additive

The calorific value of the sludge dewatered to a Dry Substance Ratio (*DSR*) of typically *DSR* ≈ 25…30% can be calculated as follows:

According to Table 2.1 the sludge at digester output contains ca. 30 g COD/(PE·d) with a calorific value of h_{COD} = 3.49 kWh/kg. The calorific value of the dry substance of digested sludge is given in the literature with h_{DS} ≈ 11 MJ/kg corresponding to 3.056 kWh/kg [30]. Taking into account the ratio of calorific values, the stream of dry substance is 34.26 g/(PE·d), the stream of humid sludge

correspondingly 1/*DSR* · 34.26 g/(PE·d). The calorific value of this humid sludge can be calculated as

$$h_{sludge} = DSR \cdot h_{DS} - (1 - DSR) \cdot h_{H_2 0} \tag{3.1}$$

where

DSR is percentage of dry substance in sludge;

h_{H_2O} is evaporation enthalpy of water (= 2257 kJ/kg).

This typically results in rather low values. By addition of a certain mass stream of coal with a relatively high calorific value h_{coal}, the overall calorific value of the mixture can be enhanced to a desired heating value h_{burn} needed for proper incineration; the required coal mass stream can be calculated as

$$\dot{m}_{coal} = \frac{\dot{m}_{sludge} \cdot (h_{burn} - h_{sludge})}{h_{coal} - h_{burn}} \tag{3.2}$$

$$\dot{m} = \dot{m}_{coal} + \dot{m}_{sludge} \tag{3.3}$$

where

$\dot{m}_{sludge}$ is sludge input mass stream;

h_{sludge} is the calorific value of the sludge before mixing with the coal;

h_{coal} is the calorific value of coal added;

$\dot{m}_{coal}$ is the mass stream of coal needed;

$\dot{m}$ is the fuel mass stream fed to incineration with calorific value h_{burn}.

3.2.2 Sludge drying

There are several conventional technical methods applied to drying of sewage sludge; the most common one is the band dryer, where a thin layer of sludge is transported on a continuously moving band and exposed to heated air, see Figure 3.2 [31]. However, the energy consumption for achieving a heating value of dried sludge appropriate for sound incineration is rather high. In section 3.3.3 it will be shown that also solar irradiation can contribute to effective sludge drying as a renewable source of heat.

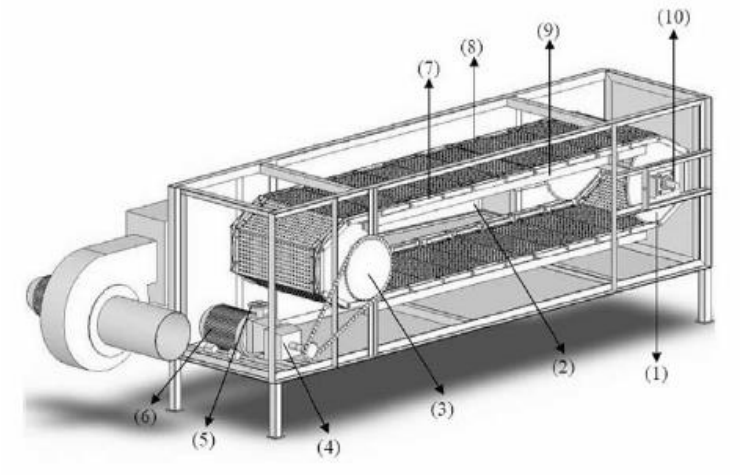

Figure 3.2: Schematic view of the dryer: sprocket (1); location of major temperature sensor (2); large scale gear (3); gearbox (4); manual rotation speed controller (5); electrical motor (6); chain(7); perforated bands (8); chain guide (9) and shaft and bearing (10) [31]

3.2.3 Sludge incineration and energy harvest

3.2.3.1 Conventional boiler

In general, a boiler is an enclosed vessel in which water is heated and circulated, either as hot water, steam, or superheated steam for the purpose of heating, powering, and/or producing electricity. The furnace of the boiler is where the fuel – in this case the dried sewage sludge – and air are introduced to combust; fuel/air mixtures are normally introduced into the furnace by using burners, where the flames are formed. The resulting hot gases travel through a series of heat exchangers, where heat is transferred to the water/steam current inside the tubes. The combustion gases are finally released to the atmosphere via the stack of exhaust section of the boiler. In [32] sewage sludge incineration in a municipal wastewater treatment plant and the principle of the boiler is shown.

3.2.3.2 Pyrobustor

The Pyrobustor system [33] operates as a two stage process of pyrolysis (under absence of oxygen), and subsequent combustion that takes place in a common rotary kiln at temperatures of approximately 800°C, see Figure 3.3; the hot exhaust gas coming out of the post-combustion chamber can be used to generate steam. In the Pyrobustor only dried sewage sludge (DSR≈ 90%) can be used, and the sludge must therefore be dried before the heat treatment.

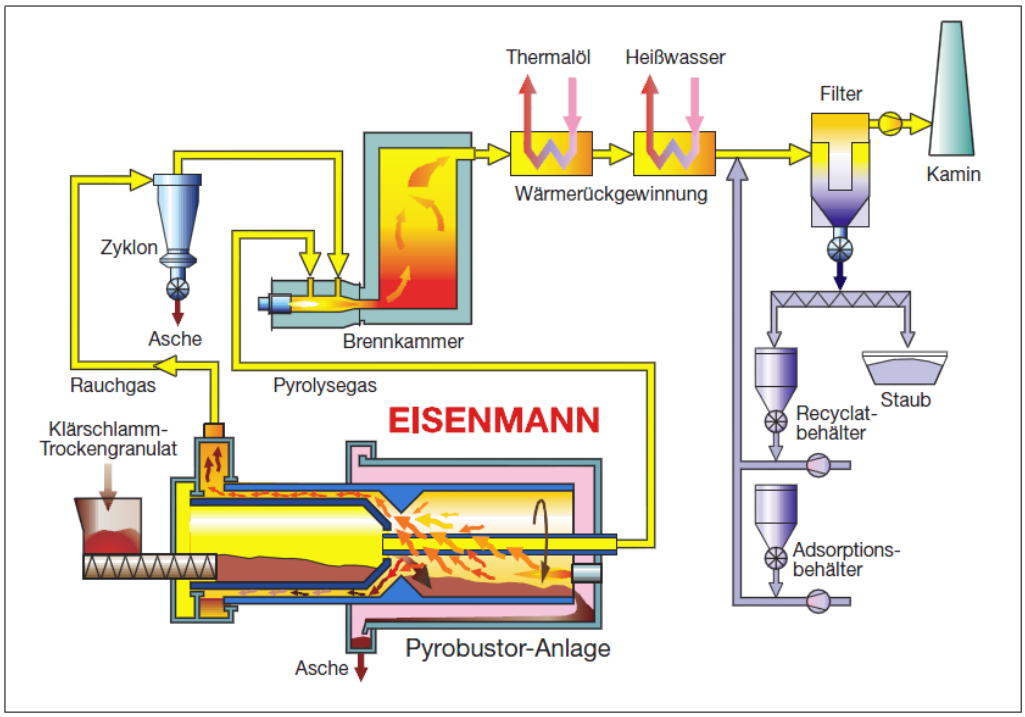

Figure 3.3: Scheme of incineration in Pyrobustor (from [33])

3.2.3.3 Steam circuit, electricity and heat generation

The heat released in a boiler or Pyrobustor can favorably be used with a steam circuit where a turbine moves a generator for electricity generation, Figure 3.4. Typical steam temperatures at the turbine input are some 400°C with pressure up to 50 bar for the order of plant size relevant to this work; and at the turbine output the temperature is in the range 30…60°C at low pressure [34]. Exemplary values from practice can be found in Table 3.1, and Figure 3.5 shows a photo of such a small steam turbine.

The waste heat of the condenser is eligible for low temperature heating issues, for instance to maintain the digester temperature at 37…38°C, see 2.3.2.2. If needed, a partial steam stream can be tapped from the turbine at higher temperature, see Figure 3.4: in this case, the electricity output is correspondingly decreased.

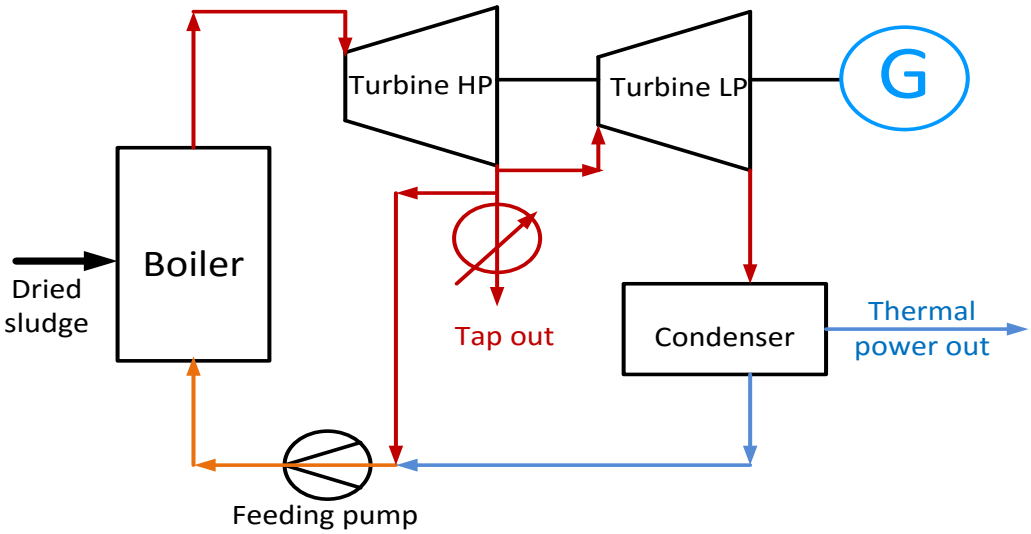

Figure 3.4: Steam process

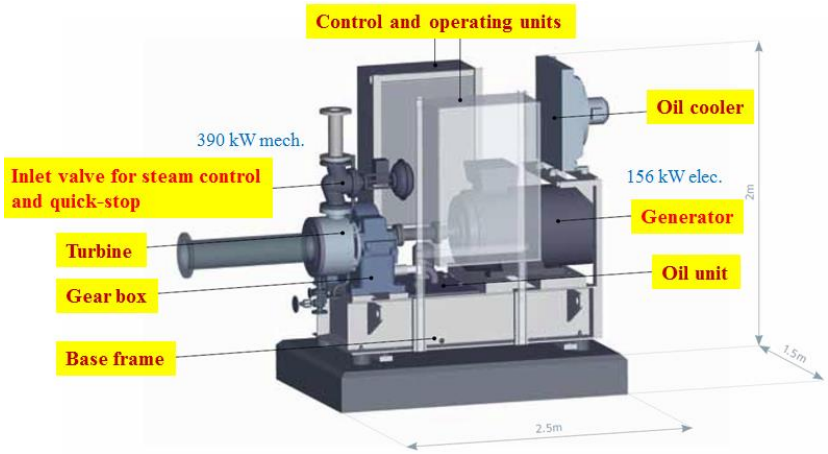

Figure 3.5: Small steam turbine [34]

Table 3.1: Technical data (example) of Siemens Turbine ST030 [34]

Data	Specification	Unit
Power output	75 … 300	kW
Inlet pressure	2 … 40	bar
Inlet temperature	up to 400 (dry/saturated)	°C
Exhaust pressure	typ. 0.1	bar
Dimensions	1.5 · 2.5 · 2 (breadth · length · height)	m
Weight	approximately 4.5	ton
Cost	average 450 (for both steam turbine and generator)	€/kW

3.3 Renewable resources on the ground of wastewater plants

3.3.1 Small hydro generation

The simplest way of renewable energy harvest at a wastewater plant is the use of the almost constant output stream of clarified water for small hydro electricity generation, provided that output flow rate and height difference are suitable. Appropriate small turbine/generator sets with different technologies are available on the market; with a typical efficiency of about 75% the power output can roughly be assessed by

$$P_{el}/(kW) \approx 7 \cdot Q/(m^3/s) \cdot h/(m) \tag{3.4}$$

3.3.2 Wind energy

The location of wastewater plants distant from populated areas relieves the erection of wind turbines on the ground, which can significantly contribute to cover the electricity demand of the plant if the local wind profile is appropriate. The electrical power output depends on the wind speed to a power of 3 and is proportional to the rotor size. A variety of wind generators in the relevant power range (100 kW up to 5 MW) based on different aerodynamic and electrical principles are commercially available [35, 36].

3.3.3 Thermo-solar sludge drying

Thermo-solar sludge drying can be used for sludge conditioning for subsequent incineration [37], instead of adding coal to the humid sludge (section 3.2.1) or application of energetically unfavorable conventional drying methods (section 3.2.2). Glass houses of appropriate size and properties as well as ploughing systems for homogenization of the drying process are state of the art, see Figure 3.6.

Figure 3.6: Glass house for sludge drying [38, 39]

The drying process is mostly conducted in batch operation. Besides floor heating – allowing to exploit low temperature waste heat for instance from the condenser of a steam circuit – air heating at higher temperatures is applied; the latter can for instance be fed by waste heat from cooling jacket or exhaust gas of a combustion engine. Even in moderate climatic zones about 20…25% of the required energy for drying can be obtained via the solar radiation [40]. Approximately 2.5 tons of water can be evaporated per m^2 and per year, which admits to assess the required size of the glass house [41]. About 960 kWh of thermal energy are needed for the evaporation of 1 ton of water; the electricity demand for conveyors, ploughing systems etcetera is specified in the wide range of 20…130 kWh per ton of water evaporated [39, 42].

Drying up to 20% remaining humidity will result in heating values of sludge similar to that of lignite coal (~ 9 MJ/kg); a typical dwell time for the sludge of almost 1 month is needed.

3.3.4 Solar thermal collector

For boosting the solar contribution for sludge drying as well as for covering other heat demand up to ca. 100°C, thermal collectors can additionally be installed. Such systems (see Figure 3.7) are state of the art and offered by many manufactures at moderate cost.

Figure 3.7: Solar-thermal collector [43]

3.3.5 Heat pump

While the use of waste heat from a CHP unit or a steam power plant creates an inter-dependency of heat availability from electricity generation, a heat pump provides the opportunity to generate heat from electricity with a typical performance coefficient $P_{th}/P_{el} \approx 4$ [44], see principle shown in Figure 3.8.

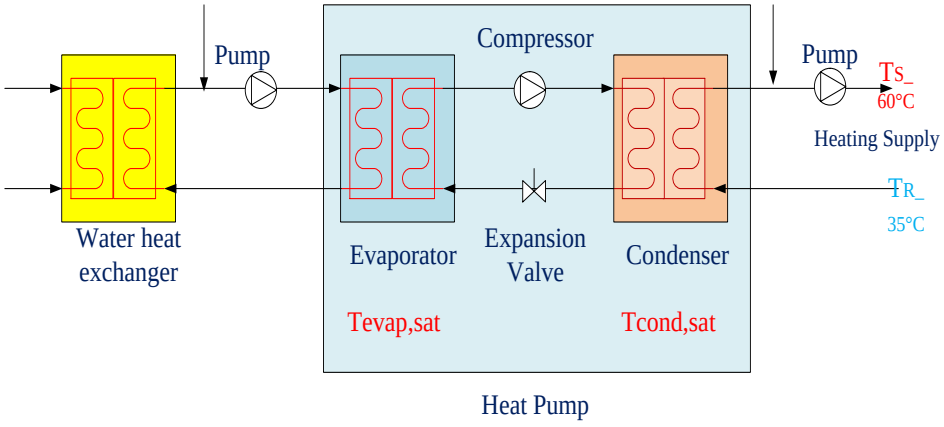

Figure 3.8: Heat pump schematic [44]

Heat from soil, groundwater or the air is introduced into the heat pump via a heat exchanger, the so-called evaporator, and transferred to a liquid refrigerant. This refrigerant has a very low boiling

point, so it heats up quickly and vaporizes at low temperatures. Now, a compressor compresses the gaseous refrigerant, thus increasing its temperature. The heat generated in this way is output through a second heat exchanger, the condenser, completely to the heating system. Thus, the refrigerant cools down and liquefies again. Subsequently, the refrigerant flows through the expansion valve where it is expanded to the original pressure, and back to the evaporator.

3.3.6 Photovoltaics

Typically, the large extent of wastewater plants would also allow for harvesting electricity from solar energy by photovoltaics. Even if the investment costs are rather high and the efficiency is quite low, the technology of modules and required DC/AC converters is well developed, and application may be useful in particular in very sunny regions.

3.4 Energy storage

In order to adapt the steady fluctuations of wind and solar based energy harvest to the load demand, energy storage may be necessary. Not only the technical and environmental aspects play an important role in selecting the most suitable storage devices, but the functionality of each individual technology as well as cost considerations can also determine the suitable ones. In the following applicable storage principles for both electricity and heat are briefly sketched.

3.4.1 Electricity storage

There is a plenty of principles of direct or indirect electricity storage such as super-capacitors, accumulators, flywheels, compressed air and many other [45]. Regarding mid and long term storage, pumped hydroelectric is the most commonly applied technology [46]; however, this principle is most eligible for larger quantities of stored energy and rated power, and requires certain geographic conditions. Regarding relevant storage capacity (< few hundred MWh) and charging/de-charging power (< 1 MW), a hydrogen storage path has proven as an applicable solution [47] and will therefore be pursued further in this work.

Surplus electricity is fed to an electrolyzer which produces hydrogen gas (as well as oxygen); so called “high-pressure electrolyzers” have an output pressure of hydrogen up to 30 bar (more recently, values up to 60 bar are also mentioned in the literature [48]), which allows for hydrogen storage in a moderately sized tank of relatively simple construction, and omits an extra compressor and its energy demand. Often electrolyzer operation in certain power steps (e.g. 25, 50, 75, 100% of nominal power) for longer periods of time is stipulated in order to reduce strain.

The oxygen which is also produced by electrolysis could be used for aeration in the clarification process, see 2.2.4, but this is not further pursued in this work. Also, the waste heat of this process is not considered here.

The reconversion of hydrogen to electricity can be done by

- fuel cell which is an innovative but still rather expensive solution;
- combustion engine driven generator as a relatively simple and more economical solution.

In case that a biogas-fed CHP unit exists anyway – as it may be given in a sewage plant for exploitation of biogas from the digester, see section 3.1 – a certain share (up to 15%) of stored hydrogen may be added to the biogas, thus sparing an extra generator set. In this case, simply an accordingly higher rated power of the generator set must be chosen, thus making this solution even more economical. Therefore, this approach will be pursued further in this work.

3.4.2 Thermal energy storage

Especially longer periods of low solar irradiation may necessitate storage of heat. For purposes as given in this work a simple, thermally isolated and unpressurized water tank is the most suitable solution. Storage temperatures may range up to 95°C; the size can be designed individually according to given temperature levels and storage needs.

4. PLANT DESIGN AND MODELING OF THE ENERGETIC COMPONENTS

4.1 Plant design

Summarizing the previous sections, the following components can be regarded in aiming at vast energetic independence of wastewater plants; as it will be shown later, the particular composition of energetic components has to respect geographic, meteorological and other individual conditions given at the plant location:

4.1.1 Sources of electricity and/or heat:

- small hydro generation at output of clarified water (→ electricity);
- CHP unit for combustion of biogas from digester (→ electricity and heat);
- incineration of dried sludge for small steam power unit (→ electricity and heat);
- wind power generation (→ electricity);
- photovoltaic (→ electricity).

4.1.2 Sinks of electricity and/or heat:

- existing sewage clarification process (→ electricity);
- digester tempering (→ heat);
- glass house for thermo-solar sludge drying (→ heat and some electricity for auxiliaries).

4.1.3 Storage of electricity or heat:

- hydrogen storage path via electrolyzer and combustion engine based generator (→ electricity);
- isolated hot water tank (→ heat).

Furthermore, despite the goal of energy independence, a connection with the public grid is desirable for

- buffering of short time electrical power peaks;
- backup in case of failure of plant components.

A very first rough assessment of the electricity balance based on values given in Table 2.1 in section 2.4.2, as well as typical efficiencies of processes, shows that the average electricity demand of an

existing wastewater plant (3.2 W/PE, Table 2.2) cannot completely be covered by the electrical outputs of both CHP and steam units (with usually negligible contribution of small hydro generation at water output stream), see Table 4.1:

Table 4.1: Rough assessment of electricity balance in sewage plant

	From Table 2.1	Typical efficiency	W/PE
CHP unit	5.38 W/PE	35%	1.883
Small steam unit	4.363 W/PE	20%	0.8726
Sum			2.7756
El. demand of plant (Table 2.2)	3.2 W/PE		3.2

Thus, in order to compensate the deficit of 0.4444 W/PE, wind and/or solar based electricity generation including a storage path has to be involved to achieve energy independence. (A very much more detailed consideration also comprising the thermal balances will be made later in chapter 8 for two examples cases).

In consequence, the overall plant design proposed with the principal energetic components is depicted in Figure 4.1; as it will be shown later in this work, the roles of wind power, photovoltaic and small hydro generation, as well as thermal components required, largely depend on local specific conditions.

4.2 Modeling of energetic components

In the following, the properties of the particular components that have to be regarded in modeling for simulation purposes of such kind of plant will be discussed. Their main properties are summarized in Table 4.2.

For simulating the energetic behavior of the complete plant over longer periods of time in 1 hour intervals, models of the particular components as listed in Table 4.2 were created as MATLAB code. These models will be described in the following and, where appropriate, their functionality is shown as Simulink blocks in the appertaining figures.

Table 4.2: Principal features of energetic components

No.	Model	Input	Output	Notes
1	Electric load of sewage plant	Electricity		Assumed constant at 3.2 W/PE (see Table 2.1)
2	Small hydro generation	Clear water flow	Electricity	0.12 m^3/(PE·d) (see 2.4.1); power output see 3.3.1
3	Digester	Wet sludge, heat	Biogas (mainly CH_4)	19.6 liters/(PE·d) [50]; heat demand according to 2.5.2
4	Combustion engine based generator	Biogas (from digester); hydrogen from storage	Electricity, heat	Typ. efficiencies: 35% (el.) and 55% (th.), (see 3.1)
5	Fuel cell	Hydrogen from storage	Electricity, heat	Option, not further pursued, see 4.1
6	Thermo-solar sludge drying	Solar irradiation, waste heat from CHP and steam units	Dried sludge	Typical values of performance see 3.3.3
7	Steam power unit	Dried sludge	Electricity, heat	Typ. efficiencies: 20% (el.) and 53% (th.), see 3.2.3.3

No.	Model	Input	Output	Notes
8	Wind converter	Wind speed (temporal profile)	Electricity	Variable power output, see section 3.3.2
9	Photovoltaic	Solar irradiation (temporal profile)	Electricity	Option; typical efficiency incl. inverter ca. 14%
10	High pressure electrolyzer	Electricity	Hydrogen (+oxygen)	Often operated in power steps; typ. efficiency ca. 60% [83]
11	Hydrogen storage	Hydrogen	Hydrogen	Pressure up to 30 bar (see 3.4.1)
12	Thermal storage	Heat	Heat	Used for thermal balance; 5% losses assumed generically
13	Heat exchangers	Heat at temperature level 1	Heat at temperature level 2	Used for combustion engine, steam condenser, digester, glass house
14	Public grid	Electricity	Electricity	Providing electrical balance in short term range; limited power capacity when indicated

No.	Model	Input	Output	Notes
15	Control system	Process variables, commands	Process control, visualization	see 5.4

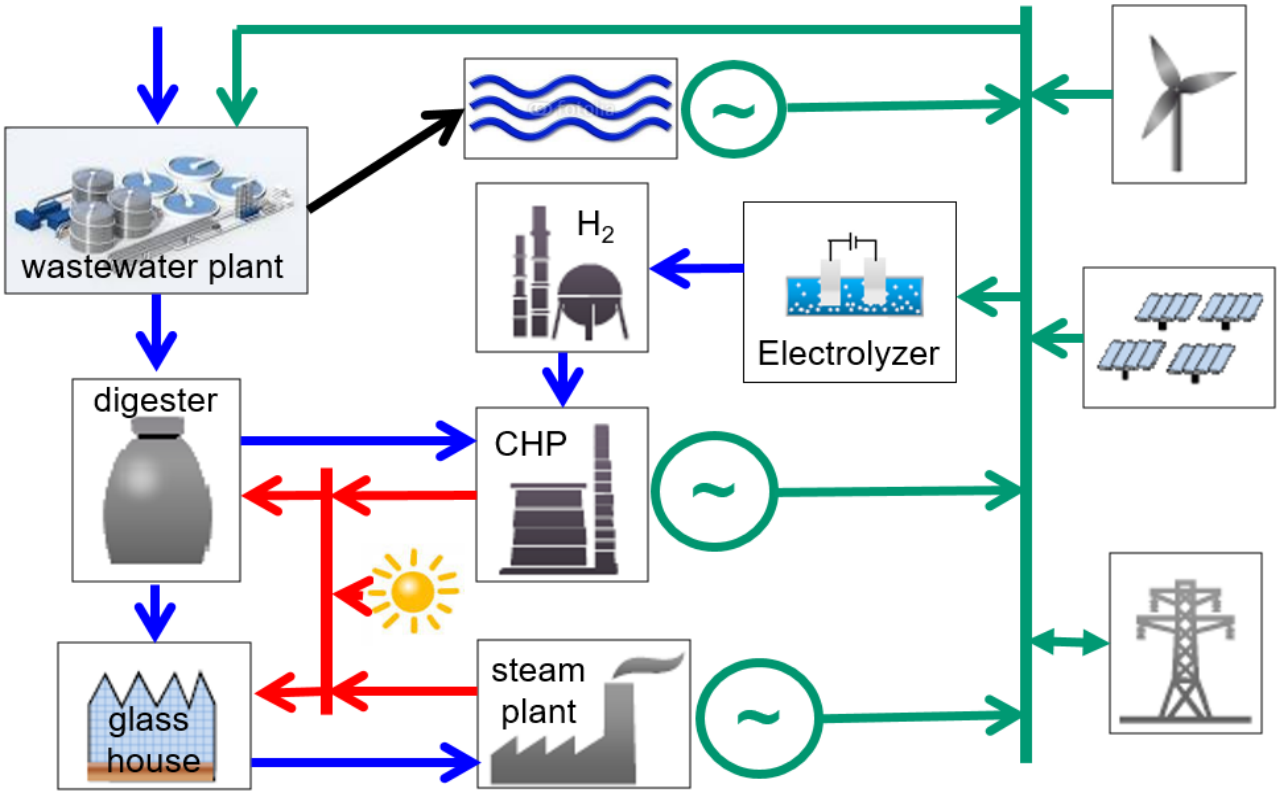

Figure 4.1: Overall plant design with principal energetic components

4.2.1 Electrical load

As outlined in section 2.5.1, the electrical load of the sewage plant can be assessed as rather constant at 3.2 W/PE; for the electrical devices needed for thermo-solar sludge drying (ventilation, conveyors, ploughing system etcetera) another constant load component is added, see section 3.3.3.

4.2.2 Small hydro generation model

The relatively simple model considers flow, height difference and an estimated efficiency, see equation (3.4) and Figure 4.2.

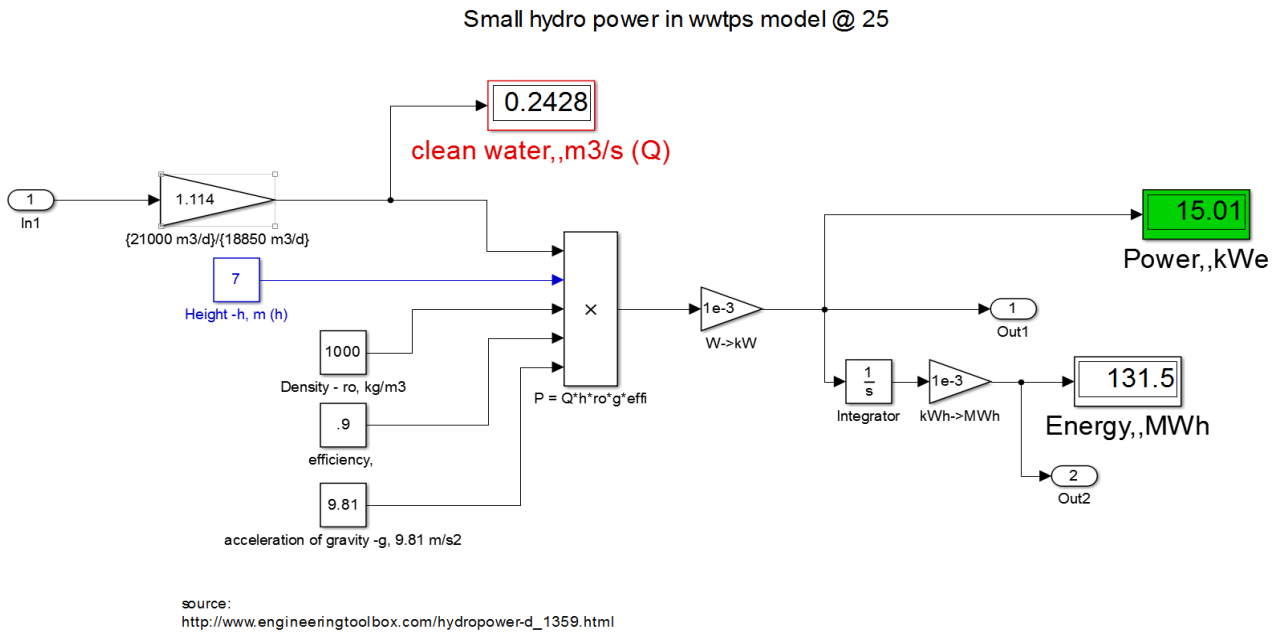

Figure 4.2: Simulink® model of small hydro generation [49]

4.2.3 Digester model

According to [50] the typical biogas production is about 19.6 liters/(PE·d); with a methane (CH_4) contents of approximately 65% the gas comprises ca. 6.5 kWh/m^3 at atmospheric pressure. Thus, the model calculates a chemical power of 5.38 W/PE (see Table 2.1) fed to the CHP unit. The heat demand of the digester – depending on ambient temperature – is calculated according to equation (3.1) and equation (3.2).

4.2.4 Model of CHP unit

In the relatively simple model the electrical and thermal output power is calculated from the energy contents of the input biogas stream – and the added hydrogen gas stream if required – multiplied with the electrical respectively thermal efficiencies as given in Table 4.2.

4.2.5 Fuel cell model

Even if finally not applied in the later simulation of example cases, an easy fuel cell model was also developed, Figure 4.3. Constant electrical and thermal efficiencies are regarded; the latter would also allow for exploitation of the waste heat. In the electrical path the efficiency of a DC/AC inverter is foreseen as well.

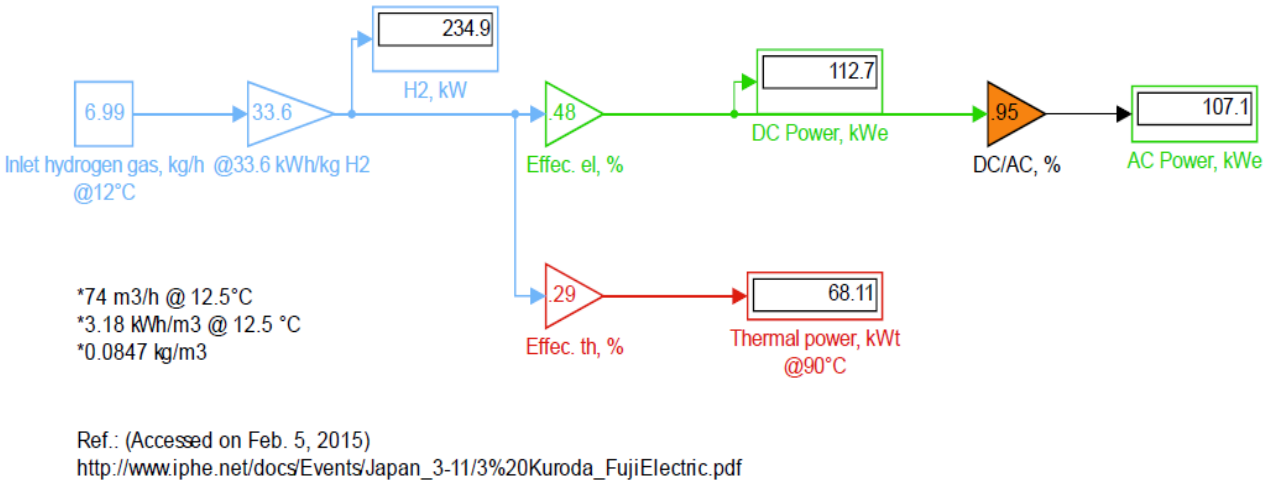

Figure 4.3: Simulink® model of fuel cell system; parameters from [51]

4.2.6 Model of thermo-solar sludge drying

The conditions and interdependencies within the glass house for sludge drying are more complex and thus required to create a more comprehensive model as shown in Figure 4.4. Basically, with given hourly profiles of ambient temperature and solar irradiation, the thermal power demand is calculated as

- power needed to heat up the input sludge with given humidity from varying ambient temperature to glass house temperature assumed constant at 55°C;
- power needed for water evaporation to the desired rest humidity of sludge (20%);
- power losses derived from given surface area of the complete glass house, heat transmission factor – 2 W/(m^2·K) assumed here – and varying ambient temperature.

This demand is diminished by the power input of solar irradiation calculated from given hourly irradiation profile, ground area of glass house and heat transmission efficiency (65 % approx.). The output of the model is the lacking thermal power which must be covered by other sources, concretely the waste heat of both CHP and steam power units (see Figure 4.5) and, if applicable, by a heat storage or tapping of the steam circuit. The balance is made in the model of the complete plant, see section 5.3.

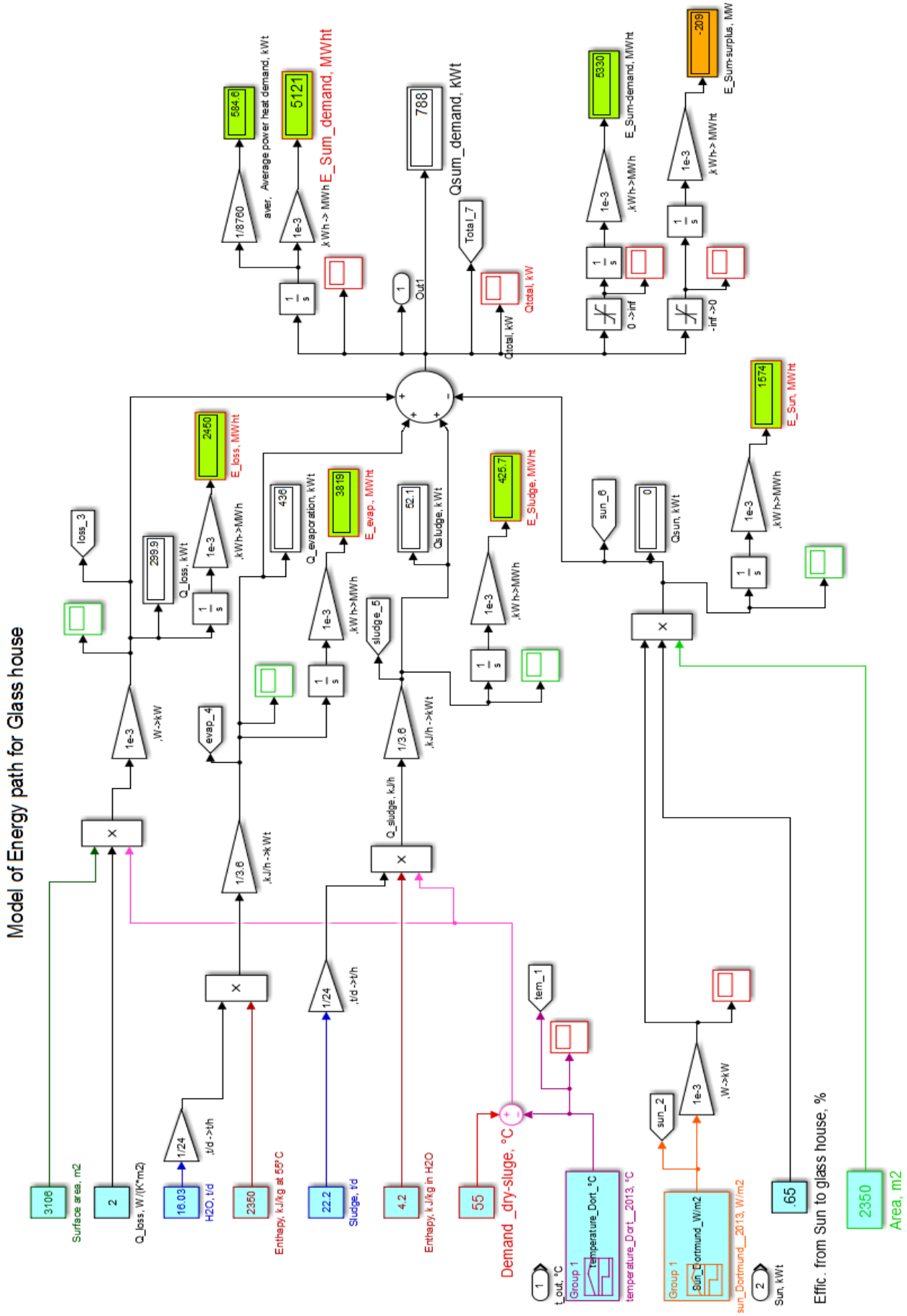

Figure 4.4: Simulink® model of thermo-solar sludge drying

With known throughput of sludge, the ground area of the glass house can be assessed by the fact that typically 2.5 tons of water per m^2 and per year can be evaporated even in moderate climatic zones [52]. For typical shapes of such glass houses the surface area (glass hull) is about 30 % larger than the ground area.

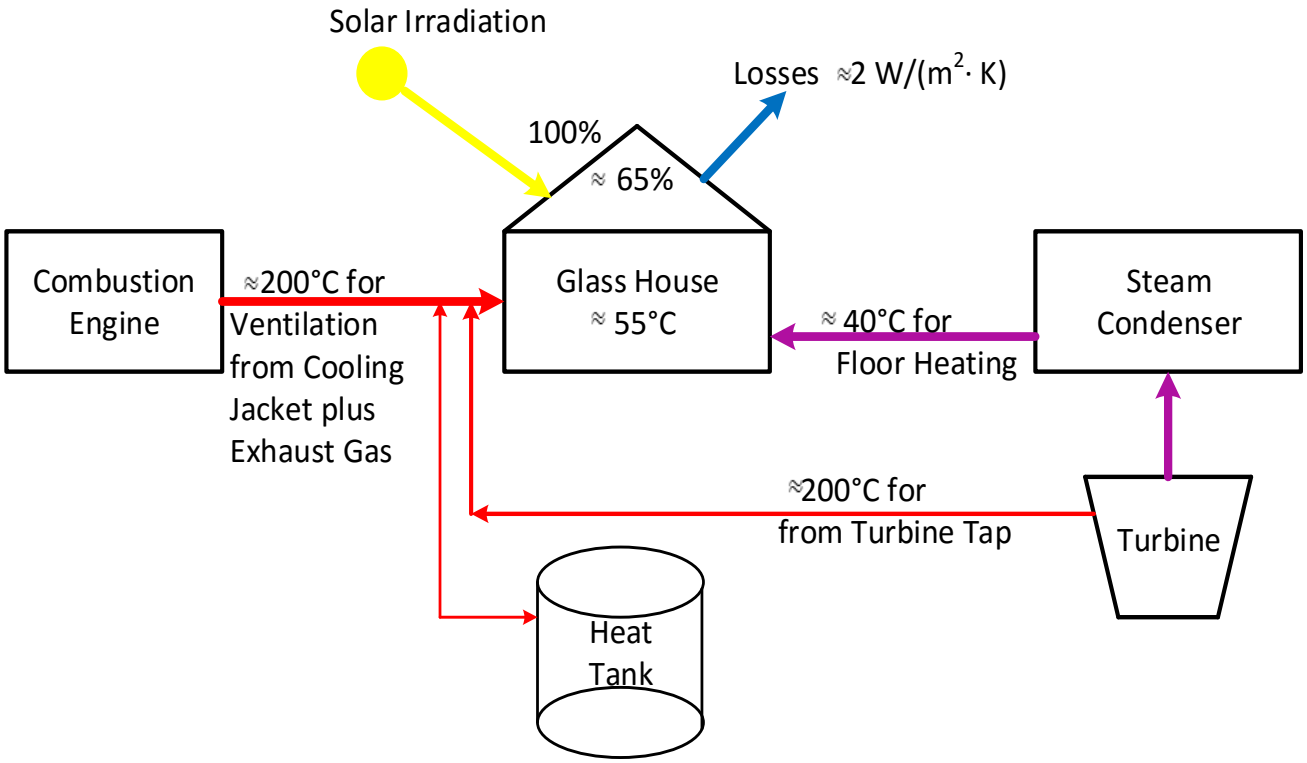

Figure 4.5: Heat supplies versus heat demand of the glass house

4.2.7 Steam power plant model

In order to allow deliberate tapping of steam, the model of the steam power unit is based on the enthalpies of water/steam at the particular stages, shown as h_1 ... h_5 in Figure 4.6.

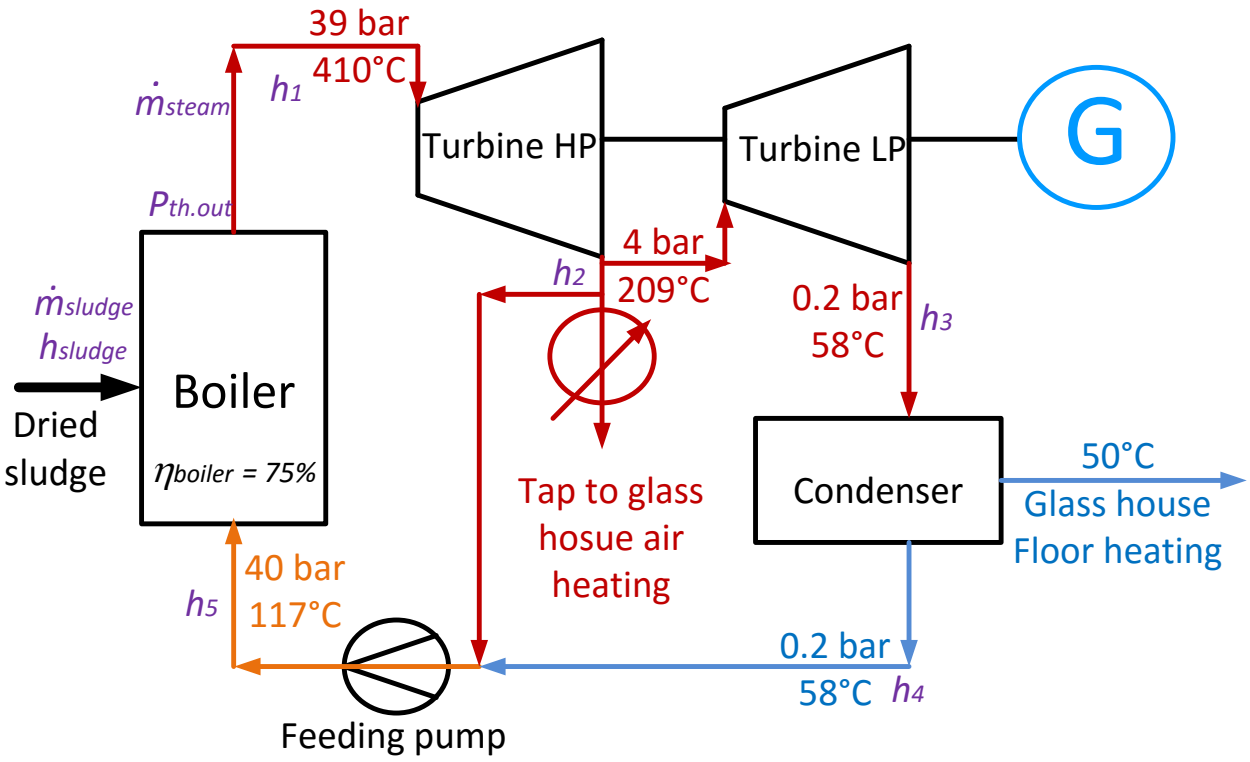

Figure 4.6: Scheme of steam turbine model with steam tapping

For assumed stoichiometric combustion the thermal output of the boiler can be calculated from the properties of dried sludge input as

$$P_{th.in} = \dot{m}_{sludge} \cdot h_{sludge}$$
$$P_{th.out} = \eta_{boiler} \cdot P_{th.in} \quad (4.1)$$

where

$P_{th.in}$ is the heat input power of boiler (kW_{th});

$\dot{m}_{sludge}$ is the mass stream of sludge to boiler for incineration (kg/h);

h_{sludge} is the heating value of sludge (MJ/kg) (1kW = 3.6 MJ/h);

$P_{th.out}$ is the thermal output power of boiler (kW_{th});

η_{boiler} is the efficiency of boiler (%).

With boiler input and output water/steam properties as given set points the mass flow of the working fluid is calculated:

$$\dot{m}_{steam} = \frac{P_{th.out}}{\left[h_{steam}(p_{\max}, T_{\max}) - h_{lH2O}(p_{\min}, T_{\min})\right]} \tag{4.2}$$

where

$\dot{m}_{steam}$ is the mass stream of steam after over-heating (kg/h);

$P_{th.out}$ is the thermal output power of boiler (kJ/h);

p_{max} is the maximum pressure at outlet of boiler (bar);

T_{max} is the maximum steam temperature at outlet of boiler (°C);

T_{min} is the temperature at inlet of boiler (°C);

$h_{steam}(p_{max}, T_{max})$ is the enthalpy of steam at boiler outlet (kJ/kg);

$h_{lH2O}(p_{min}, T_{min})$ is the enthalpy of water at boiler inlet (kJ/kg).

The relevant enthalpies are calculated from given temperatures and pressures by a special program for thermodynamic properties [53] which was firmly integrated into the code of the model.

For the purpose of steam tapping (for feed water pre-heating as well as for covering lacking heat demand in the plant) the turbine was separated in two individual sections – see Figure 4.6 –, where in between a deliberate steam stream can be diverged. From the enthalpies at input and output the mechanical power of the turbine(-sections) is calculated:

$$P_{mech} = \dot{m}_{steam} \cdot (1 - Tap) \cdot \begin{bmatrix} h_{in}(p_{in}, T_{in}) - \{h_{out.steam}(p_{out}, T_{out}) \cdot X \\ + h_{out.liquid}(p_{out}, T_{out}) \cdot (1 - X)\} \end{bmatrix} \tag{4.3}$$

where

P_{mech} is the mechanical power of turbine;

$\dot{m}_{steam}$ is the mass stream of steam at turbine inlet (kg/h);

Tap is the relative share of tapped steam;

X is the relative steam fraction;

$h_{in/out.steam/liquid}(p_{in/out}, T_{in/out})$ is the enthalpy at turbine inlet/outlet of steam/liquid, respectively.

In case of steam tapping the steam flow in the second turbine section is decreased accordingly, thus reducing the mechanical power available.

The electric power output of the generator results from the mechanical power of both turbine sections (small mechanical losses are neglected here):

$$P_{el} = \eta_{gen} \cdot (P_{mech.1} + P_{mech.2}) \tag{4.4}$$

where

P_{el} is the electric power output of the generator (kW_{el});

η_{gen} is the efficiency of generator (%);

$P_{mech.1}$ is the mechanical power of turbine section 1 (kW);

$P_{mech.2}$ is the mechanical power of turbine section 2 (kW).

The thermal power transferred by the condenser (the steam fraction at turbine outlet can be set in the model) is

$$P_{out.th} = \dot{m}_{steam} \cdot (1 - Tap) \cdot \begin{bmatrix} \{h_{steam}(p_{\min.}, T_{\min.}) \cdot X + \\ + h_{liquid}(p_{\min.}, T_{\min.}) \cdot (1 - X)\} - \\ - h_{liquid}(p_{\min}, T_{\min}) \end{bmatrix} \tag{4.5}$$

where

$P_{out.th}$ is the heat power from condenser (kW_{th});

Tap is the ratio of tapped steam (%);

X is the steam fraction;

$\dot{m}_{steam} \cdot (1 - Tap)$ is the mass stream of steam at inlet of condenser (kg/h);

$h_{steam}(p_{min}, T_{min})$ is the enthalpy of steam fraction at condenser inlet (kJ/kg);

$h_{liquid}(p_{min}, T_{min})$ is the enthalpy of liquid fraction at condenser inlet, as well as the enthalpy of water at outlet of condenser (kJ/kg).

According to given set point, the feeding water of the boiler is preheated by adding tapped steam and then pressurized up to boiler pressure p_{max}, thus being regarded in equation (4.2).

In the model the flow losses of the system are generically considered by a given slight enthalpy reduction of the overheated steam between boiler outlet and turbine inlet.

4.2.8 Wind turbine model

The model is based on the steady-state power characteristics of the turbine. As the wind speed fluctuates, the output power $P_{Wind}(t)$ follows the variations of the wind speed with a cube function and is limited at rated power as indicated in equation (4.6).

$$P_{Wind}(t) = \begin{cases} 0 & if \quad v_t < v_c \\ 0.5 \cdot c_p \cdot \rho \cdot A \cdot v_t^3 & if \quad v_c \le v_t \le v_r \\ P_{rated} & if \quad v_r \le v_t \le v_f \\ 0 & if \quad v_t > v_f \end{cases} \tag{4.6}$$

where:

c_p is the performance coefficient of the turbine; a constant value of 0.48 was applied here [54];

ρ is air density (kg/m^3);

A is swept area of rotor (m^2);

v_t is wind speed (m/s);

v_c is cut in speed (m/s);

v_r is rated speed (m/s);

v_f is furling speed (m/s);

P_{rated} is rated power (kW).

The typical behavior of a wind turbine as described by equation (4.6) is shown in Figure 4.7 as an example [55].

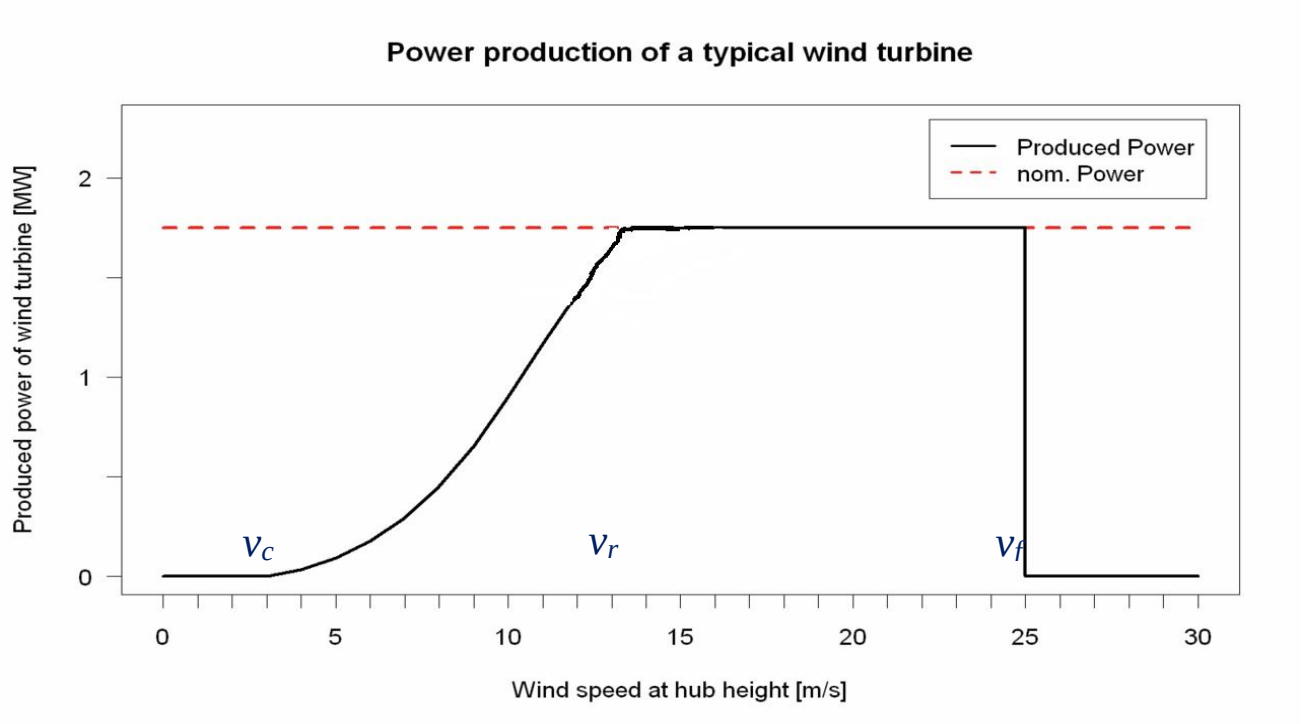

Figure 4.7: Output power of wind turbine (reworked from [55])

4.2.8 Photovoltaic plant model

The photovoltaic plant model is relatively simple and considers the solar irradiation (according to a given profile), the surface area, and an efficiency which at the same time can comprise that of the inverter (typically 14 … 15 % in total), see Figure 4.8.

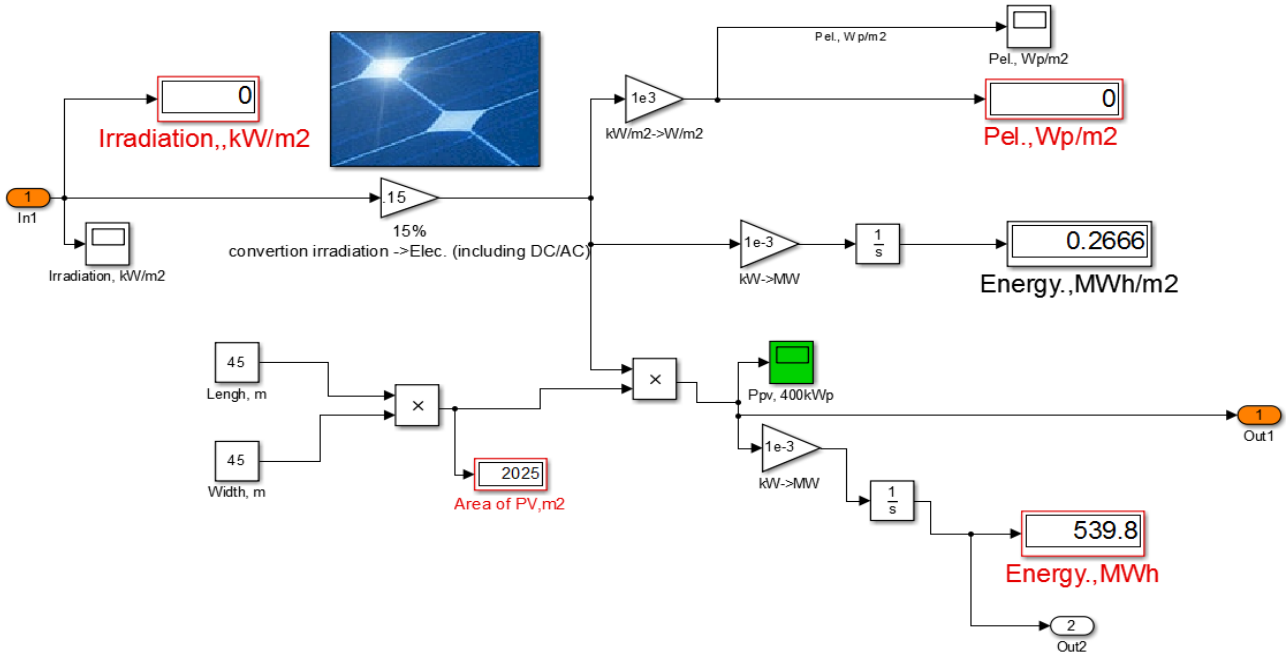

Figure 4.8: Simple Simulink® model for photovoltaic plant

4.2.9 Model of electrolyzer and hydrogen storage tank

According to section 3.4.1, a hydrogen path appears as an appropriate way for mid-term indirect electricity storage. The mentioned high pressure electrolyzer was modeled by efficiency factors of both the electrolyzer itself as well as of the inverter providing DC as electrolyzer input. The output hydrogen stream (still in terms of a power flow) is integrated over time, thus representing the storage tank. Upper and lower filling levels of the tank are given as limitations. For practical reasons (lifetime expectancy) the electrolyzer is operated in certain steps (related to nominal power) for a minimum period of time. This has to be considered in the strategy of plant operation, see section 5.4. The re-conversion of hydrogen to electricity is done at need by additive hydrogen fueling of the biogas driven CHP unit – see section 4.2.4 – up to a maximal share of 15%.

4.2.10 Models of heat exchangers and thermal storage

Heat exchangers are simply modeled by a given efficiency between the power of primary and secondary circuits.

Also for heat storage a simple model was chosen: An integrator with given upper and lower limits; thermal losses are neglected in this case.

4.2.11 Model of public grid

The public grid is electrically considered as an infinite bus. However, for later economic optimization of the plant, individual in-feed and supply tariffs can be assigned.

4.2.12 Control system

For proper situation dependent operation of the plant a certain control strategy is required. The implemented system will be discussed in the subsequent chapter 5 together with the complete plant model.

Furthermore, for operators' interaction a clearly arranged human-machine interface is needed. In chapter 6 a relevant approach is proposed. This can be used for realistic control of the plant simulation model, but it will also be sketched how this operational surface could be connected to a real plant process.

5. Simulation of plant operation

5.1 Modeling the complete plant

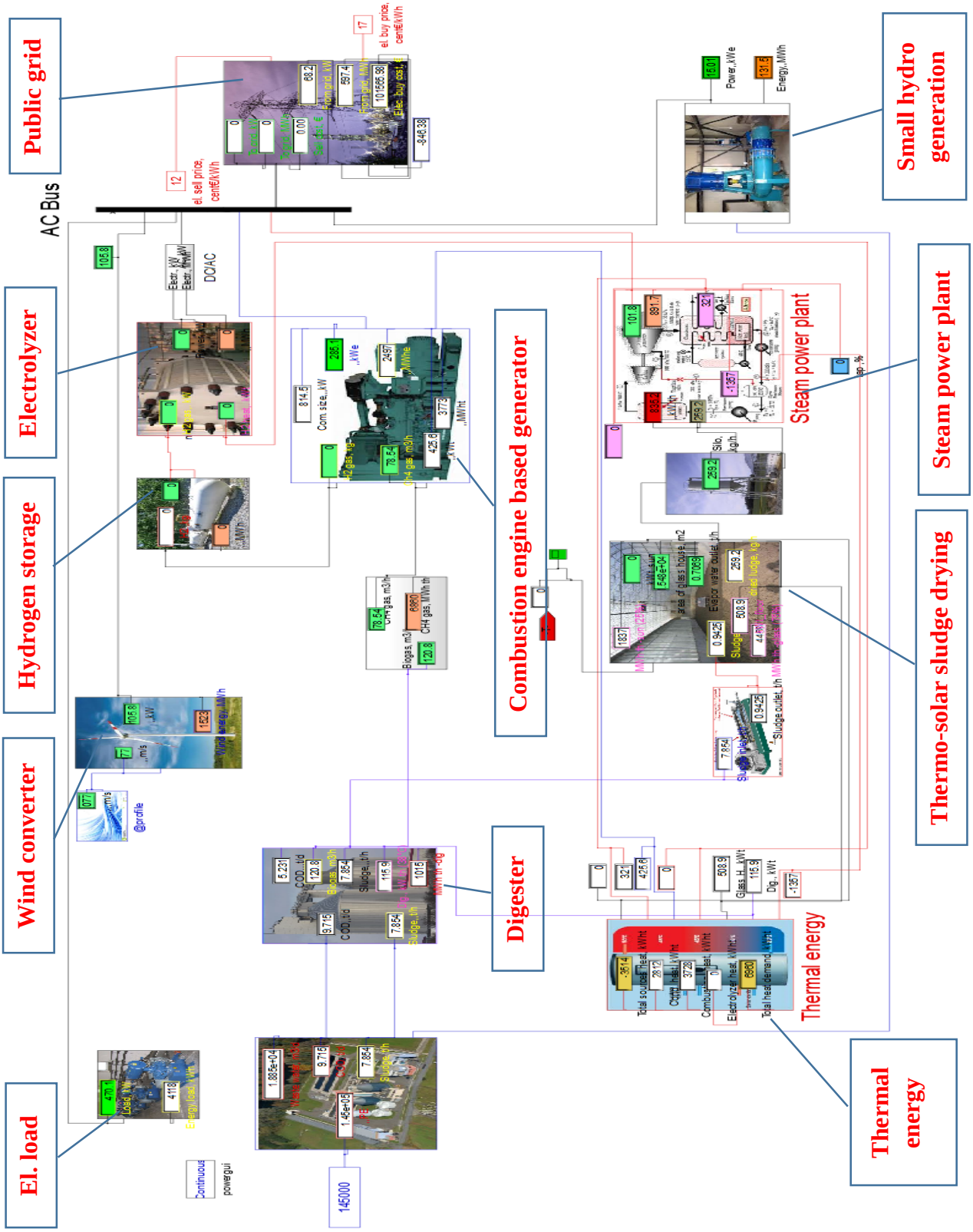

Figure 5.1: Survey of MATLAB/Simulink® structure of plant model

Composition of the relevant component models as particularly described in chapter 4 results in the complete plant model which was also implemented in MATLAB, see rough survey in Figure 5.1. The model is designed to run in hourly steps which allows for simulating longer periods of time (for instance one complete year) after input of relevant time-variant profiles such as solar irradiation, wind speed or ambient temperature; an example is shown in Figure 5.2.

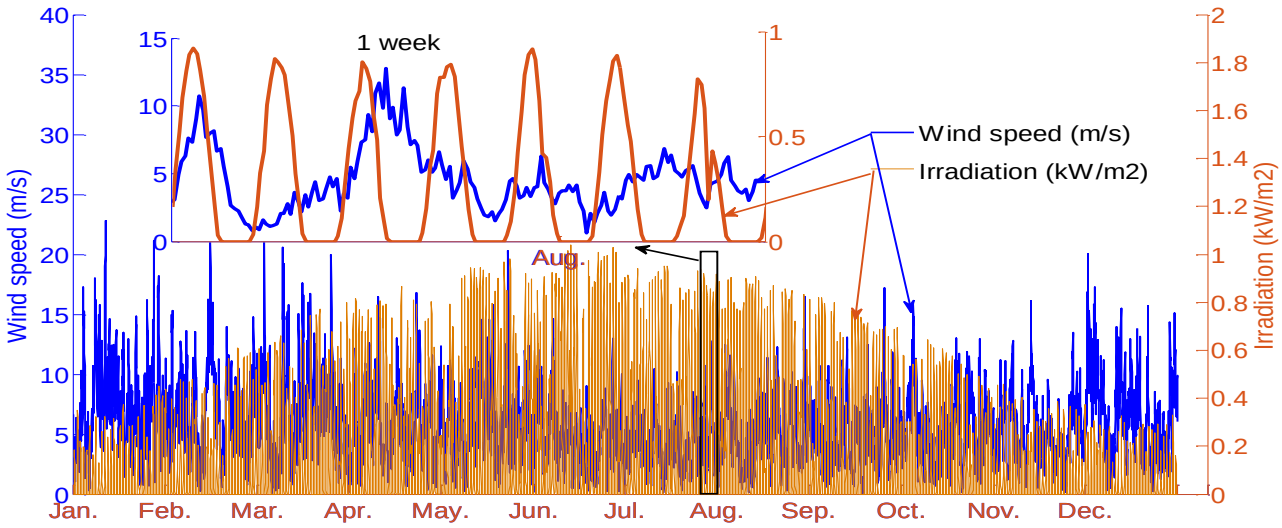

Figure 5.2: Annual profiles of wind speed and solar irradiation for simulation (example)

5.2 Central electricity node

All electric sources and loads, as well as the public grid, are connected by a central node nominated "AC Bus" in Figure 5.1 Here for each time step (1 hour) the actual balance of electrical power is made – which can be visualized on the operation surface as shown in chapter 6. Based on this, power balance situation-dependent control commands (for instance for activating the electrolyzer in case of actual and expected generation surplus and other decisions) can be derived, see below in this chapter.

5.3 Heat node

In similar way for each time step of simulation the heat balance is made in a central thermal node; however, in this case the individual temperature levels have to be regarded, which would require a more complex heat management system for a real plant. Table 5.1 gives a survey of temperature levels of thermal components. In the considerations done in this work, for the heat balance it was

ensured that heat flows realistically are only from higher to lower temperature levels; in practice this could be achieved by mixing of fluids and/or appropriate design of heat exchangers.

Table 5.1: Temperature levels of thermal components

	Medium	Inlet temperature	Outlet temperature
CHP	Cooling water	72…75°C	91°C
	Exhaust gas	-	550°C
Steam turbine	Intermediate steam tapping	-	208°C
	Cooling water condenser	35°C	50°C
Digester	Sludge	Ambient temperature	37.5°C

5.4 Operation control

5.4.1 Introduction

As mentioned above, relevant and meaningful operation decisions for activating or deactivating certain devices (in particular the electrolyzer in this work) or assigning power set points have to be derived from the actual operational status of the plant. In order to allow long-term simulations (e.g., over one full year) which also have to consider such operational decisions, an “intelligent” control system had to be developed and implemented running together with the simulation model.

For setting up such kind of control system, the following circumstances have to be considered:

- The dependencies where operational decisions can be based on are only roughly known and can be formulated as (if … then …) rules.
- The exact values to trigger the particular rules are not exactly known but can be derived from sample data.

5.4.2 ANFIS

For circumstances as described above so called Adaptive Neuro-Fuzzy Inference Systems (ANFIS) have proven useful [56], and such approach was also adopted here. The advantage of ANFIS is that the process behavior can be trained to a neural network from sample data which, of course, must be available before, and is then internally transposed to a fuzzy system. This fuzzy system – or more precisely, its rule base – can be interpreted by the user, and in this way it is possible to obtain a comprehensible description of the process control behavior or, with other words, a controller with an easily interpretable performance.

5.4.3 Approach adopted in this work

More concretely, in the control of electricity flows of the plant considered in this work the electrolyzer plays a predominant role when there is electrical power surplus in the system. The reason is that by operation of this device the distribution of surplus power to storage (via controlled conversion to hydrogen) respectively to the public grid (the rest of surplus power) is decided; on the other hand, the electrolyzer is assumed to be only allowed to operate in certain steps (in the work here 0, 25, 50, 75 or 100% of nominal power) for at least 1 hour in order to increase lifetime expectancy. Thus, electrolyzer control was implemented as an ANFIS which is available as a MATLAB tool [57]. However, here the question arises where from to take the training data (see section 5.4.2). This was solved as follows:

In chapter 7 the optimal sizing of the components will be shown, based on a meta-heuristic approach which makes use of a full-year hourly simulation of the complete plant and then derives the rating of components; as side-effect this optimization includes optimal annual plant operation data for the considered year, which also concerns optimal electrolyzer operation. Since the operational power steps of the electrolyzer were considered in the optimization, too (see chapter 7), this optimized behavior of the entire plant for the specific year was used as training data of the implemented ANFIS for electrolyzer control presented here. Of course, this proceeding must be applied individually for a given plant, see examples in chapter 8.

The electrolyzer control principally has to regard

- the amount of actual electrical power surplus;
- the distribution of this surplus to hydrogen storage (electrolyzer power set point) and grid (rest);
- the admitted power steps of electrolyzer operation (0, 25%, 50% 75%, 100% of nominal power);
- the actual power import from grid, whereby the total annual energy import was limited to 5% of total yearly load demand; besides covering periods of actual power deficit, the import power from grid sub-serves to replenishing the electrolyzer power to certain set point steps as described above;
- the actual hydrogen storage filling level;

Thus, these signals respectively those signals comprising this data have to be chosen as input of the controller; output is the electrolyzer power set point in mentioned power steps. As training data of the ANFIS the following signals were used from the annual optimization, each as hourly values for one year (8760 h):

- power exchange with grid (input 1, Figure 5.3 a); only positive values (export) considered;
- power surplus sent to electrolyzer, diminished by the import power from the public grid (input 2, Figure 5.3 b);
- hydrogen storage filling level (input 3, Figure 5.3 c);
- power set point of electrolyzer (output, Figure 5.3 d).

For easier understanding of the annual curves particularly shown in Figures 5.3 a) and b), Figure 5.3 e) depicts an excerpt of power curves of involved components within one week as an example. Thus, curve 5.3 a) is the sum of curves “compensation from grid to electrolyzer” and “power exchange with grid” in Figure 5.3 e). Curve 5.3 b) is the actual power to the electrolyzer (following the mentioned power steps), diminished by the “compensation from grid to electrolyzer” in Figure 5.3 e).

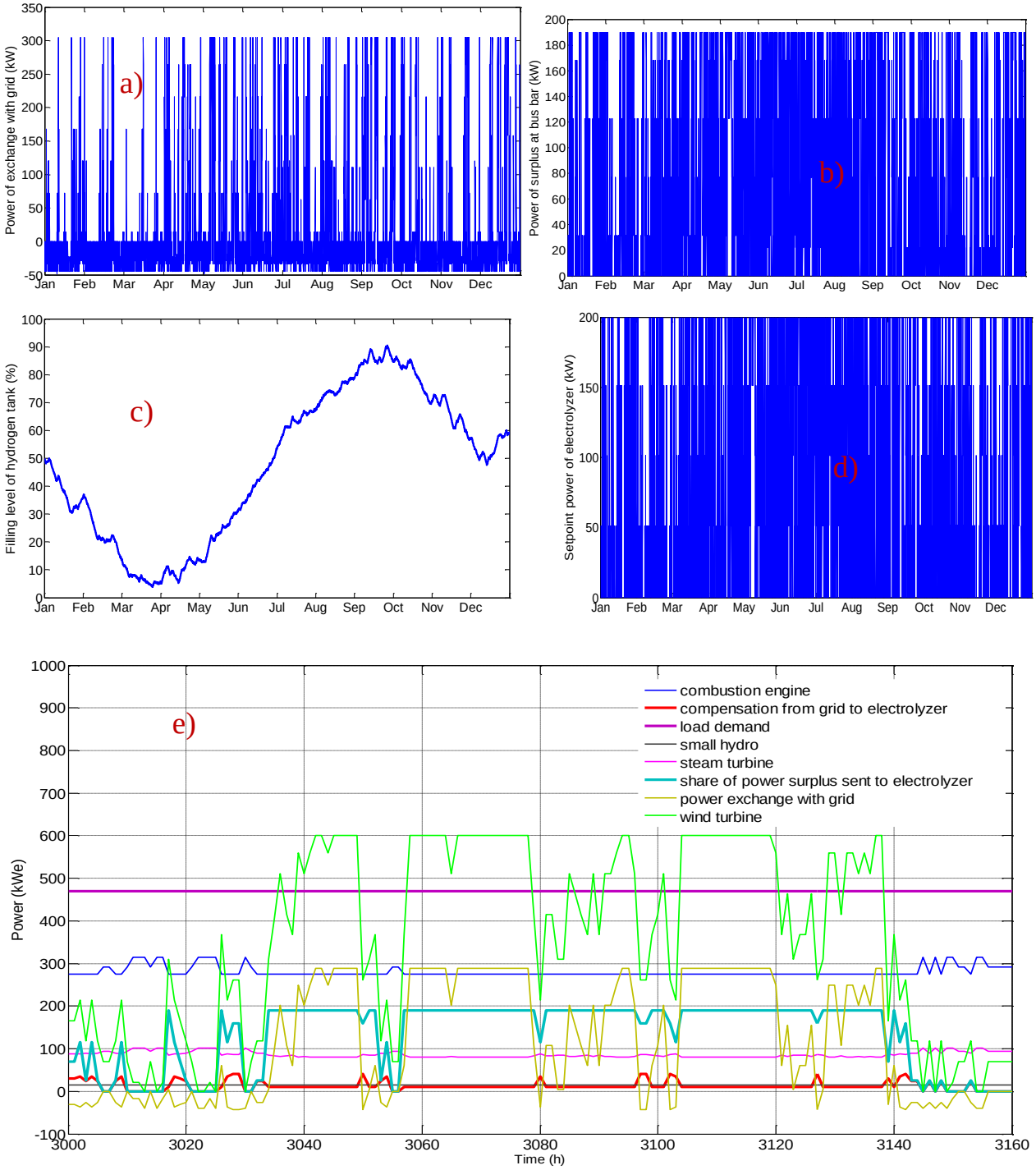

Figure 5.3: Training data for ANFIS taken from optimization (chapter 7):

a) Power exchange with grid (positive values are input 1, see text);

b) Share of power surplus sent to electrolyzer (input 2, see text);

c) Filling level of hydrogen storage (input 3);

d) Power set point of electrolyzer (output);

e) Power of components (excerpt of one week as example).

The sum of both positive values of input 1 and input 2 is, of course, the total actual surplus power, but in this separated form they also contain the information of optimal distribution between electrolyzer and grid from the optimization for each hourly time step, which should also be trained. Consequently, the ANFIS internal neural network has 3 input nodes and one output node, see Figure 5.4. The resulting matrix of 3 inputs + 1 output and 8760 hourly steps (4 · 8760) was given to the ANFIS for training as pointed out later.

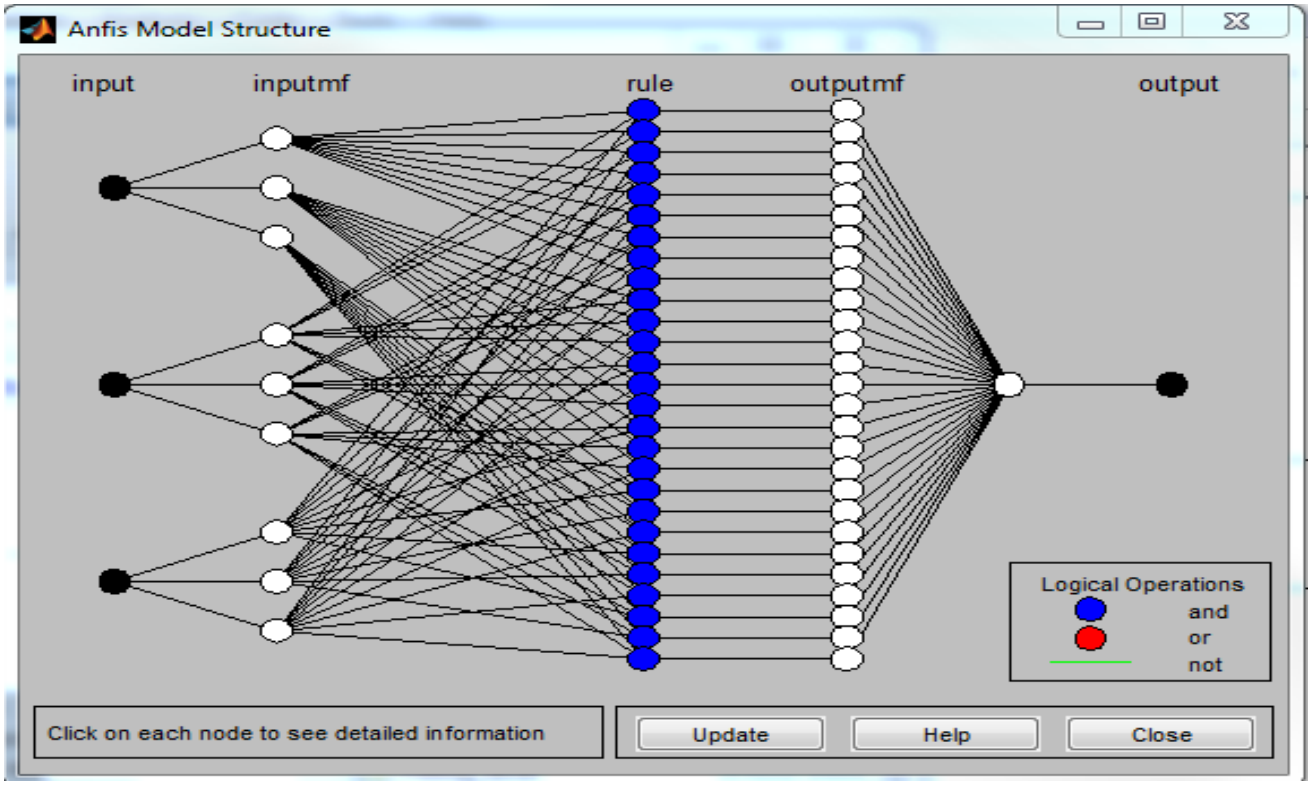

Figure 5.4: ANFIS model structure with 5 layers in MATLAB®

For the assignment to membership functions of the fuzzy system included in MATLAB each of the 3 inputs can be member of the variables “high” / “medium” / “low” which results in (3·3) = 9 nodes of the second layer “inputmf” as shown in Figure 5.4. Combinatorial interrelation of node outputs of the second layer leads to (3·3·3) = 27 rules, the layer of which is marked accordingly in Figure 5.4. The rules themselves can be visualized, checked or altered within a control window as depicted in Figure 5.5. The 27 conclusions of rules (“outputmf” in Figure 5.4) are again membership functions and thus have to be de-fuzzified to the concrete set point values 0, 25, 50, 75, 100% of electrolyzer nominal power) as output.

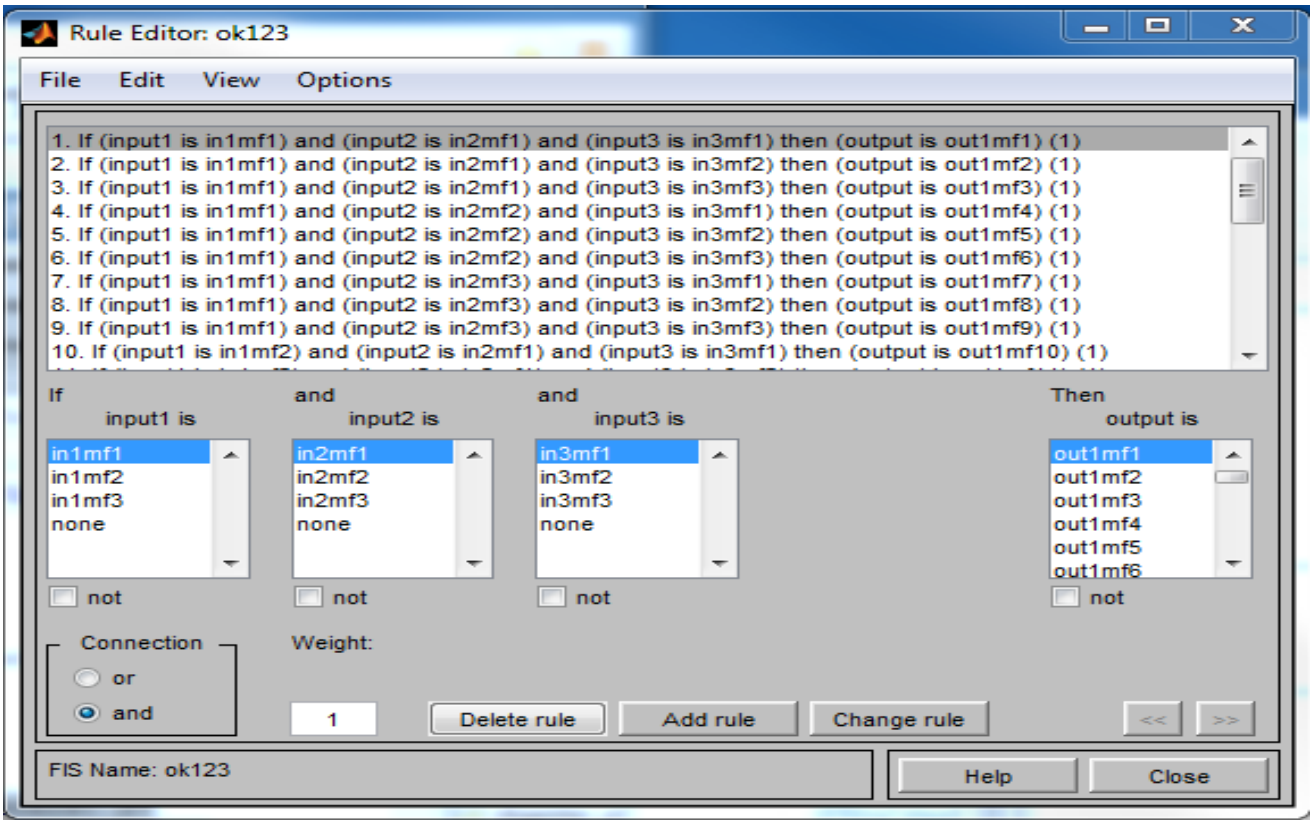

Figure 5.5: Control and test window for the rules in MATLAB® ANFIS tool

In order to set up the system, the matrix given by annual hourly values of in/outputs from the optimization (as described above) is fed to the ANFIS for training; this process running iteratively in “epochs” can be observed in a control window as shown in Figure 5.6. For the given problem in both example cases (see chapter 8) the complete training process lasted about 1 hour. Table 5.2 contains ANFIS parameters used in this work.

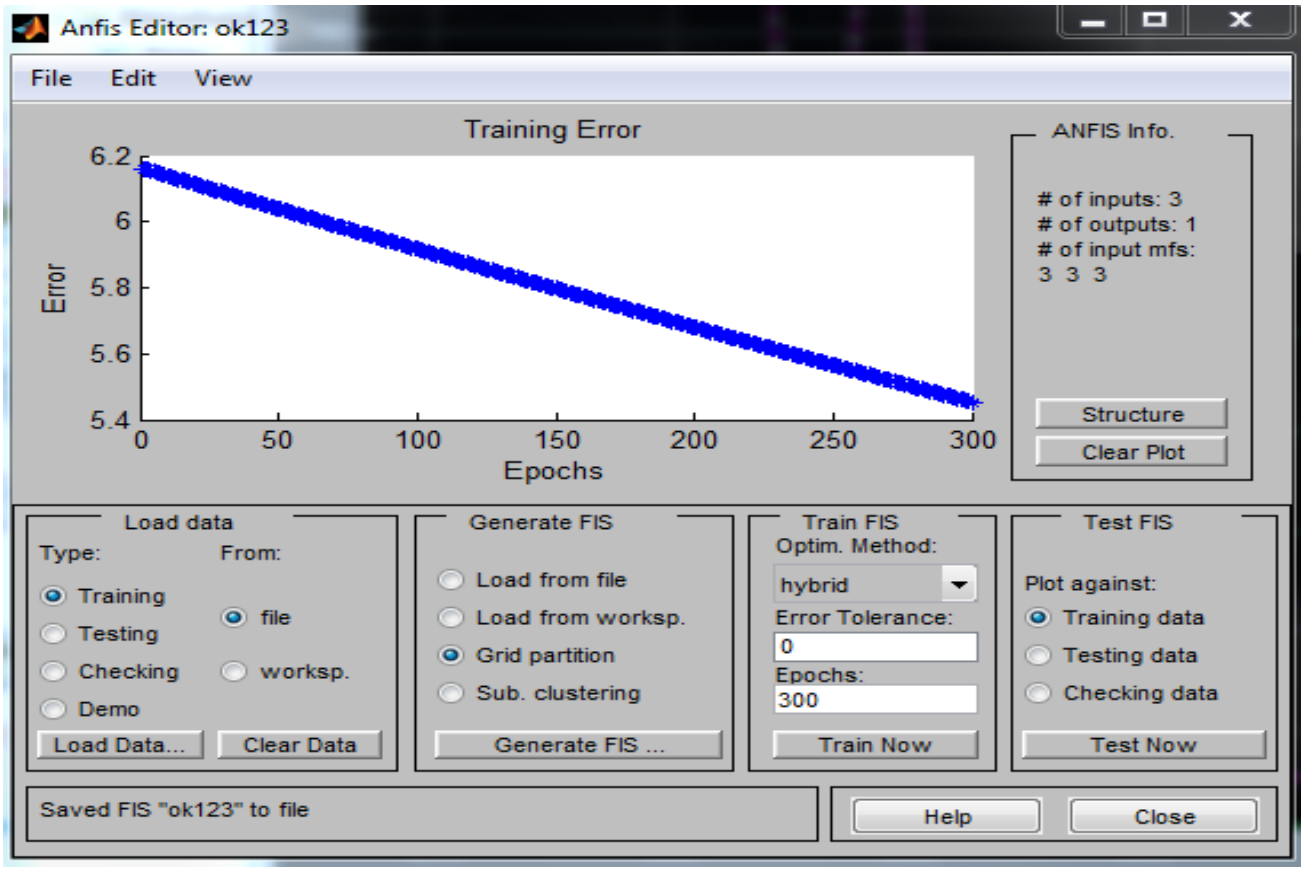

Figure 5.6: Observation of training in ANFIS (MATLAB® tool)

Table 5.2: ANFIS parameters

Parameter of ANFIS	Values
Number of nodes	78
Number of linear parameters	27
Number of nonlinear parameters	36
Number of training data pairs	8761
Total number of parameters	63
Number of checking data pairs	0
Number of fuzzy rules	27

After completion of training, from the ANFIS toolbox a file can be exported to be used in MATLAB/Simulink simulation; in the present case it is the adapted controller for electrolyzer operation. In Figure 5.7 it can be seen that, in comparison with conventional control, ANFIS control

is rather smooth, draws less electricity from the grid for short time, and reduces electrolyzer operation cycles, thus extending electrolyzer lifetime.

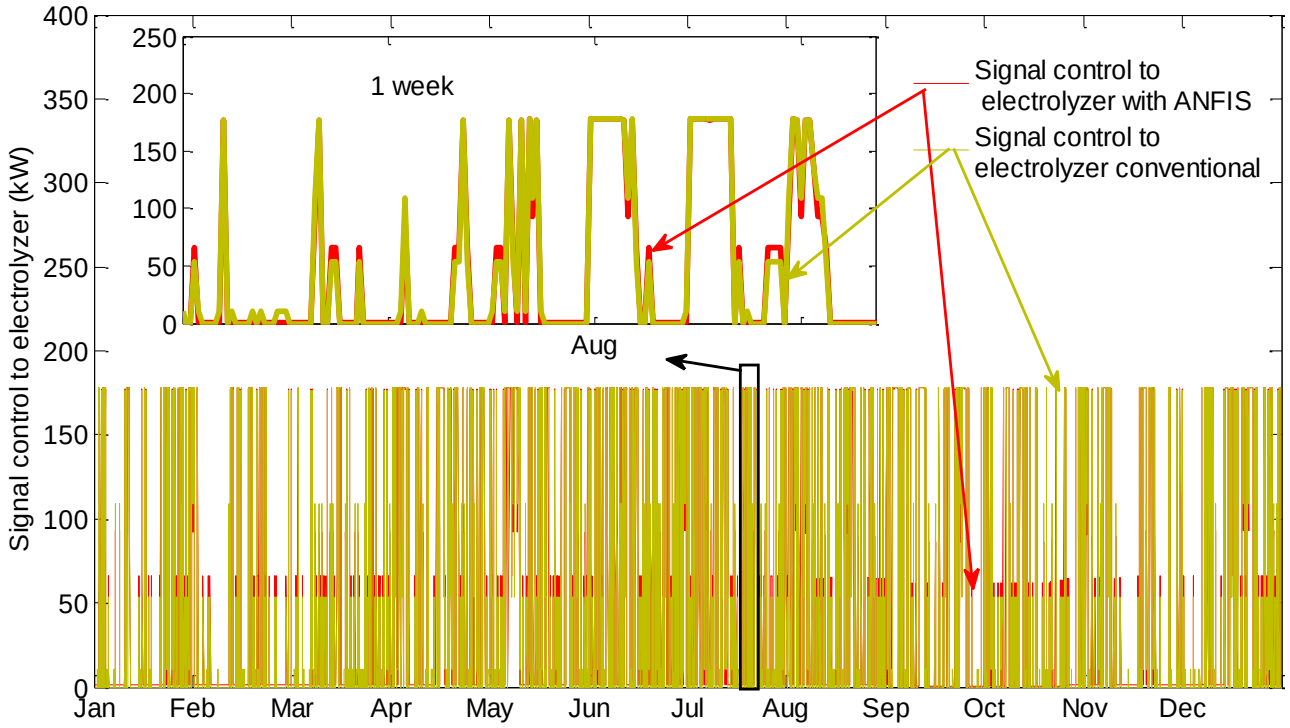

Figure 5.7: Comparison of results ANFIS / conventional control

6. OPERATIONAL SURFACE

6.1 Introduction

Operation of a technical plant requires a subsystem which provides a clear and well-arranged indication and/or visualization of the current plant status by using direct and/or prepared process information, as well as allowing for human interventions to the current process. Therefore, a realistic operational surface was created which – by coupling with the plant simulation as described in the previous chapter 5 – enables to "operate" the simulation model like a real plant in either real time or preferentially – for destined studies over longer time periods – in accelerated temporal mode. After giving a survey of the functionality of the implemented approach, in the following it will also be sketched how this solution could be applied to real plant control when indicated.

6.2 Process variables

Relevant external and internal data of the energetic parts of the plant to be supervised are for instance

- meteorological information such as ambient temperature, wind speed, solar irradiation;
- mass streams of sewage, sludge, cleaned water etcetera (for the simulations in this work assumed constant);
- balances of electricity and heat;
- flows of el. power and heat between plant components and central nodes;
- actual set points of components (e.g., electrolyzer or steam tapping);
- detail process information of partial systems (for instance steam power unit or CHP plant);
- filling levels of storages;
- actual values such as temperature or humidity in glass house;
- metering values as, for instance, total energy from/to public grid.

6.3 Operational windows and data handling

Various individually customized control windows were created. As an example, in Figure 6.1a) the indication of actual power values of components is depicted; the panel for input of set points to components such as electrolyzer or steam tapping valve is shown in Figure 6.1b) as another example. In similar way more detailed windows for, e.g., observation and control of particular plant components such as the steam power plant, the CHP unit or the electrolyzer could be displayed,

too. Since internally the data are stored in a buffer (archive) it is also possible to analyze the plant behavior retrospectively – see Figure 6.2a – or to derive trends from historical data as shown in Figure 6.2b and Figure 6.1b at the bottom.

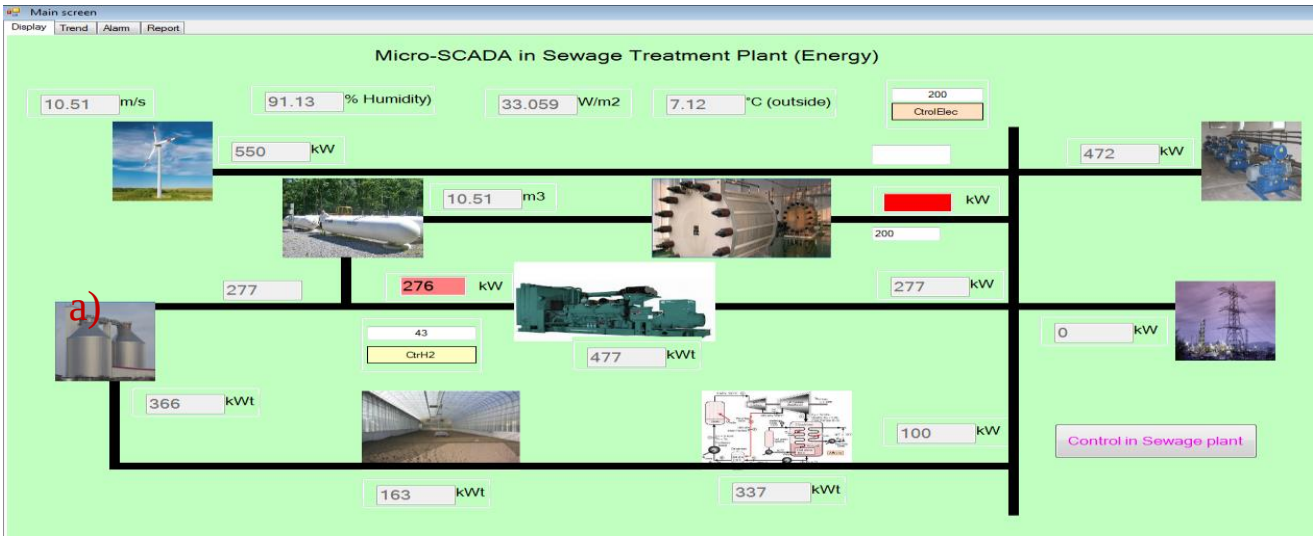

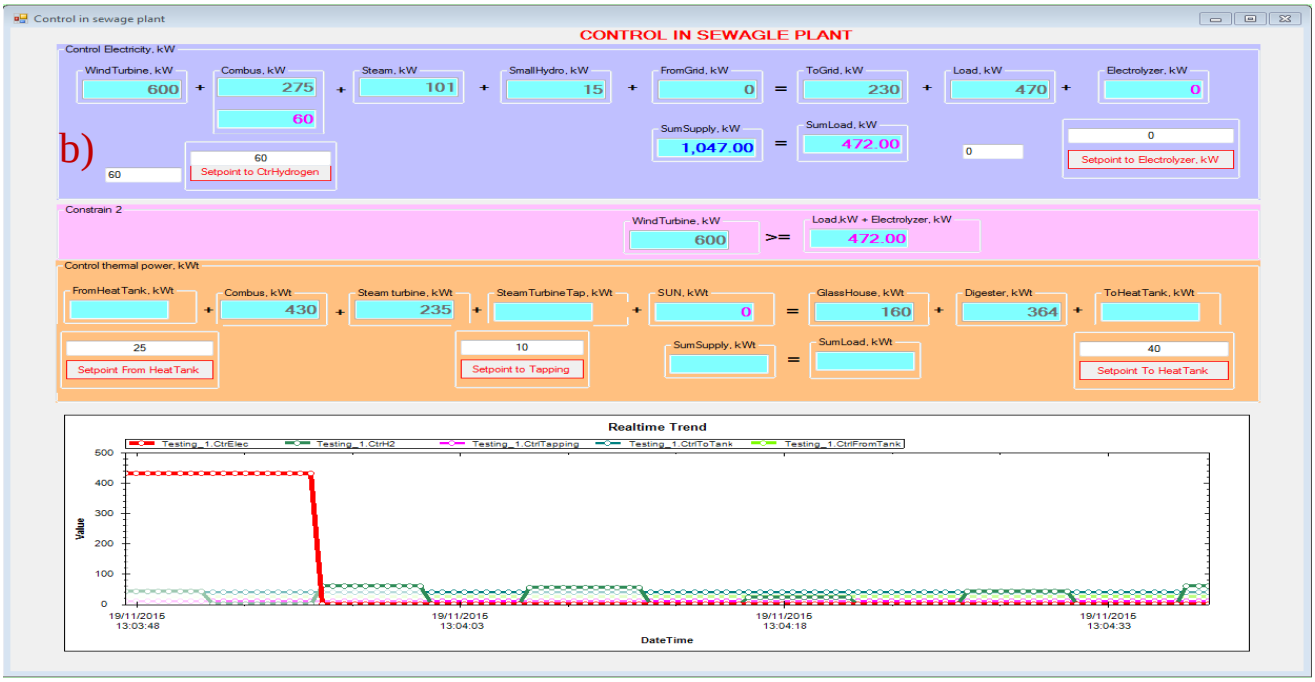

Figure 6.1: Examples of operation surface (I):

a) Indication of actual power of components

b) Panel for control input

Figure 6.2: Examples of operation surface (II):

a) Charts of historical data

b) Trend analysis

The operational displays were all programmed in visual C# using the Integration Development Environment (IDE) tool of Microsoft Visual Studio 2013 [58] as shown in Figure 6.3. This software has also the ability to communicate with OPC (OLE Processing Control), see below.

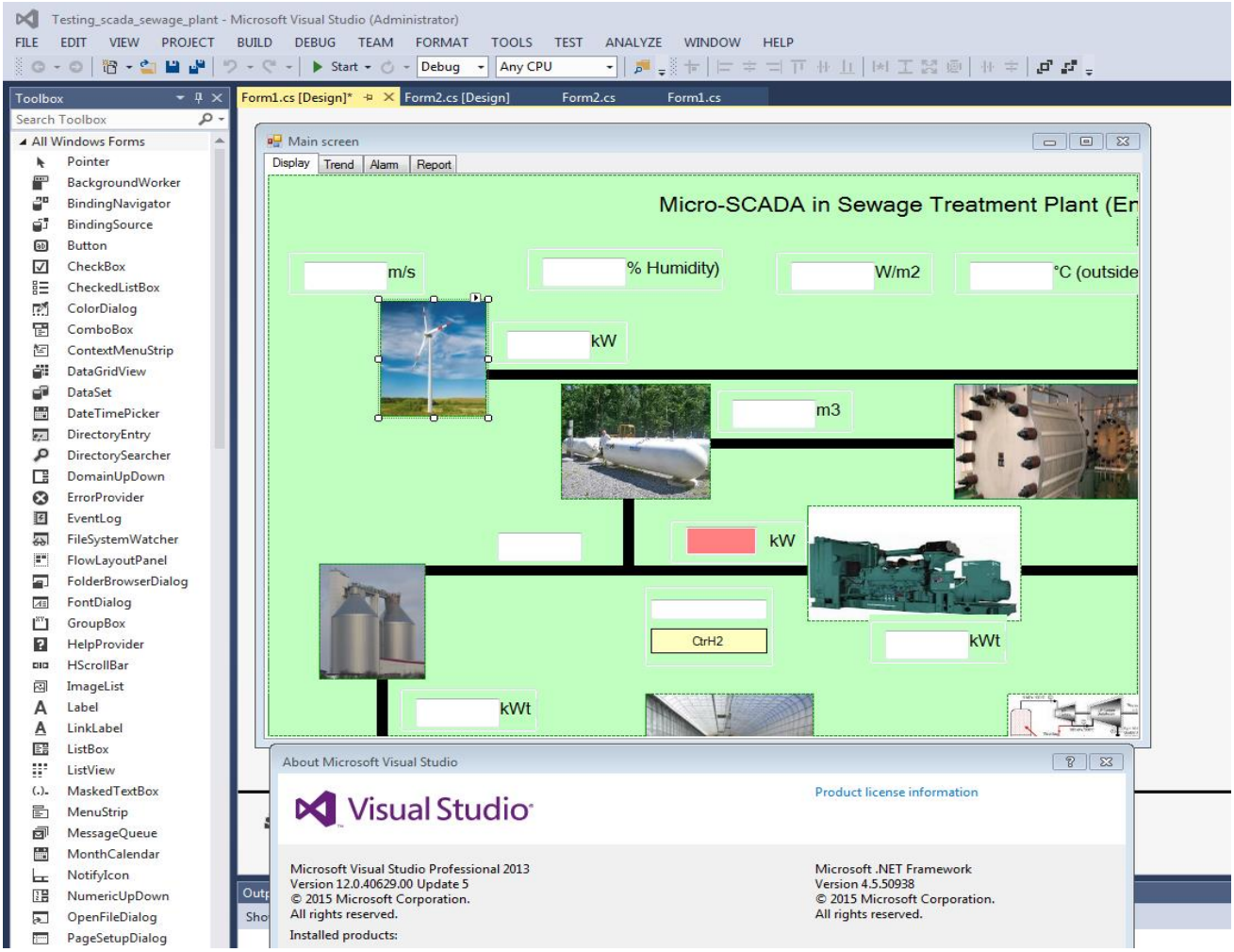

Figure 6.3: IDE (Integration Development Environment) tool of Microsoft Visual Studio 2013

The refresh rate of the displays can be adapted to the actual temporal simulation resolution; in this work this was chosen uniquely at 1 h in order to allow for long term studies, see chapter 8; for real plant control – see below – considerably shorter rates of, e.g., 1 minute or even few seconds are possible, too.

As communication platform between the MATLAB plant simulation and the operational surface via file transfer, the KEPServerEx software [59] is being used, see Figure 6.4; a full functional demo-version (only limited in run time at 2 hours) is freely available on the internet. KEPServerEx is based on "Open Platform Communications" (OPC), an interoperability standard in automation industry [60], as well as on customary communication protocols. Especially these features would also allow for easy adaption of the developed operational surface to control a real plant.

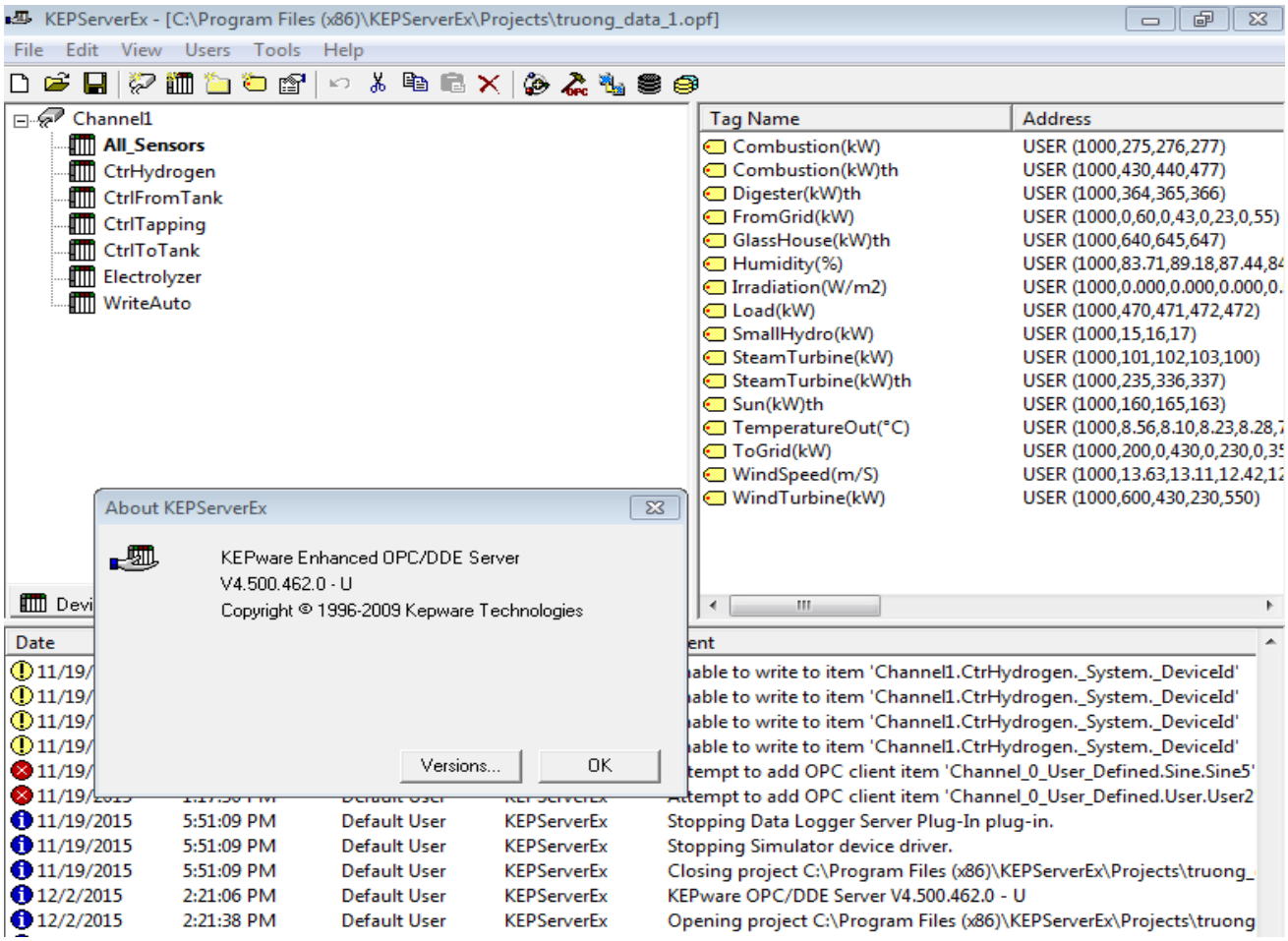

Figure 6.4: OPC interface *KEPServerEx* [59]

6.4 Real plant control

For control of a real plant, instead of being retrieved from the MATLAB based simulation, the current process data would be directly transferred between the relevant constituents of the plant and the control computer which also would host the operational surface, see light colored lines in Figure 6.5.

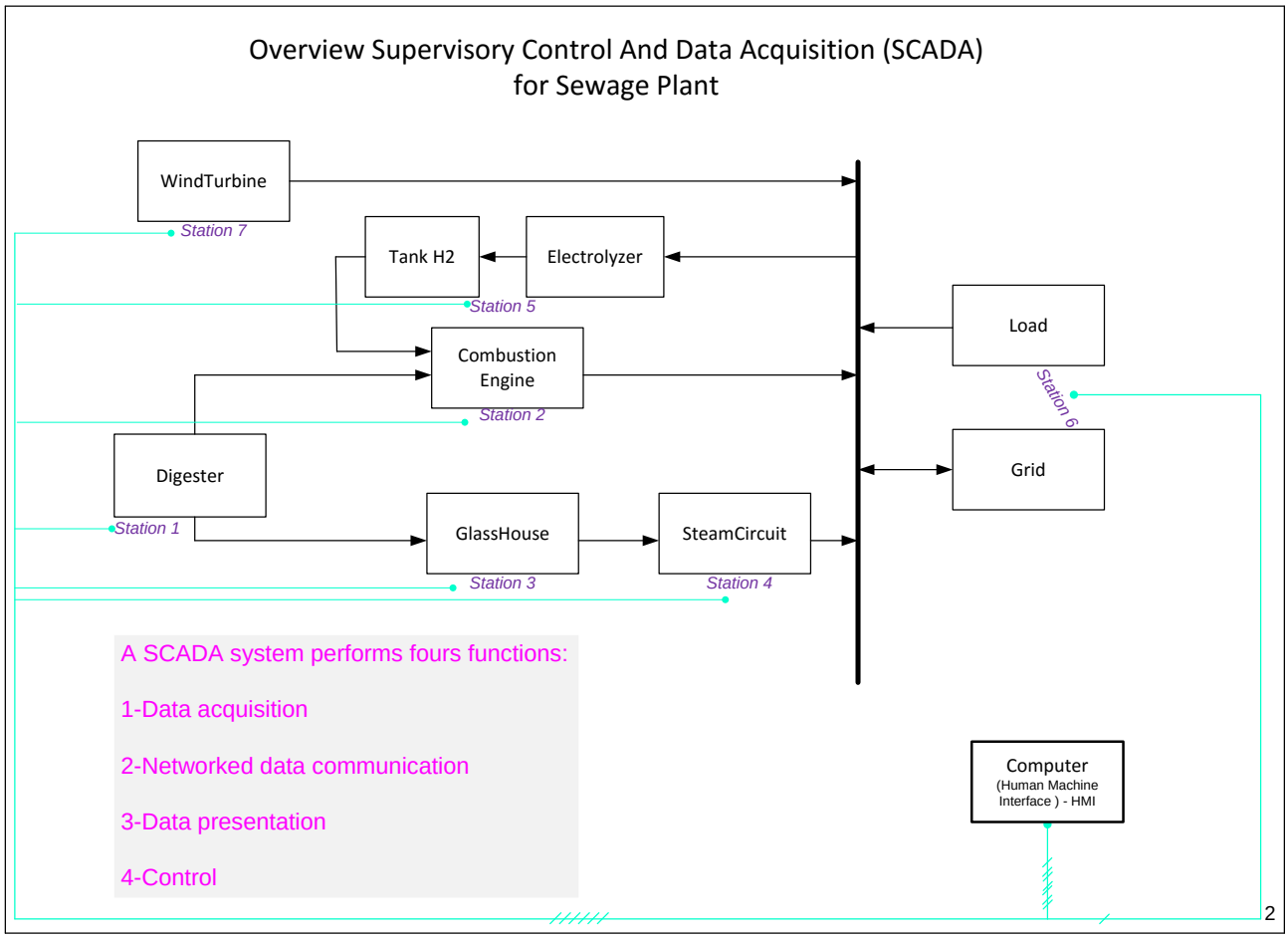

Figure 6.5: Overview supervisory control and data acquisition for sewage plant

Within the particular entities (“Stations”, see Figure 6.5) local control computer units would manage the distribution of information from/to sensors respectively actuators; while for more complex components such as the steam power unit this local instance is the dedicated process control system on site which has to be installed anyway, for less intricate components such as the glass house a simple micro-controller can be implemented which at the same time converts analog input data to digital signals, see Figure 6.6. Depending on the given distances within the plant, the data transmission can be realized via standard RS232/RS485 or TCP/IP connections.

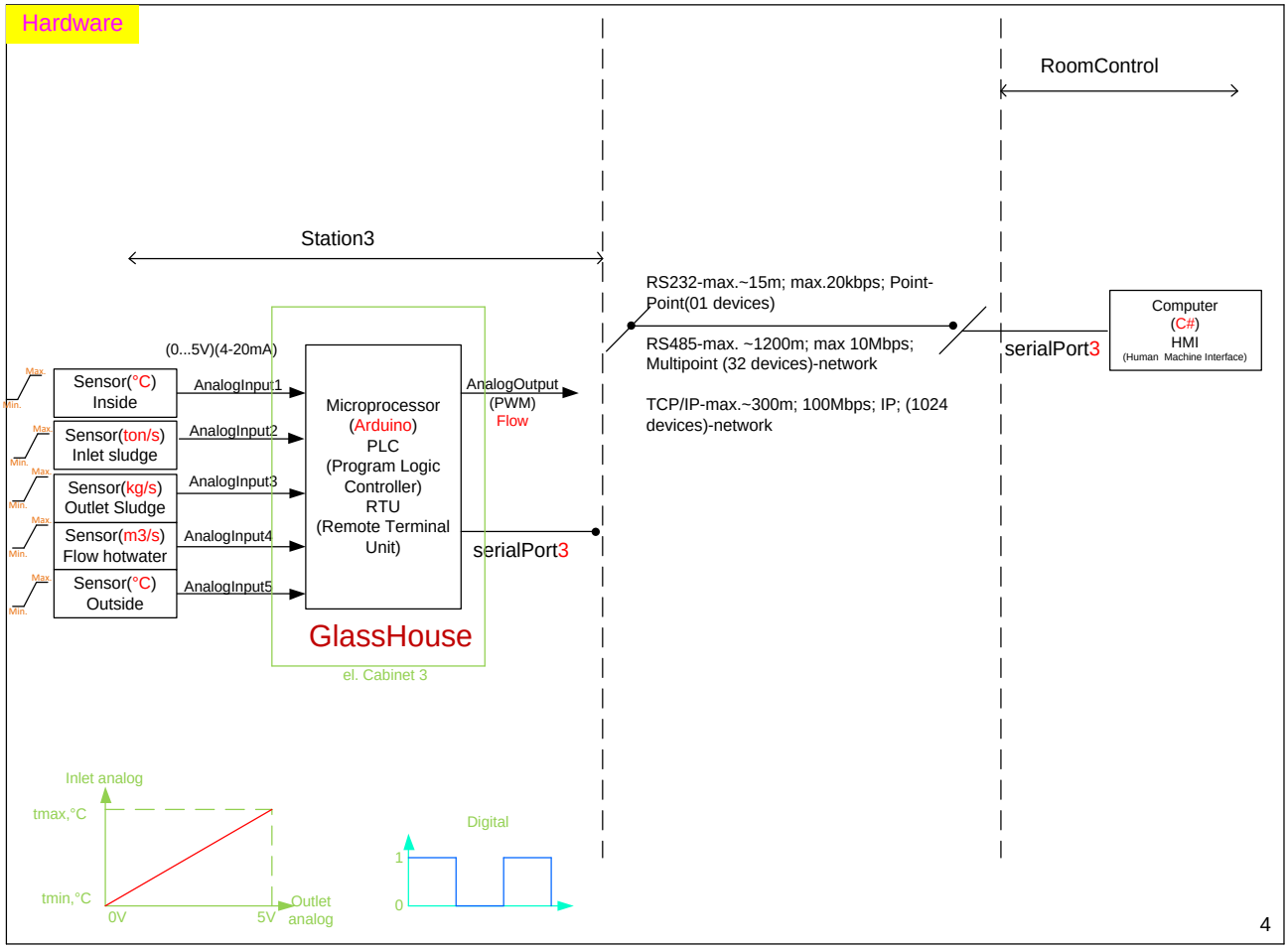

Figure 6.6: Local data treatment and transmission in real plant control for glass house (Station 3) as an example

7. Optimization of components aiming in energetic independency of plant

7.1 Introduction

In chapter 4 the principal design of the proposed plant was developed; from Figure 4.1 it is evident that some of the energetic components are determined in size by the sewage respectively sludge throughput, while other components – in particular the fluctuating renewable sources and energy storage paths – have to be rated individually according to the given local – mainly meteorological – conditions.

Thus, for constant wastewater/sludge streams – appropriately burnished by intermediate basin/silo storage – the base rating of

- combustion engine driven generator set (CHP unit),
- steam power unit,
- small hydro unit, as well as
- the size of the glass house for sludge drying

can be calculated directly. In contrast, because of the complexity of dependencies, the sizes of

- wind converter,
- photovoltaic modules,
- nominal power of the electrolyzer,
- hydrogen storage,
- additional capacity of combustion engine driven generator set for hydrogen re-conversion and
- capacity of el. feeder (mainly needed for short term balance, but to be provided for emergency supply in case of device failures anyway)

need extensive consideration, in particular under the aspect that cost optimal plant operation is desired.

Since the latter leads to a typical mixed-integer optimization problem, an appropriate algorithm has to be applied for the solution, together with simulative modeling of entire plant behavior over a longer period of time with given temporally varying quantities. In section 7.2 the meta-heuristic "Mean-Variance Mapping Optimization" (MVMO) will be briefly proposed as a sound approach.

As mentioned above, the optimization objective is cost minimization for electricity supply of the sewage plant. Thus, the cost of all components and their operation as well as given grid tariffs has to be considered. This will be outlined in section 7.3.

7.2 MVMO Optimization approach

Generally, for the solution of mixed-integer optimization problems meta-heuristic approaches such as genetic or evolutionary algorithm, particle swarm optimization and many other have proven to be advantageous because of their robustness and the feature not to be captured in local optima [61]. As another variant, in direct comparison with these approaches, the "Mean-Variance Mapping Optimization" (MVMO, detail information see [62]) has proven superior in performance at lower number of parameters to be preset [63]. Thus, this approach was adopted here.

After definition of the k optimization variables x_i ($i = 1 \ldots k$) – in the actual application the cost of particular plant devices – they are normalized within their upper and lower boundaries to a range [0 …1], and the objective function is evaluated iteratively until a termination criterion is satisfied, Figure 7.1. During the iteration those sets of variables ("populations") which fulfil the boundary conditions are successively stored in a list ordered according to their quality ("fitness") in meeting the optimization goal. For each subsequent iterative step, a new set of variables x_i is derived by use of a "mapping function" (see Figure 7.1) which introduces the randomness needed to extend the search space of the optimization, but at the same time accentuates the currently best solution (details of MVMO see [62]). These results of objective function evaluation are de-normalized to the original range – in the present application denoting the costs of particular plant devices. The convergence performance of MVMO can be exemplarily seen in Figure 8.5 for two practical examples with 250 respectively 400 object function evaluations. Appendix A7.1 contains some MVMO parameters used for the application in this work.

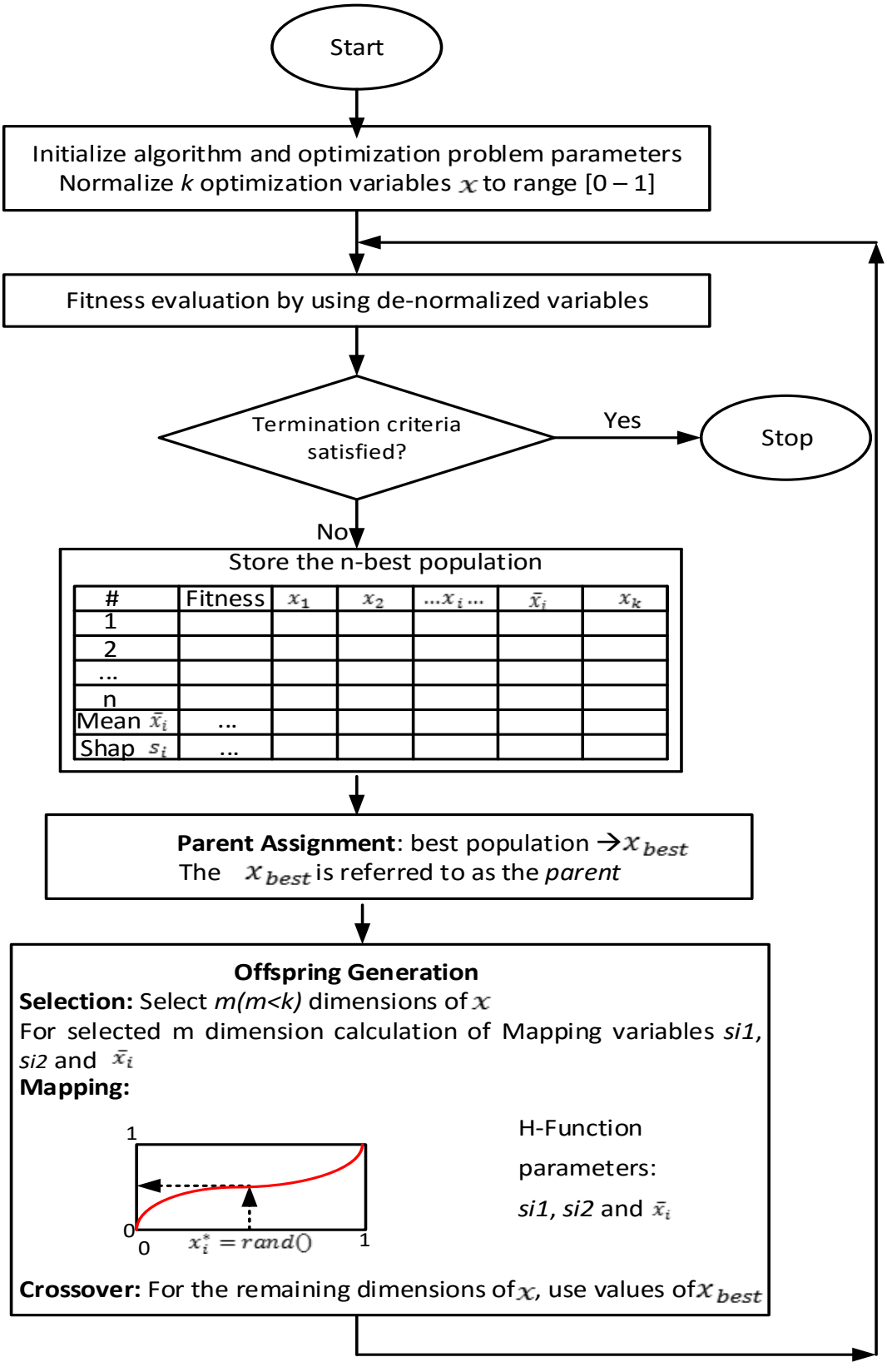

Figure 7. 1: Flowchart of the MVMO algorithm [64]

7.3 Objective function

Goal of optimization is the energy supply of a sewage plant widely based on local energy harvest – as discussed chapter 4 – at minimal cost over a calculated operation period of 20 years; this in particular means regard of

- the investment cost of all additional energetic components;
- the replacement cost of components with expected lifetime of less than 20 years, in particular the engine of the CHP unit, and
- the cost of energy exchange with the public grid.

Thus, besides the investment cost $\Sigma C_{constant}$ of those energetic components the rating of which can be calculated and fixed in advance based on given sewage/sludge throughput (see section 7.1), the objective function for minimization of total cost C_{total} contains as variables the cost Σx_i of renewables based sources, components of energy storage paths as well as and electricity grid exchange, actually indexed by 'i'. Owing to the technical nature of this thesis, which mainly focuses on energetic issues, the maintenance cost of the plant (servicing and personnel) as well as financing cost was not regarded in the optimization.

Objective function:

$$C_{total} = \sum C_{\text{Constant}} + \sum x_i \rightarrow \min \tag{7.1}$$

- $\Sigma C_{Constant}$: cost of all components having been rated before the optimization such as steam circuit, base power of CHP unit, glass house etcetera; typical values used for the optimization can be found later in Table 8.3 for example cases.
- For power sources: $x_i = C_i \cdot N_i \rightarrow N_i = \frac{x_i}{C_i}$

  where C_i: device cost per kW;

  N_i : rated power of source in kW.
- For energy storage: $x_i = C_i \cdot E_i \rightarrow E_i = \frac{x_i}{C_i}$

  Determination of storage size:

$$E_i = \{\max[\int \eta_{iIn} \cdot P_{iIn}(t) - \frac{1}{\eta_{iOut}} \cdot P_{iOut}(t)]dt - \min[\int \eta_{iIn} \cdot P_{iIn}(t) - \frac{1}{\eta_{iOut}} \cdot P_{iOut}(t)]dt\}$$

where C_i : storage cost per kWh;

E_i : rated energy capacity of storage in kWh;

$P_{iIn/Out}$: power to/from storage in kW;

$\eta_{iIn/Out}$: conversion efficiency into/from storage.

- For grid exchange:

$$x_i = C_{Grid} \cdot N_{Grid} + C_{EnergyFromGrid} \cdot \int P_{FromGrid}(t)dt - C_{EnergyToGrid} \cdot \int P_{ToGrid}(t)dt$$
$$\rightarrow N_{Grid} = \frac{x_i - C_{EnergyFromGrid} \cdot \int P_{FromGrid}(t)dt - C_{EnergyToGrid} \cdot \int P_{ToGrid}(t)dt}{C_{Grid}}$$

where C_{Grid} : cost of feeder capacity per kW;

N_{Grid} : rated feeder capacity in kW;

$C_{EnergyFrom/ToGrid}$: cost of electricity import/export per kWh;

$P_{From/ToGrid}$: grid exchange power in kW.

For the objective function equation (7.1) the following subjections have to be considered:

1. El. power balance at any hourly time interval:

$$\sum P_{elGenerated}(t) \geq P_{Load}(t) + P_{elToStorage}(t) + P_{ToGrid}(t) \qquad (7.2)$$

where $P_{elGenerated}$: sum of generated el. power from all existing sources including import from public grid (varying);

P_{Load} : electric load (assumed constant);

$P_{elToStorage}$: varying el. power fed to storage (via electrolyzer);

$P_{To/FromGrid}$: varying grid exchange power.

2. Thermal power balance at any hourly time interval:

$$P_{thSteam}(t) = P_{thCH4}(t) + P_{thH2}(t) + P_{Sun}(t) + P_{thFromStorage}(t) \geq P_{Digester}(t) + P_{GlassHouse}(t) + P_{thToStorage}(t) \quad (7.3)$$

where $P_{thSteam}$: heat power from the steam turbine's condenser plus – in case of steam tapping – the extracted heat;

P_{thCH4} : heat power of the CHP combustion engine resulting from constant feed of biogas;

P_{thH2} : additional varying heat power of the combustion engine caused by supplementary feed of hydrogen;

P_{Sun} : varying contribution of solar power to glass house heating;

$P_{thTo/FromStorage}$: varying input / output of thermal storage;

$P_{Digester}$: heat demand of the digester for biogas generation – varying with ambient temperature;

$P_{GlassHouse}$: heat demand of the glass house for sludge drying – depending on ambient temperature.

3. The electrical power harvest from renewable sources must cover the el. power to storage (via electrolyzer) and the power exported to the grid at any time interval:

$$P_{Renewables} \geq P_{ToStorage} + P_{ToGrid} \quad (7.4)$$

where $P_{Renewables}$: sum of varying el. power from renewable sources;

$P_{ToStorage}$: varying el. power sent to the storage (via electrolyzer);

P_{ToGrid} : varying power sent to the public grid.

Relying on the MATLAB based annual plant simulation in steps of 1 hour, the objective function as given above, with sizing variables x_i, was applied to optimal component rating using the MVMO method [65]; further internal variables are the distribution of el. surplus power to storage (via electrolyzer) and external grid, the ratio of el. deficit power drawn from grid and from hydrogen storage, as well as, if applicable and required, the percentage of steam tapping (*Tap*) from the turbine.

7.4 Optimization process

After initial input of the possible ranges of component sizes the first MVMO generation of variables is randomly set up and the MVMO process is iteratively performed as sketched in section 7.2. In this course, for each iteration generation of variables the plant behavior for the complete year is calculated in hourly steps, respecting the varying (meteorological) parameters, power balances, the mutual dependencies of components and boundaries, as well as subjections given in equations (7.2) to (7.4), and the "fitness" of the objective function is checked, see Figure 7.2. In parallel, the energy is counted up, thus giving the grid exchange and the storage filling level(s). After having satisfied the termination criterion, the resulting annual cost is given out. For the depreciation period of 20 years this result is simply multiplied by 20, but lower lifetime expectancy of components (e.g., combustion engine) is also considered accordingly.

In chapter 8 results of this optimization approach will be shown for two example cases.

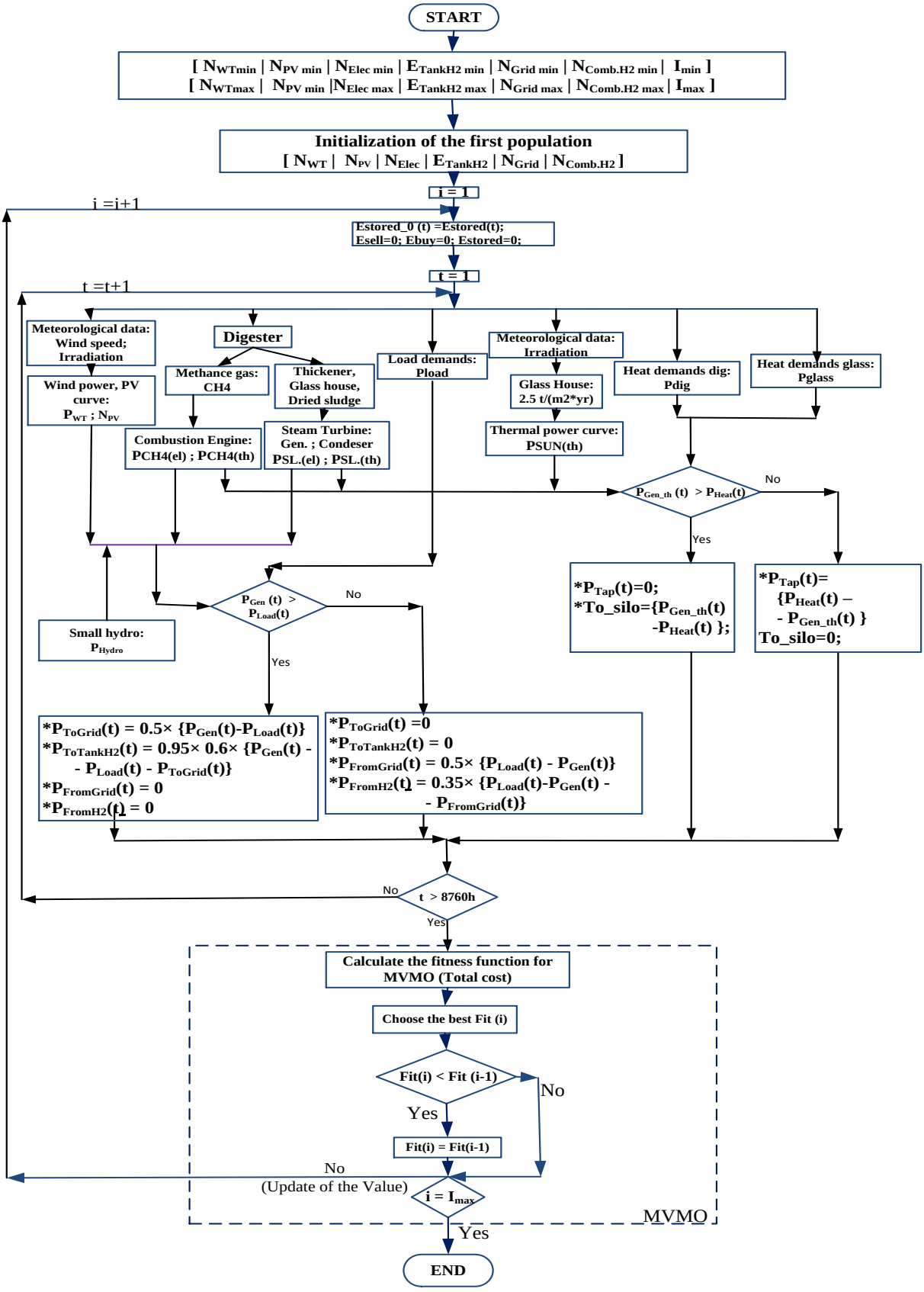

Figure 7. 2: Flow chart of optimal component sizing

8. DESIGN AND PERFORMANCE INVESTIGATION OF TWO EXAMPLES (GERMANY AND VIETNAM)

In the following, the energy autonomy and cost of two exemplary wastewater plant configurations – rather different regarding the geographic and climatic circumstances and thus the relevance of renewable (solar and wind) resources as well as temperatures – are investigated in detail:

- for a city located in the west of Germany serving for 145,000 person equivalents (PE);
- for city Quy Nhon located in the middle of Vietnam serving for 180,000 PE.

For both cases comprehensive energy harvest on the ground of the plants will be assumed in order to make them utmost independent from external energy supply, see chapter 3. Thus, the complete systems investigated make not only use of biogas from sludge digester in a small CHP unit which is state of the art at many places already; rather solar thermal sludge drying and subsequent incineration for a small scale steam power plant is included with further contribution of waste heat from CHP and steam unit for sludge drying. Furthermore, wind power and, where applicable, photovoltaic electricity generation on the ground of the plant is integrated, including a hydrogen storage path.

For both examples the particular composition and the global power streams are sketched first. Then, optimal sizing of the particular components is described, see chapter 7; and finally several results of simulative plant operation over a full year are shown, the latter in particular highlighting the mutual operational dependency of plant devices and proving that reasonable performance at extensive energy independence and at cost significantly below conventional supply of the wastewater plants from the public grid can be achieved for both cases.

8.1 Configuration, mass and energy streams

Table 8.1 contains the mass and energy streams for the energetic plant composition according to the configuration as shown in Figure 4.1 for the two example cases in Germany and Vietnam. The base values were given in chapter 2 and Table 4.1, respectively; the particular flows are derived as follows:

The base electricity demand of the conventional part of the sewage plant can be assessed from wastewater input stream at 22 W/(m^3·d) [22, 66].

Energy contents of the sewage respectively sludge streams can be expressed in form of the "Chemical Oxygen Demand" (COD), see chapter 2 and 3, and the equivalence of 1 kg COD to 3.49 kWh.

Approximately 20 liters/(PE·d) of biogas being generated in the digester typically comprise 65% of methane (CH_4) [67] and provide a related heating value of 0.13 kWh/(PE·d). At constant operation the corresponding flow of chemically bound power can be identified, which can be converted to electricity by means of a combustion-engine driven generator set (typical el. efficiency approx. 35%, see section 3.1); waste heat which can be recovered from cooling jacket and exhaust gas in CHP operation mode arouses a thermal efficiency of approx. 55% [29, 68].

The heat demand of the digester for keeping the internal temperature constant at 37.5 °C is mainly caused by the necessity to warm up the input sludge from ambient temperature to internal temperature, see section 2.5.2; the mass stream of this wet sludge is in the range of 1…5 % of sewage input [69]. The number specifically given for Germany in [70] leads to about 1.55 % which will be assumed in this work for further calculations in both examples. Thermal losses are assessed at ca. 5%. Thus, assuming the heat capacity of the wet sludge being that of water, the average heat power to the digester is

$$P_{Digester} = 1.05 \cdot \dot{m}_{sewage-input} \cdot 1.5\% \cdot c_{H_2O} \cdot (37.5°C - T_{ambient}) \tag{8.1}$$

with c_{H2O} = 4.182 kJ/(kg·K). Of course, in consequence of largely different ambient temperatures in Germany and Vietnam, respectively, the individual heat demand is rather different, see Table 8.1.

The stabilized sludge leaving the digester still has a COD of about 30 g/(PE·day) [16, 71] – corresponding to approx. 0.11 kWh/(PE·day). After de-watering and drying, this sludge can be matter of local incineration.

Despite the use of filter presses in order to reduce the volume of the sludge, the remaining water contents is still in the range of 75%, thus preventing immediate efficient incineration for a steam process; on the other hand, waste heat of this steam process as well as from the biogas-driven combustion engine as CHP unit (see above), and furthermore additional comprehension of solar heat, can be applied for thermo-solar drying (see section 3.3.3) in order to dry the sludge to a

remaining water contents of 20% with an effected heating value in the range of that of lignite coal (ca. 9 MJ/kg), thus allowing for effective incineration [30, 72].

The total energy demand for sludge drying from a given humidity of 75% (output of filter press, see above) to desired 20% – procuring a heating value of ca. 9 MJ/kg, see section 3.3.3 – can be calculated as follows:

Of course, the energy is contained in the dry substance of sludge; at the output of filter presses (i.e. input of thermo-solar drying process) this is about 25% of total mass stream consisting of another 75% of water. After solar drying the same mass stream of pure dry substance has only 20% rest humidity, and thus contributes to 80% of total mass stream. The heating value of the sludge at this point is 9 MJ/kg (see above), corresponding to 2.5 kWh/kg. According to Table 2.1, the related power stream of the sludge at digester output is 4.363 W/PE, which remains unchanged in the subsequent process steps. From this value, the PE related mass stream of dry substance can be calculated:

$$\dot{m}_{ds} = (4.363\ \text{W/PE}) / (2500\ \text{Wh/kg}) = 1.75\ \text{g/(h} \cdot \text{PE)} \tag{8.2}$$

With the shares of dry substance d_{s1} before and d_{s2} after thermo-solar drying the water mass stream to be evaporated can be derived:

$$\dot{m}_{H_2O-evap} = \dot{m}_{ds} \cdot (1/d_{s1} - 1/d_{s2}) \tag{8.3}$$

As described above, for both examples considered here (Germany and Vietnam) the shares of dry substance are assumed to be d_{s1} = 25% and d_{s2} =80%; using the related sludge mass stream as derived in equation (8.1), according to equation (8.2) the mass stream of water to be evaporated results in about 4.8 g/(h·PE); the individual results are entered in Table 8.1.

Assuming further that, according to [37, 73], about 960 kWh are needed to evaporate 1 ton of water in a thermo-solar sludge drying process, the thermal power demand can be derived:

$$P_{thermo-solar} = \dot{m}_{H2O-evap} \cdot\ 960\ \text{Wh/kg} = 4.6\ \text{W/PE} \tag{8.4}$$

Again, the concrete values are entered in Table 8.1. The dimensioning (ground area) of the required glass house for thermo-solar sludge drying can be assessed as follows:

In Western Europe, with a typical yearly solar irradiation $I \approx 950$ kWh/m^2, a share of approximately 25% of evaporation energy is contributed by the sun in yearly average according to practical experience [38, 74], whereby the transmission factor of the glass house is about 65 % [39, 75]. Accordingly, 75% of thermal energy needed for evaporation has to be covered by other (waste) heat sources such as CHP unit and/or steam circuit. In Vietnam the yearly solar harvest is almost double of that in Western Europe ($I \approx 1900$ kWh/m^2). Thus, the needed glass house ground size for Vietnam is only about $1/(2 \cdot 25\% + 75\%) = 0.8$ times of that in Western Europe. Based on these considerations and the specific heat demand as given in Table 8.1, the glass house size can be assessed for the German case:

$$A_{GlassHouse} = 0.25 \cdot P_{thermo-solar} \cdot 1/I \cdot 1/0.65 \tag{8.5}$$

For the Vietnam example, only 80% of this value would be required for the same sludge throughput, see above, but the higher number of person equivalents (180,000) in this example case has to be considered, too, thus leading to a very similar size, see Table 8.1.

Finally, the additional electricity demand of the thermo-solar drying process has to be taken into account. For continuously operating conveyors, ventilators, ploughing systems etcetera a typical demand in the wide range of 20…130 kWh per ton of water evaporated is given in the literature [39, 76]; for the investigations made in this work, a value of 80 kWh per ton of water evaporated is assumed in order to calculate on the secure side. The relevant values for both examples can also be found in Table 8.1 and must consequently be added to the original electricity demand of the sewage plant.

In this way, provided that the necessary heat for thermo-solar drying is procured (see below), the energy contents in the dry solids of the sludge can widely be exploited in a small scale thermal steam power plant [34, 77]. With a typical boiler efficiency of 73% and a thermal efficiency of the steam process of approx. 22% for the relevant order of size, an electrical output efficiency of 16 % can be achieved in constant operation mode; typically, 53 % of the energy of fuel can be retrieved from the condenser as thermal energy at a temperature level of about 50 °C.

Last, but not least, if height difference between wastewater plant and supplied river admits, another constant electrical power can be gained from the steady output of clarified water by use of a small

hydro unit, see section 3.3.1 and equation (3.4). The relevant values assumed for the two example cases and the resulting output powers are also entered in Table 8.1.

Table 8.1: Mass and energy streams

No.	Example case	Germany	Vietnam
1	Person equivalents (PE)	145,000	180,000
2	Sewage input (m^3/d)	18,850	21,000
3	COD input sewage (kW)	2,530	2,818
4	COD to digester (kW)	1,413	1,574
5	COD biogas (kW)	783	872
6	Average ambient temperature (°C)	13	25
7	Heat demand of digester (kW)	364	134
8	El. output CHP unit, $\eta \approx 35\%$ (kW)	275	306
9	Thermal output CHP unit, $\eta \approx 55\%$ (kW)	430	479
10	COD digester out / dried sludge (kW)	630	702
11	El. output steam process (untapped), $\eta \approx 16\%$ (kW)	101	113
12	Thermal output steam process (untapped), $\eta \approx 53\%$ (kW)	335	373

No.	Example case	Germany	Vietnam
13	El. load of conventional sewage plant @ 22 W/(m^3·d) (kW)	415	462
14	Mass stream of water evaporated $\dot{m}_{H_2O\ evap}$ (kg/h)	696	864
15	Ground size glass house (m^2)	2350	2333
16	Additional electricity demand of plant (kW)	55	63
17	Height difference for small hydro (assumed) (m)	10	6
18	Power of small hydro generation according to eq. (3.4) (kW)	15	10

Thus, based on the considerations made above, the global power flows of the plant can be set up. Figure 8.1 and Figure 8.2 in their inner parts (light blue background) depict the mass/power streams according to the values given in Table 8.1 for the example cases in Germany and Vietnam, respectively.

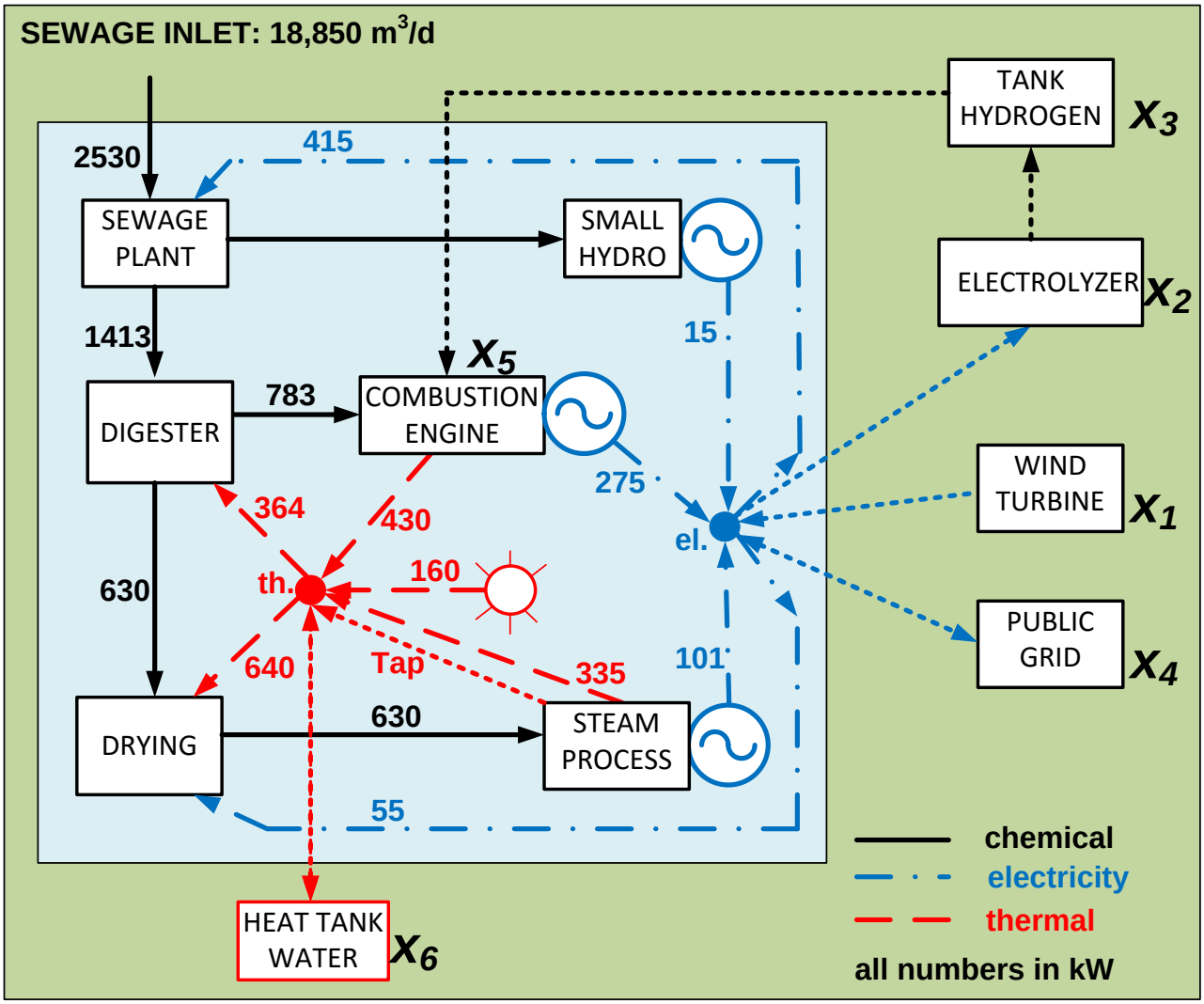

Figure 8.1: Average power streams related to energy recovery at example waste water treatment plant for 145,000 person equivalents (PE) in Germany

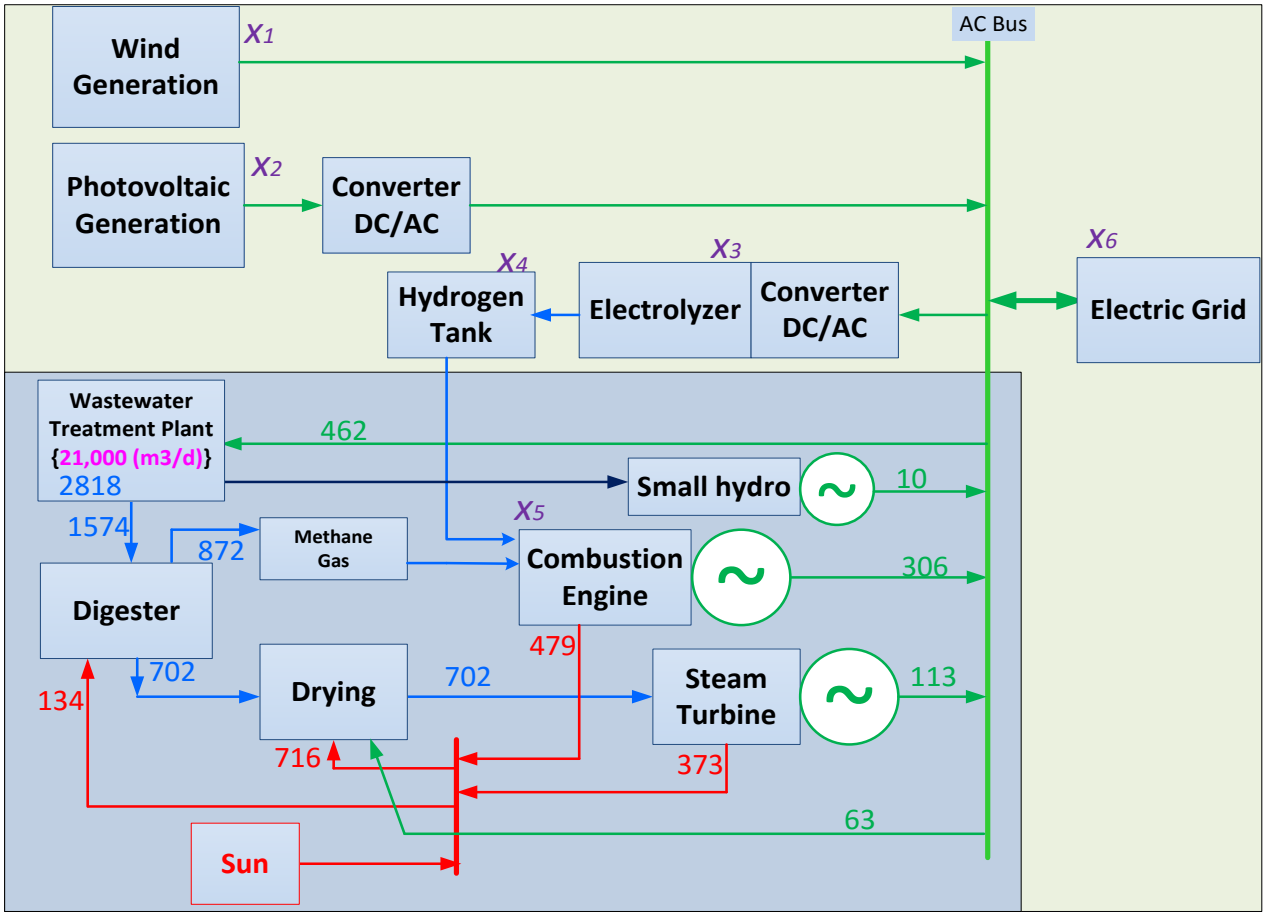

Figure 8.2: Average power streams related to energy recovery at example waste water treatment plant for 180,000 person equivalents (PE) in Vietnam; all numbers in kW: bound chemical (blue); thermal (red); electricity (green)

8.2 Global power balances

In order to design the sewage plant for utmost energetic autonomy, the balances of both thermal and electrical power must be properly adjusted. The first principal survey given in Figures 8.1 and 8.2 is based on annual averages and at this point does not yet consider seasonal or operational variations, which in particular depend on location of the plant and many other specifics and will be discussed later.

Nevertheless, looking at the global balances of both thermal and electrical nodes shown in Figures 8.1 and 8.2 it can be stated that in both cases they are widely settled, with minor deficiencies as indicated in Table 8.2 (negative sign means power lacking).

Table 8.2: Global electricity and thermal power balances

Example	Germany	Vietnam
Electrical balance	-79kW	-96kW
Thermal balance	-79kW	+02kW

These deficiencies, together with compensation of temporal variations and fluctuations of the entire process, can be covered by additional wind and solar power based electricity generation on the ground of the wastewater plant and appropriate energy storage – see Figures 8.1 and 8.2 outer parts – which will be investigated in the following. Of course, which additional renewable sources are used in particular depends on the local conditions which are rather different for the two investigated examples in Germany and Vietnam.

8.3 Compensation of temporal fluctuations by renewable based generation and energy storage

At a closer view, the rough estimative balances based on annual averages need some detailing since several of the quantities significantly vary over time: for instance, the heat demand to keep the digester temperature at constant 37.5°C varies with seasons (inlet sludge temperature) and weather (thermal losses of digester according to outside temperature); furthermore, the contribution of sun irradiation to sludge drying in a glass house varies with weather and seasons. Typical annual profiles in 1 h resolution are shown in Figures 8.3 and 8.4 for the relevant example locations [78].

These dependencies, in connection with the aim to cover the deficits of the electricity and thermal power balances, necessitate providing an additive local energy source.

In order to maintain the idea of vast independency of external supply, local installation of a wind turbine and/or a photovoltaic (PV) plant appears a reasonable approach. For wind generation there is the beneficial aspect that typical locations of waste water plants outside the cities relieve the administrative admittance for the erection, and at the same time the typical dimension of terrain also favors ample PV installation.

The electricity harvest from renewable based generation can firstly be used to cover the deficit of the electricity balance (see Table 8.2). However, since solar irradiation as well as wind speed are continuously fluctuating and calms may occur (see Figure 8.3 a), energy storage is needed which can reasonably be realized by a hydrogen path [79] consisting of a high pressure electrolyzer (delivering up to 30 bar of hydrogen output pressure [80]), a storage tank for the produced hydrogen, and reconversion of hydrogen to electricity by either an (expensive) fuel cell, a separate combustion engine driven generator set or, even better, by combined use of the biogas from the digester and, if needed, additive hydrogen from the storage tank in one and the same combustion-engine driven generator set; up to a share of approx. 15% of H_2 this should be admissible without change of the engine adjustment. The additive waste heat of the latter, caused by supplementary additional hydrogen combustion, secondly can contribute to cover the deficit of the thermal energy balance – if any (see Table 8.2) – and, when indicated, be equalized by a hot water storage tank of appropriate size, see below.

For the two example cases of Germany and Vietnam the appropriate renewable sources as well as energy storage paths are shown in the outer regions of Figures 8.1 and 8.2. It is clear from the yearly profiles in Figures 8.3 and 8.4 that in Germany wind is favored, while for Vietnam photovoltaic is also an option, in particular since module prices tremendously dropped recently.

In order to comply with the issue of consistent and reliable supply, equitable ratings of devices as well as a prudent operation strategy are needed; both were afforded on the basis of a sound plant model (see chapter 4) and simulation over longer periods of time, typically one year, with appropriate temporal resolution of 1 hour.

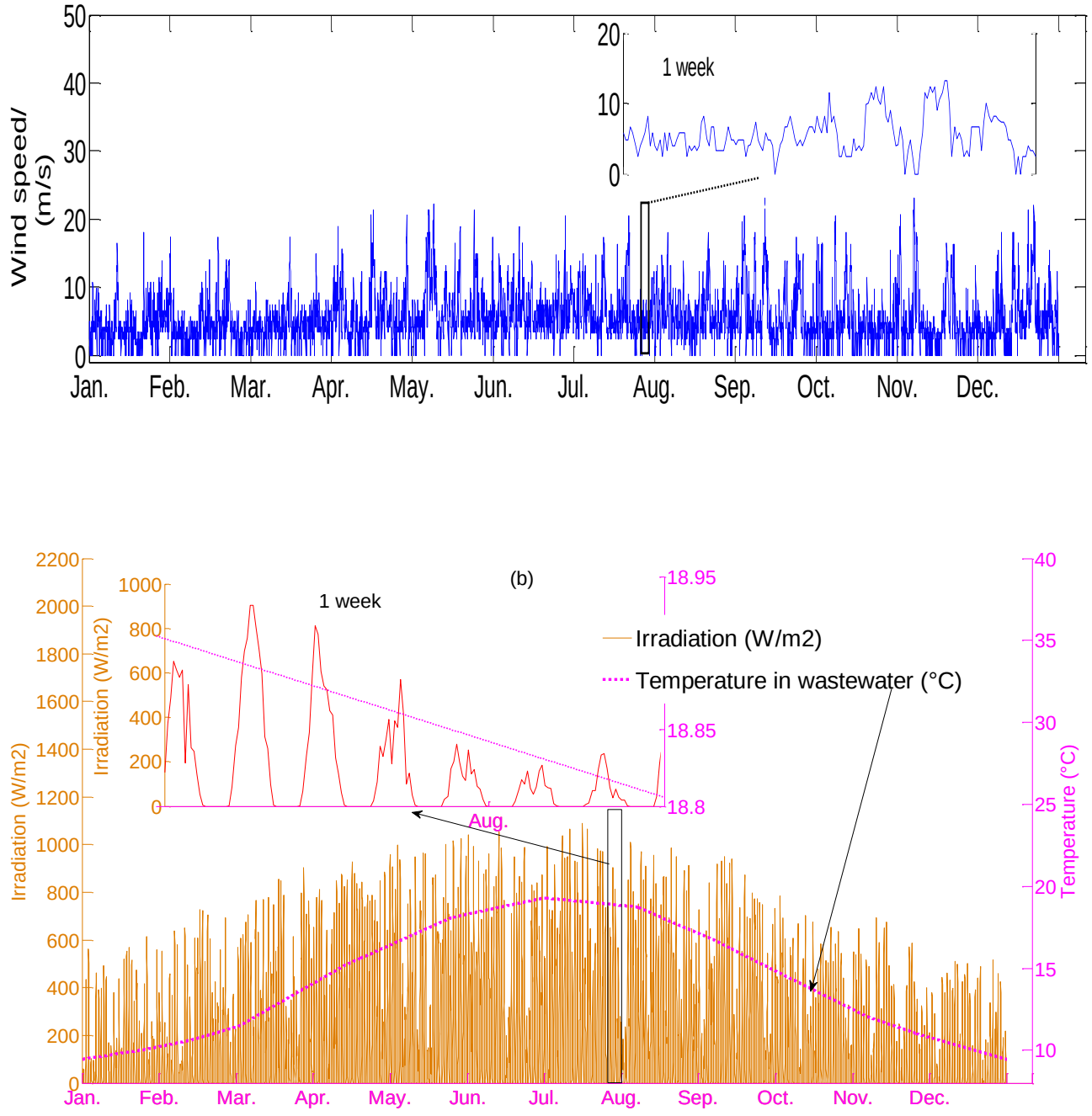

Figure 8.3: a) Annual profiles of wind speed (Germany) [78]

b) Temperature and solar irradiation at plant site

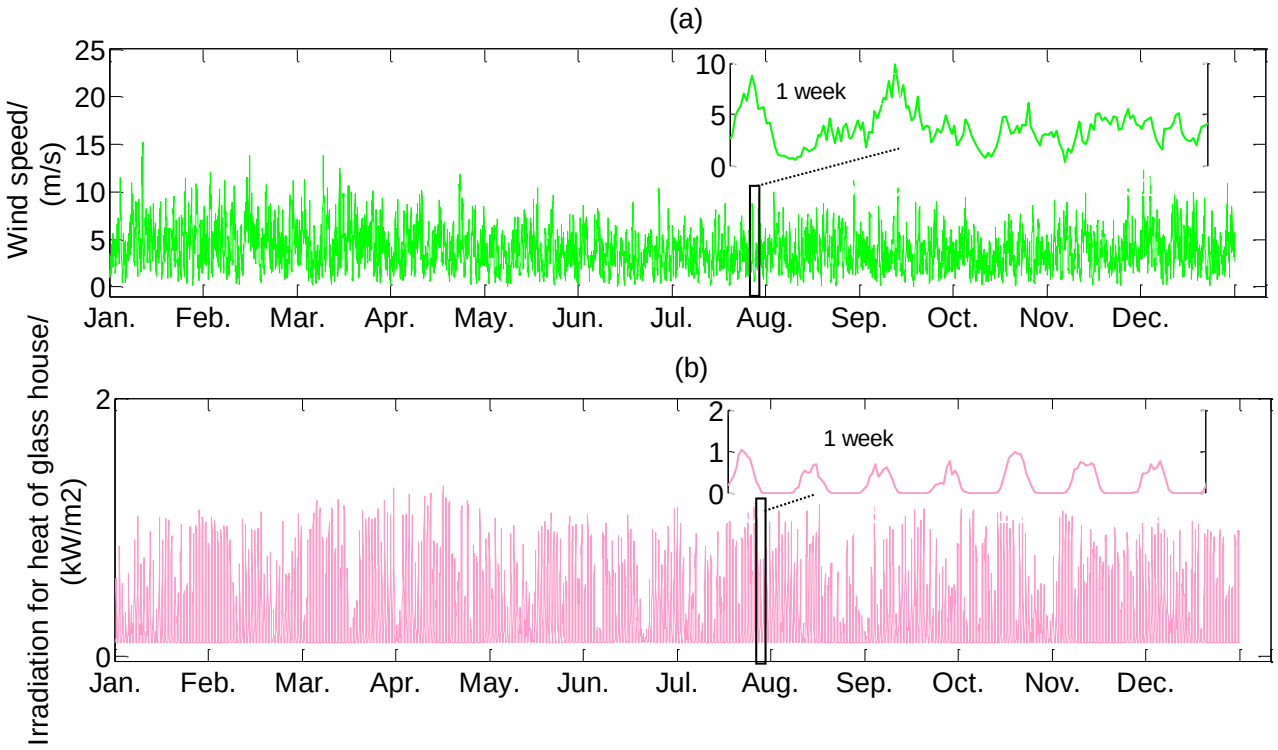

Figure 8.4: Annual profiles at Quy Nhon wastewater treatment plant in Vietnam [78]; the ambient temperature is only very slightly varying here and was considered as constant at 25°C

a) Wind speed
b) Solar irradiation

8.4 Optimal sizing of devices for the example cases

As shown above, for both examples the base rating of combustion engine driven generator set, steam power unit and small hydro unit, as well as the size of the glass house for sludge drying can primarily be calculated for constant wastewater/sludge streams – appropriately burnished by intermediate basin/silo storage, see Table 8.1. In contrast, the sizes of

- renewable generation (wind converter, photovoltaic where applicable),
- nominal power of electrolyzer,
- hydrogen storage,
- additional capacity of combustion engine driven generator set for hydrogen re-conversion,
- capacity of el. feeder,
- thermal storage, if needed, and
- fraction of steam tapped from the turbine for balancing the varying heat demand if needed

were subjected to the optimization algorithm according to chapter 7, which – under simulation of the hourly plant behavior for one full year with the varying quantities as shown in Figures 8.3 and

8.4 – determined their optimal rating. Investment and operation cost in terms of external grid tariffs for electricity import and in feed were considered, aiming at full electrical and thermal power supply of the sewage plant under minimal overall cost; parameters see Table 8.3, which also contains the cost of devices with rating fixed in advance (see Table 8.1). For the depreciation period of 20 years the results gained by annual optimization was simply multiplied by 20; rather, the moderate lifetime expectancy of the combustion engine (5 years, see Table 8.3) was also considered.

Because of the technical nature of this paper focusing on energetic issues the maintenance costs of the plant (servicing and personnel) as well as financing costs were not regarded in the optimization.

Table 8.3: Parameters of optimization and component sizing for the example cases; for Vietnam (VN) the cost were transposed to €

Cost	Device	Varying quantity	Cost (estimated)	Cost reference	Lifetime (years)	Example case (variable no. in Fig. 8.1/8.2)
C_{Wind}	Wind turbine	Wind speed	1000 €/kW	[79]	25	DE (x_1); VN (x_2)
C_{PV}	Photovoltaic	Irradiation	1450 €/kW$_p$	[79]	25	VN (x_2)
$C_{elToStorage}$	Electrolyzer	Surplus power	1600 €/kW	[82]		DE (x_1); VN (x_2)
$C_{elStorage}$	Hydrogen tank	Surplus energy	0.32 €/kWh	Estim.	20	DE (x_3); VN (x_4)
C_{Grid} C_{Export} C_{Import}	Connection to public grid	Surplus/deficit power	1000 €/kW; Export: 0.12 €/kWh; Import: 0.17 €/kWh	Actual values for Germany	20	DE (x_4)
C_{Grid} C_{Export} C_{Import}	Connection to public grid	Surplus/deficit power	1000 €/kW; Export: 0.09 €/kWh; Import: 0.12 €/kWh	Actual values for Vietnam	20	VN (x_6)

Cost	Device	Varying quantity	Cost (estimated)	Cost reference	Lifetime (years)	Example case (variable no. in Fig. 8.1/8.2)
C_{CombH2}	Supplementary nominal power of combustion engine set for added hydrogen	Deficit power	300 €/kW	[81]	05	DE (x_5); VN (x_5)
$C_{thStorage}$	Hot water tank	Surplus/deficit thermal	0.60 €/kWh	Estim.	20	DE (x_6)
$C_{Digester}$	Digester Volume	3500 m^3	700 €/m^3	Estim.	20	VN
C_{Steam}	Complete steam circuit	101 kW const.	2000 €/kW	[79]	20	DE
C_{Steam}	Complete steam circuit	113 kW const.	2000 €/kW	[79]	20	VN
$C_{CombCH4}$	Base rating of comb. engine set	275 kW const.	700 €/kW	[84]	05	DE
$C_{CombCH4}$	Base rating of comb. Engine set	306 kW const.	700 €/kW	[84]	05	VN
$C_{SmallHydro}$	Small hydro unit	15 kW const.	1000 €/kW	[79]	20	DE
$C_{SmallHydro}$	Small hydro unit	10 kW const.	1000 €/kW	[79]	20	VN
$C_{GlassHouse}$	Glass house with infrastructure	2350 m^2	600 €/m^2	[84]	20	DE

Cost	Device	Varying quantity	Cost (estimated)	Cost reference	Lifetime (years)	Example case (variable no. in Fig. 8.1/8.2)
$C_{GlassHouse}$	Glass house with infrastructure	2613 m^2	600 €/m^2	[84]	20	VN
$C_{Heat\ Exchanger}$	Heat exch. at various places	Σ (1004 kW)	40 €/kW	Estim.	20	DE; VN
$C_{Heat\ Exchanger}$	Heat exch. at various places	Σ (850 kW)	40 €/kW	Estim.	20	VN

While for Germany wind power appears as the only eligible renewable generation source, for the Vietnamese example case the optimization was performed for the three scenarios:

a) renewable generation by both wind power and photovoltaic;
b) wind power as only renewable source;
c) photovoltaic as only renewable source;

the latter in particular under the viewpoint of nowadays largely dropped price of PV modules (see Table 8.3) and favorable irradiation situation at the example site, see Figure 8.4.

For solving the mixed integer optimization problem of the above mentioned plant components' rating in order to achieve minimal overall cost, the meta-heuristic Mean-Variance Mapping Optimization (MVMO, [62]) has been applied – see chapter 7 – under plant simulation for one full year in hourly steps. The objective function and subjections are explicitly given in the Appendix A8.1 and A8.2 for both example cases.

As result of the component sizing optimization the ratings as entered in Tables 8.4 … 8.7 were determined; all of them are in a reasonable range of size. For practical reasons, the nominal power of wind turbine, electrolyzer and combustion engine should be oriented at eligible models on the market next in size (as indicated in Tables 8.4 … 8.7), and the power of the electrolyzer should be controlled with limited number of discrete stages (0, 25, 50, 75 100% of nominal power) in order to enhance lifetime expectancy, see operational results below.

Table 8.4: Results of optimal components sizing for German example

Symbol	Optimization	Practical)*	Devices
N_{Wind}	583 kW	600 kW	Wind turbine
$N_{elToStorage}$	178 kW	200 kW	Electrolyzer including converter (output pressure max. 30 bar) operated in 50 kW steps
$E_{elToStorage}$	129 MWh	135 MWh (5% reserve capacity)	Hydrogen storage 1488 m^3 $(11.4m)^3$ @ 30 bar; 4018 kg H_2 {*33.6 kWh/kg H_2; 2.7 kg H_2/m^3 @ 30 bar*}
N_{Grid}	399 kW	500 kW	Maximal power exchange with grid
$N_{Comb.H2}$	(275+ **29**) kW	315 kW	Power of combustion engine set (CH_4+**H_2**)
$E_{thStorage}$	39 MWht	60 MWht	Thermal storage, 2063 m^3 @ ΔT=25 K {$Q=m \cdot c_p \cdot \Delta T$}
Tap	40 % max.	Limited at 40%	Tapping of turbine steam (~208°C)

Table 8.5: Results of optimal sizing for Vietnamese example (wind + PV)

Symbol	Optimization	Practical	Devices
N_{Wind}	514 kW	550 kW	Wind turbine
N_{PV}	390 kW_p	400 kW_p	Photovoltaic, 2025 m^2
$N_{elToStorage}$	83 kW	100 kW	Electrolyzer including converter (output pressure max. 30 bar)
$E_{elToStorage}$	29 MWh	30 MWh (3.3% reserve capacity)	Hydrogen storage 333m^3 $(6.9m)^3$ @ 30 bar; 893 kg H_2 {*33.6kWh/kg H_2; 11.2kg H_2/m^3*}
N_{Grid}	580kW	600 kW	Maximal power exchange with grid
$N_{Comb.H2}$	(306+**17**) kW	325 kW	Power of combustion engine set (CH_4+**H_2**)
Tot.cost	-	-	**157** Bil.VND (6.32 Mil.€)

Table 8.6: Results of optimal sizing for Vietnamese example (wind only)

Symbol	Optimization	Practical	Devices
N_{Wind}	994 kW	1 MW	Wind turbine
$N_{elToStorage}$	84 kW	100 kW	Electrolyzer including converter (output pressure max. 30 bar)
$E_{elToStorage}$	39 MWh	40 MWh (2.5% reserve capacity)	Hydrogen storage 444m^3 (7.6m)^3 @ 30 bar; 1190 kg H_2 {*33.6kWh/kg H_2; 11.2kg H_2/m^3*}
N_{Grid}	812 kW	850 kW	Maximal power exchange with grid
$N_{Comb.H2}$	(306+**15.5**) kW	325 kW	Power of combustion engine set (CH_4+**H_2**)
Tot.cost	-	-	**159** Bil.VND (6.41 Mil.€)

Table 8.7: Results of optimal sizing for Vietnamese example (PV only)

Symbol	Optimization	Practical	Devices
N_{PV}	840 kW_p	850 kW_p	Photovoltaic, 4356 m^2
$N_{elToStorage}$	84 kW	100 kW	Electrolyzer including converter (output pressure max. 30 bar)
$E_{elToStorage}$	14 MWh	15 MWh (7% reserve capacity)	Hydrogen storage 167m^3 (5.5m)^3 @ 30 bar; 446 kg H_2 {*33.6kWh/kg H_2; 11.2kg H_2/m^3*}
N_{Grid}	660 kW	700 kW	Maximal power exchange with grid
$N_{Comb.H2}$	(306+**11**) kW	325 kW	Power of combustion engine set (CH_4+**H_2**)
Tot.cost	-	-	**162** Bil.VND (6.53 Mil.€)

Figure 8.5 proves that the MVMO optimization algorithm firmly converges in all cases after any of three individual runs with 250, 400 evaluations for each example/scenario, respectively. On a PC with Intel® Core™i7 CPU 920 @ 2.67 GHz and 6 GB Ram under Windows 7 Professional 64 bit, the time demand was ca. 6 minutes for each run.

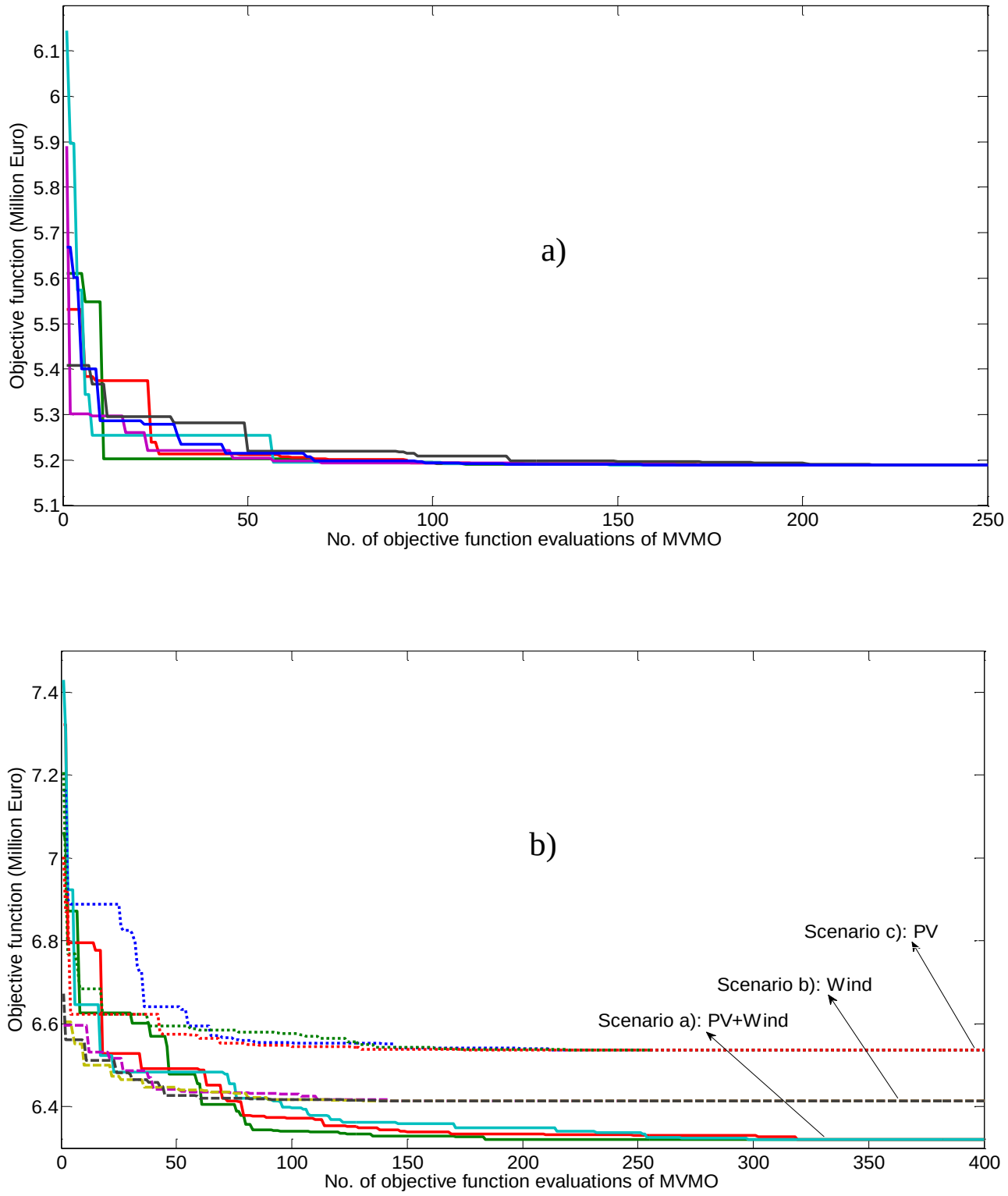

Figure 8.5: Convergence of MVMO algorithm applied to component sizing for minimal cost of electricity supply over 20 years

a) German example (6 runs)
b) Vietnamese example (3 runs each scenario)

In Table 8.8 the calculated total costs for the energetic exploitation of sewage for the intended depreciation period of 20 years are contrasted with those electricity costs which would accumulate

for the constant electricity supply of the conventional plant from the public grid (i.e. without sludge exploitation) over these 20 years.

Table 8.8: Comparison of electricity cost with sludge exploitation vs conventional supply

Case	Electricity cost with sludge exploitation (see Table 8.5 … 8.7)	Electricity cost conventional supply
Germany	5.2 Mill. €	12.36 Mill. € (0.17 €/kWh)
Vietnam scenario a	6.32 Mill. €	9.71 Mill. € (0.12 €/kWh) (~ 3.000 VND/kWh)
Vietnam scenario b	6.41 Mill. €	
Vietnam scenario c	6.53 Mill. €	

Obviously, besides solving the ecologic problem of extirpating large quantities of infectious sludge as well as CO_2 avoidance for conventional electricity generation there is also a considerable economic vantage.

From a closer look at Tables 8.4 … 8.7 it becomes evident that

- the required additional capacity of the combustion engine driven generator set for hydrogen reconversion is marginal (<30 kW) for all cases;
- obviously the given electricity tariff structures in both countries favor grid energy exchange compared to using the hydrogen path in short term range; thus, the hydrogen path primarily acts as long term storage;
- in both example cases the calculated capacity of the public grid connection would also allow for external feeding of the total electricity demand in case of failure of plant components (emergency operation).

Furthermore, comparison of the three Vietnamese scenarios in Tables 8.5 … 8.7 proves that

- covering the supplementary electricity generation only by wind power (option b) is not the most economical solution, and the required hydrogen storage is largest;
- besides its versatility, the combined wind power and photovoltaics (option a) has marginal economic advantage;

- despite the considerably decreased market prices of photovoltaics and favorable irradiation conditions at plant site this option (c) is not yet fully competitive to wind power (b); rather the hydrogen tank, primarily serving as seasonal storage, would have the most reasonable size of 167 m^3;

- the ratings of electrolyzer and combined heat and power unit are almost the same for all three options.

8.5 Simulative operational results

In the following some more detailed exemplary results of the simulative operation of the plants are analyzed, all of them proving reasonable performance; in all subsequent yearly curves the same sample week in August has been zoomed for visibility of details. The results will first be shown separately for the German and Vietnamese example cases; finally, their yearly energy balances are sketched and common conclusions are drawn.

8.5.1 Temporal behavior, German example

Figure 8.6 depicts the output power of the wind turbine (600 kW rated power, see Table 8.4), based on the annual wind speed profile as shown in Figure 8.3. It can clearly be seen that the electrical output of the combustion engine driven generator set (rated power 315 kW, see Table 8.4), generating 275 kW from constant biogas feed, is augmented maximally by another 40 kW fed from H_2 storage in case of low wind periods. Furthermore, it can be seen that the el. output of the steam turbine driven generator is slightly modulated, too, in consequence of moderate steam tapping in times of low thermal power available.

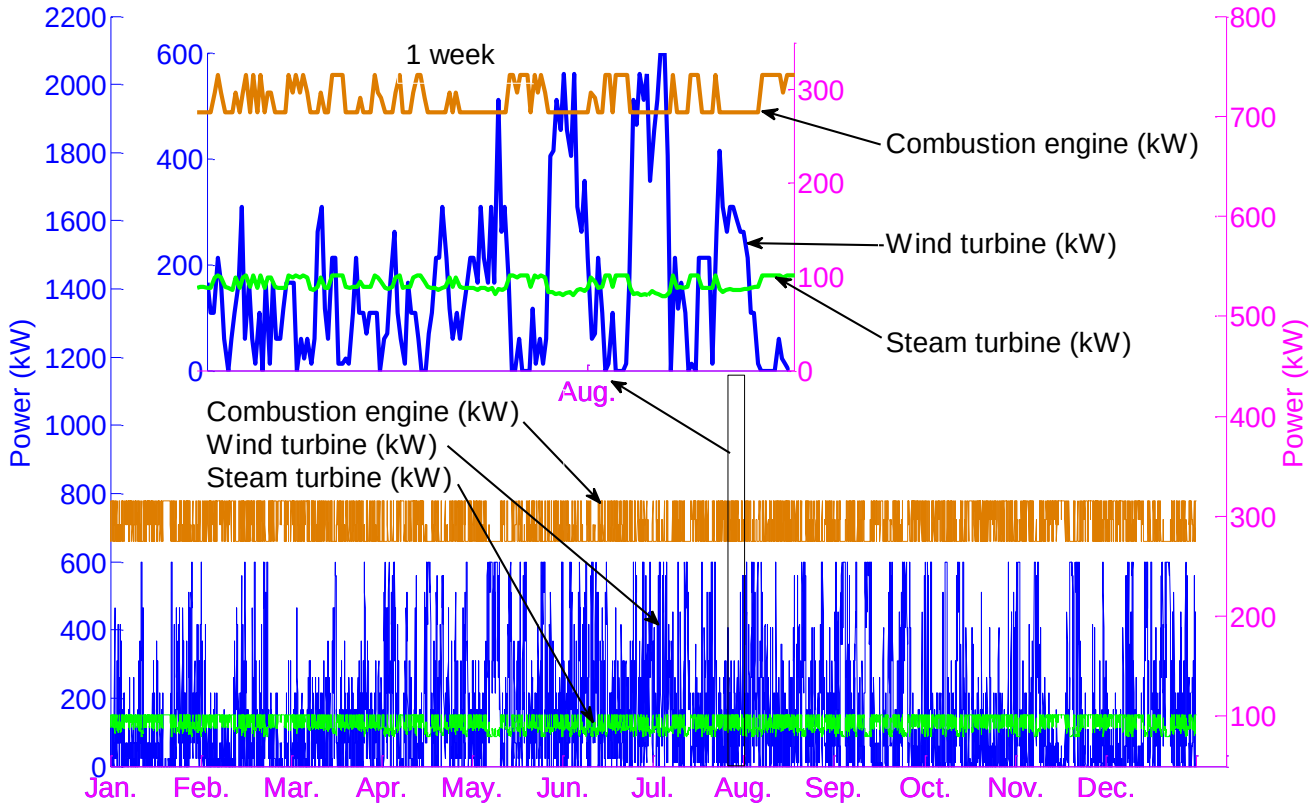

Figure 8.6: Delivered el. power of wind turbine (left power scale), as well as combustion engine and steam turbine, both right power scale

In Figure 8.7 the energy exchange with the hydrogen gas storage path is shown. When the electrolyzer is operated – in 50 kW steps of el. input –, the filling level of the hydrogen tank rises accordingly; this mainly happens in spring and autumn when winds are stronger resulting in higher generation of the wind turbine and thus more el. power surplus.

In case of el. power deficit, the output of the combustion engine driven generator is increased by additional fueling with hydrogen gas (up to 15 %), and thus the H_2 storage filling level is lowered correspondingly. The total el. energy sent to the electrolyzer in the considered year sums up to 680 MWh, from which a portion of 134 MWh is re-converted to electricity by the combustion engine, thus leading to ca. 20% total efficiency of the hydrogen storage path. The integral balance of electrical energy over the considered year can be found in Table 8.9 (see below).

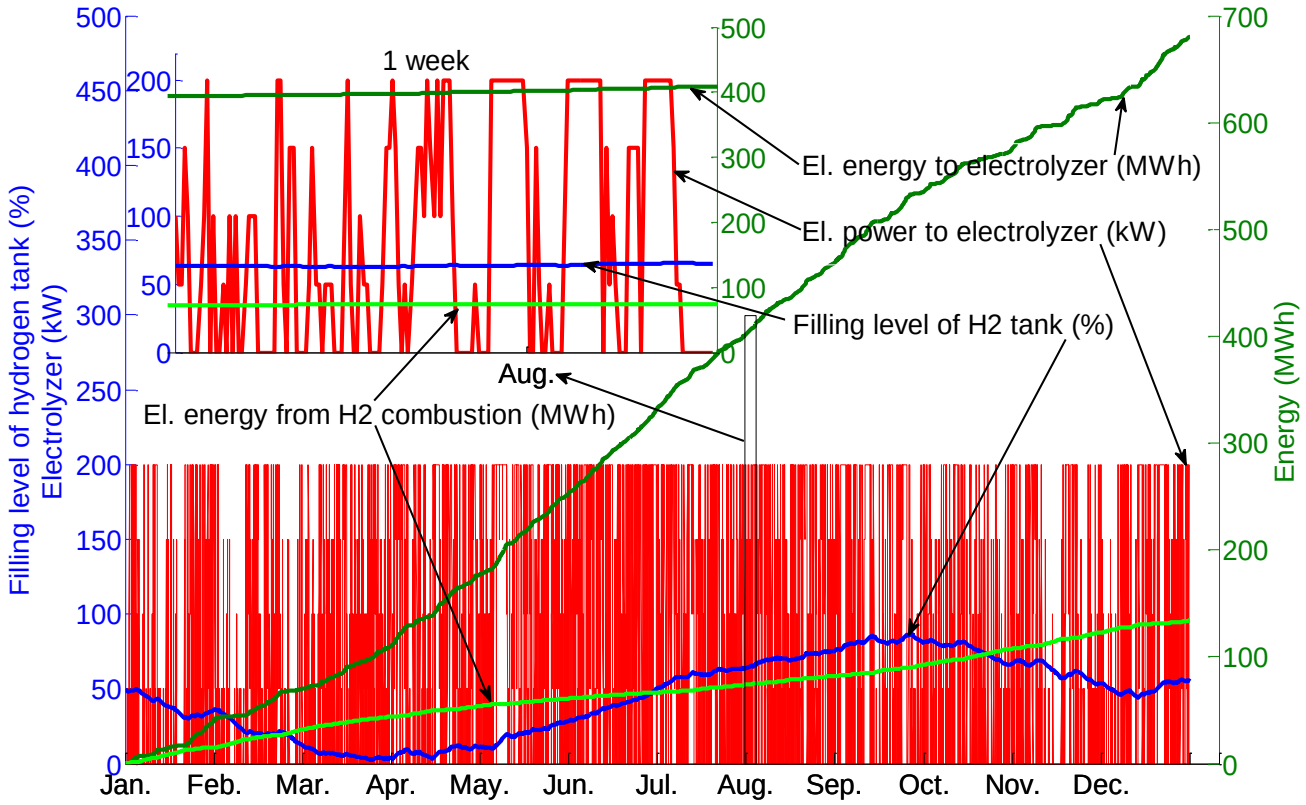

Figure 8.7: Electric power and energy to electrolyzer, electric energy via additional combustion of hydrogen and resulting filling level of hydrogen tank

Figure 8.8 illustrates the availability of thermal power from combustion engine (operated as shown in Figure 8.6, regarded efficiency of heat exchanger 95%), from steam condenser (slightly modulated by steam tapping which is also shown as a separate curve), and solar contribution to sludge drying (yearly insolation profile as depicted in Figure 8.3). From the detailed excerpt it is obvious that steam tapping – used for glass house air heating and basically needed for compensation of day/night cycles via the heat storage tank – is largely increased in periods of low solar irradiation.

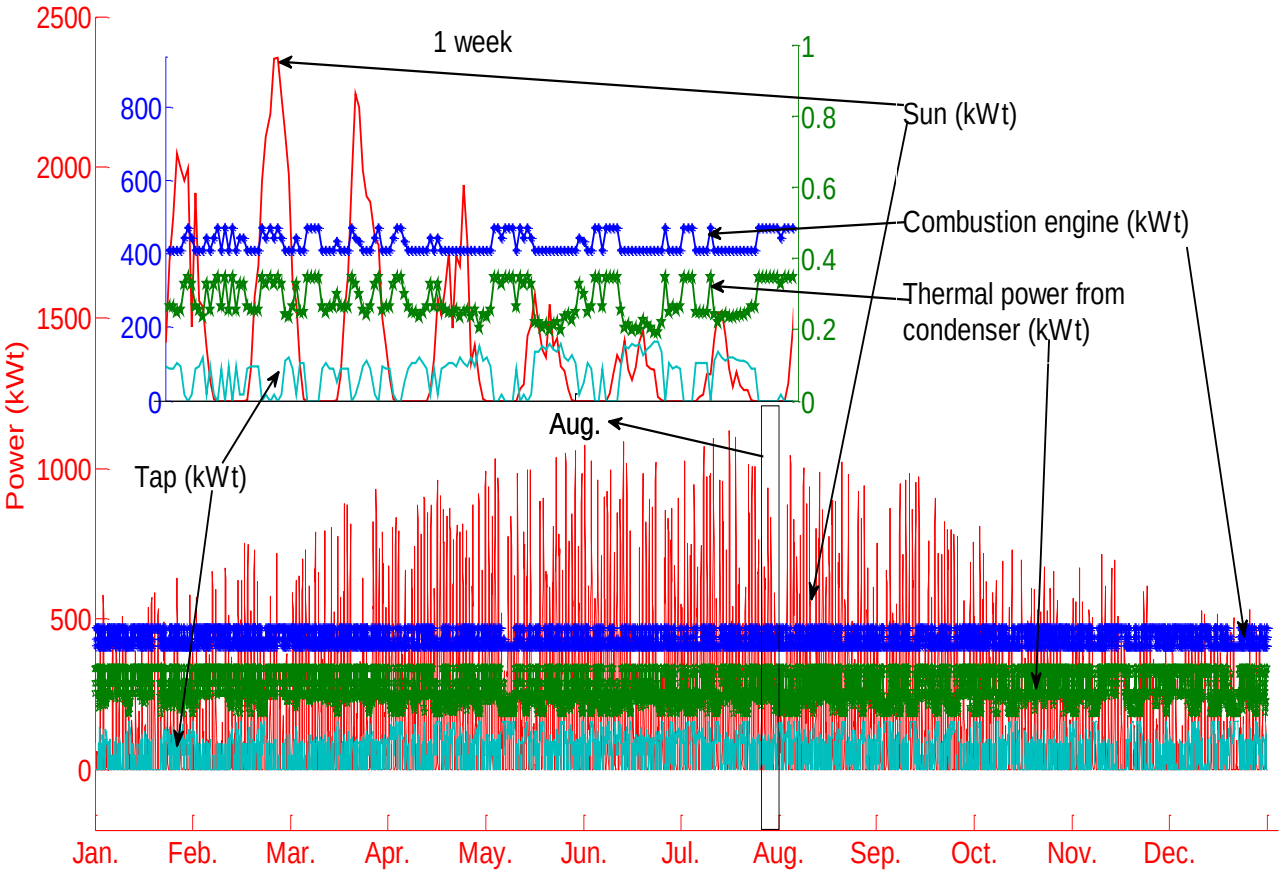

Figure 8.8: Thermal power of components

The charging/de-charging periods of the buffering thermal storage can be observed in Figure 8.9, together with the heat tank's filling level; the latter in detail mostly follows the day/night cycles (see zoomed excerpt) with strong increase at times of bright sun, and in major scale it is mainly charged during the summer months and de-charged in winter: While charging of the heat tank directly reflects the solar irradiation profile, de-charging is largely determined by annual variation of heat demand. The integral balance of thermal energy over the considered year is entered in Table 8.9 (see below).

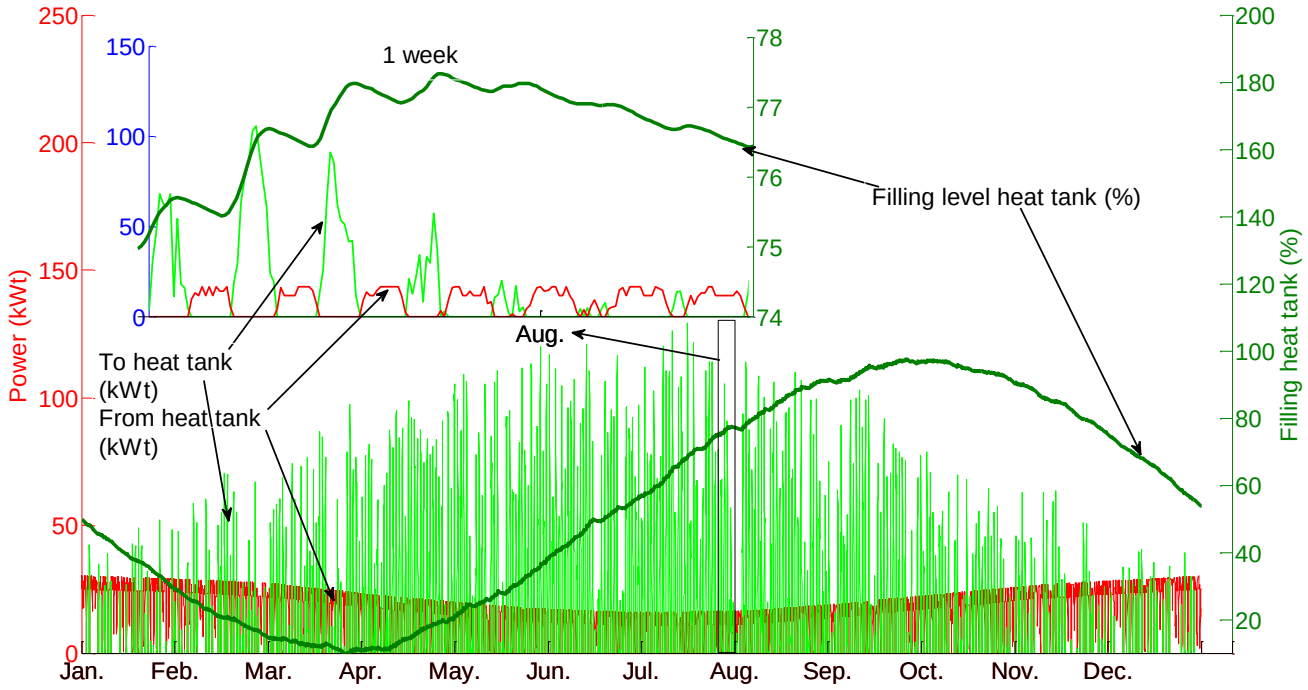

Figure 8.9: Power exchange and filling level of thermal storage

Finally, Figure 8.10 shows the electricity exchange with the public grid. While the grid mostly acts as short time electricity buffer (see oscillating curve of el. power export (positive) and import (negative), respectively), in consequence of the applied tariff the exported electricity (@0.12€/kWh) exceeds the import (@0.17 €/kWh) by approximately the inverse ratio, thus making the grid exchange energy widely cost neutral; the yearly electricity balance can also be found in Table 8.9.

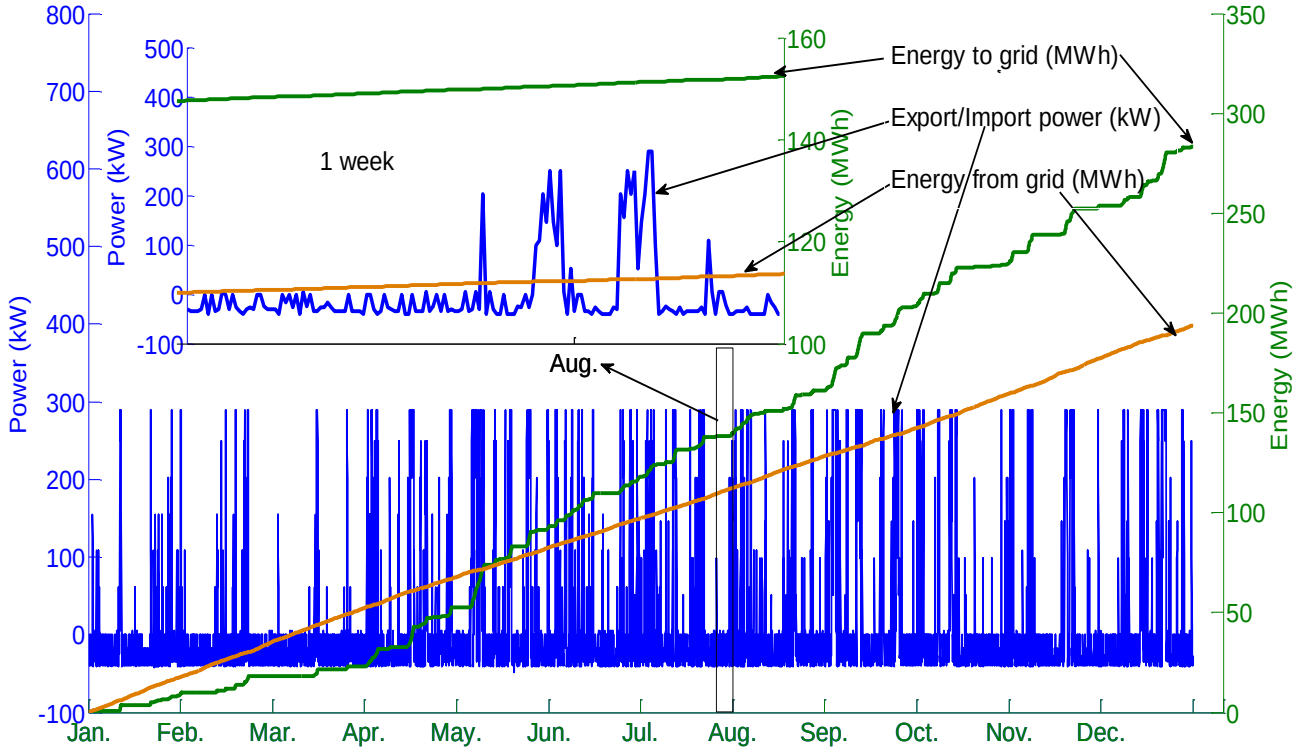

Figure 8.10: Electricity exchange with public grid

8.5.2 Temporal behavior, Vietnamese example

In contrast to the German case, in the Vietnamese example – in consequence of the climatic conditions – there is plenty of heat power available; the yearly average heat balance here (see Table 8.2) is well adjusted even without counting the solar contribution for sludge drying, which was also not yet specified in Figure 8.2. This leads to the consequences that

- making use of the additional and appreciable solar contribution for sludge drying in the glass house, a major part of waste heat from the biogas-fed CHP unit (taken at high temperature at the exhaust gas output) can be released for pre-heating the feeding water of the steam circuit (instead of tapped steam as applied in German case), thus slightly increasing efficiency and electrical output;
- no heat storage (tank) is required in this case;
- no additional steam tapping from the turbine is required for compensation of missing heat power.

Again, operation over one year was investigated by simulation in hourly steps, based on the renewable (wind and solar) profiles as shown in Figure 8.4 for Vietnam. The most economic option (scenario a with both wind and photovoltaic electricity generation, see section 8.4) was considered here in particular.

The results prove that all physical quantities experience largely less dominant annual fluctuations than in Germany. For instance, from Figure 8.11 it becomes evident that the contribution of renewables to electricity generation has no distinct seasonal disparity.

A more detailed view at one particular week shows that – as expected – the power of the CHP unit is slightly increased by additional combustion of stored hydrogen at times with low renewables harvest.

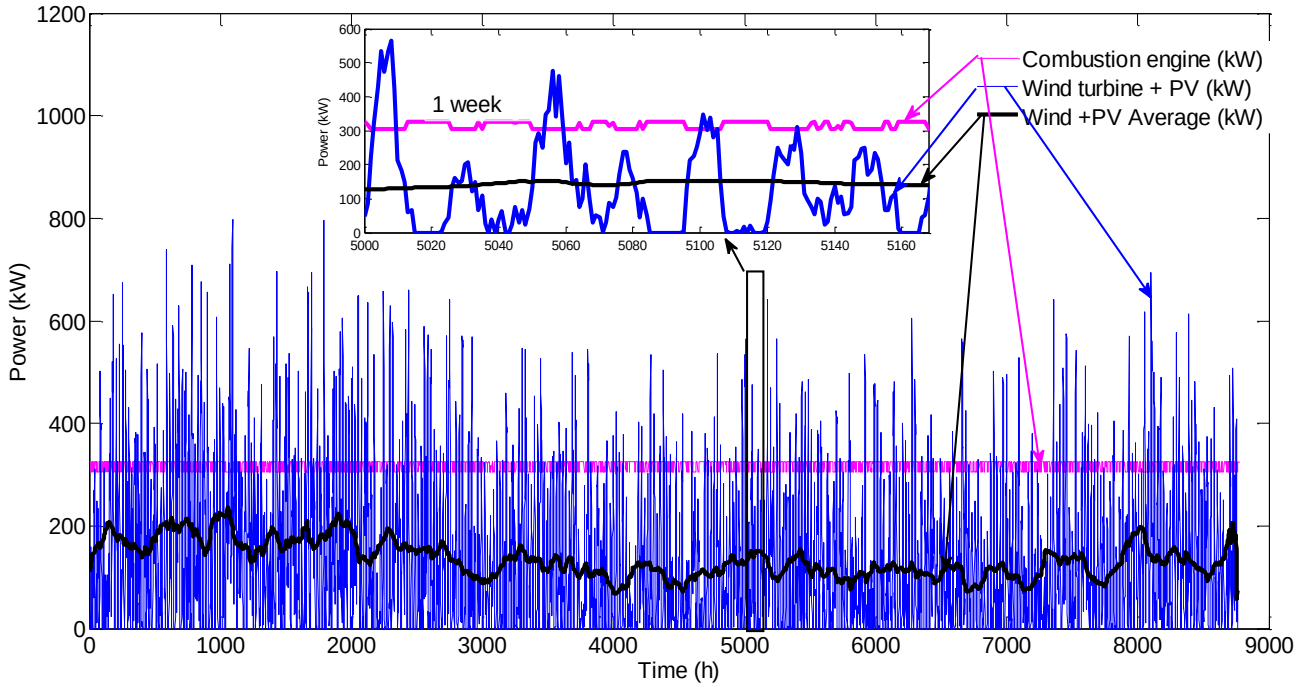

Figure 8.11: Delivered el. power of renewable sources and CHP unit

Only smoothing the annual curve by a sliding window over one week (168 hours) – black curve in Figure 8.11 – uncovers slightly higher values of electricity generation from renewables during the first quarter of the year.

However, this slight increase leads to higher surplus of electricity in the plant and, in consequence, to slightly stronger operation of the electrolyzer – black curve of sliding window in Figure 8.14 showing electrolyzer operation –, thus filling up the hydrogen storage tank within this period of time. As to be seen in Figure 8.12, during the rest of the year the hydrogen filling level is lowered by trend again. The weekly period zoomed in Figure 8.12 in detail also proves that the hydrogen storage filling level is slightly increased when the electrolyzer is operated, and decreased in other times.

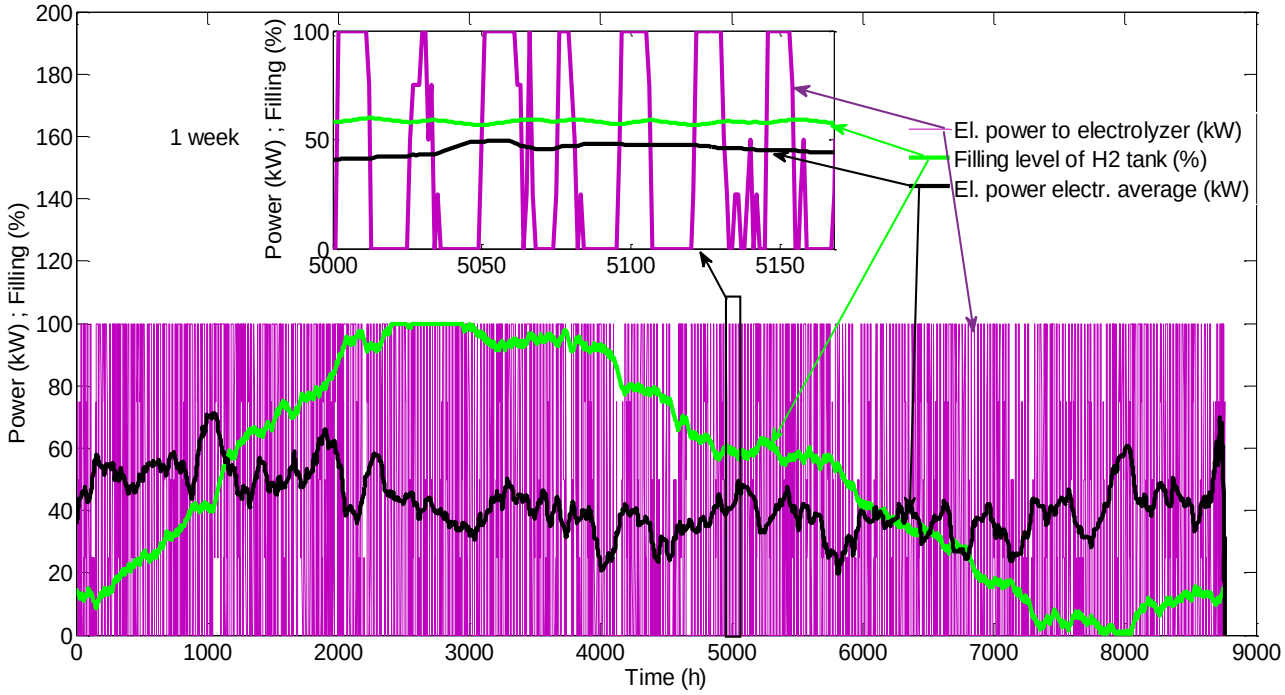

Figure 8.12: Electric power to electrolyzer and filling level of hydrogen tank

Figure 8.13 shows the power and energy exchange with the public grid. As in the German example the export energy – positive values – exceeds the import. The maximal import power is slightly lower than 100 kW at any time, resulting from situations with no renewable input, compare Table 8.2.

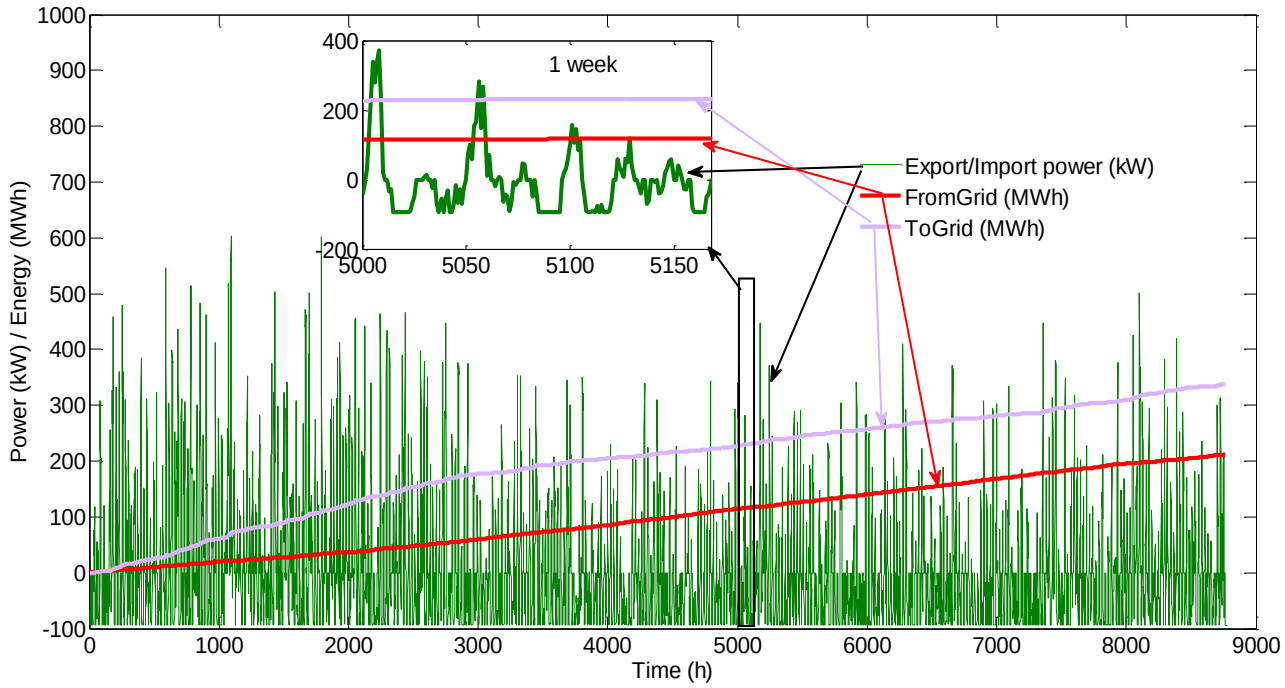

Figure 8.13: Electricity exchange with public grid

Figure 8.14 finally confirms that – except the day/night cycles of solar contribution to thermo-solar sludge drying – the thermal output power of components is fairly even all over the year – in contrast to the German example case, compare Figure 8.8.

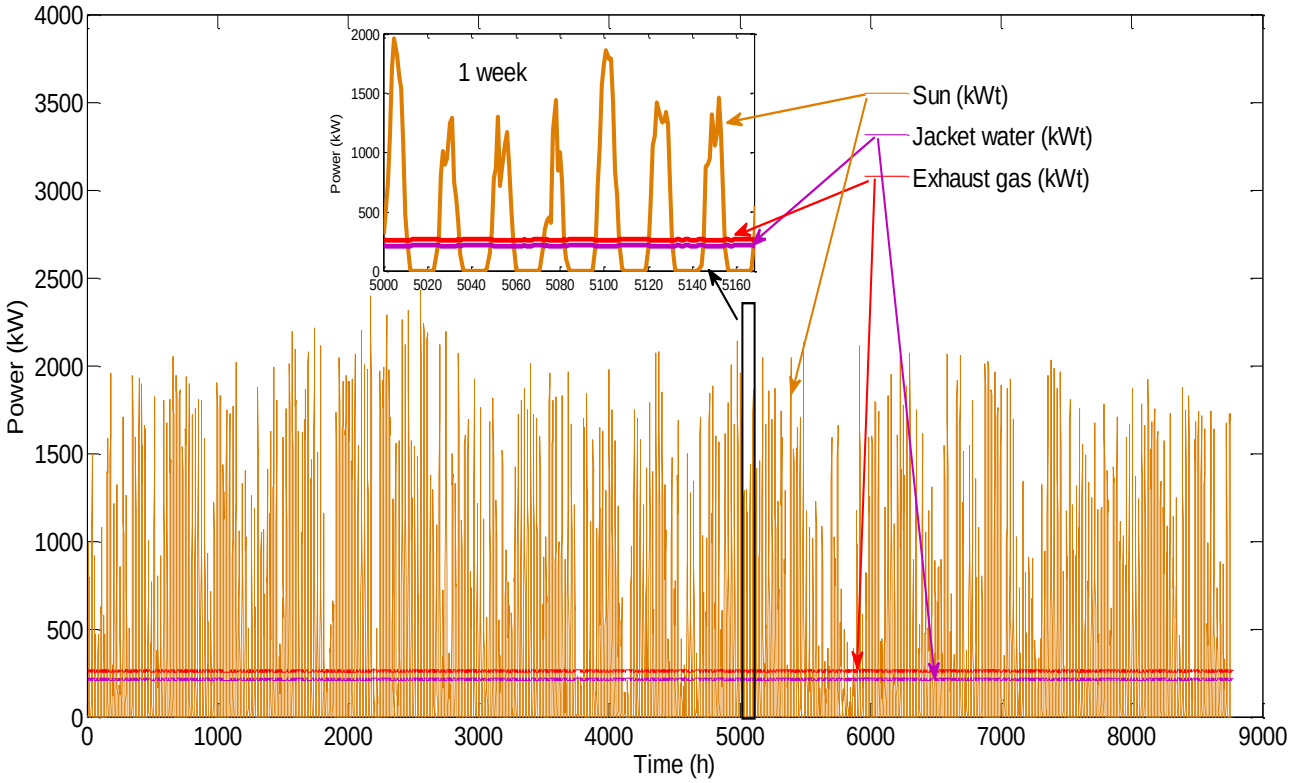

Figure 8.14: Thermal power of components

8.5.3 Annual energy balances and conclusions

In Tables 8.9 and 8.10 the global balances of both electrical and thermal energies in the considered year are summarized for both German and Vietnamese example cases, respectively; for Vietnam the most economic scenario a (wind and PV) is considered here.

Table 8.9: Energy balance of the sewage plant in one year operation (Germany)

Electricity		**Thermal energy**	
Symbol	$E = \int P_{el}(t)dt$ **(MWh)**	**Symbol**	$E = \int P_{th}(t)dt$ **(MWh)**
E_{Wind}	+1405	E_{Sun}	+1850
E_{elCH4}	+2408	E_{thCH4}	+3595
E_{elH2}	+0134	E_{thH2}	+0178
$E_{elSteam}$	+0809	$E_{thSteam}$	+2409
$E_{SmallHydro}$	+0131	$E_{TapSteam}$	+0577
$E_{FromGrid}$	+0194	$E_{thFromStorage}$	+0112
Total in	***+ 5081***	***Total in***	***+8721***
E_{ToGrid}	-0284	$E_{thToStorage}$	-0112
$E_{elToStorage}$	-0680	$E_{GlassHouse}$	-5606
E_{Load}	-4118	$E_{Digester}$	-3003
Total out	***-5082***	***Total out***	***-8721***

Table 8.10: Energy balance of the sewage plant in one year operation (Vietnam)

Electricity		**Thermal energy**	
Symbol	$E = \int P_{el}(t)dt$ **(MWh)**	**Symbol**	$E = \int P_{th}(t)dt$ **(MWh)**
E_{Wind}	+0631	E_{Sun}	+3356
E_{PV}	+0540	-	-
E_{elCH4}	+2681	E_{thCH4} • *Jacket water* • *Exhaust gas (pre-heating)*	+1891 (+2312)
E_{elH2}	+0074	E_{thH2} • *Jacket water* • *Exhaust gas (pre-heating)*	+0052 (+0064)
$E_{elSteam}$	+1041	$E_{thSteam}$	+3446
$E_{SmallHydro}$	+0094	-	-
$E_{FromGrid}$	+0211	-	-
Total in	***+5272***	***Total in***	***+8745***
E_{ToGrid}	-0338	-	-
$E_{elToStorage}$	-0346	$E_{GlassHouse}$	-7571
E_{Load}	-4588	$E_{Digester}$	-1174
Total out	***-5272***	***Total out***	***-8745***

Summarizing comparison of the contents of Tables 8.9 and 8.10 proves, that

- combustion of biogas, sludge incineration as well as small hydro largely contribute to the direct coverage of electricity demand (in total more than 80% in both example cases);
- renewables based generation directly participates in 11% (Germany, wind) and 26% (Vietnam, wind + PV) of load coverage; the majority of renewables based generation (Germany 69%, Vietnam 58%) is sent to electrolyzer and public grid for buffering;
- only 8% respectively 6% of total electricity consumption come via hydrogen (direct storage) and grid (indirect storage);
- despite considerable losses of the hydrogen storage path (efficiency ca. 20% only) this significantly contributes to energetic autonomy of the plant;
- solar irradiation delivers almost 21.5% (Germany) respectively 38% (Vietnam) of total thermal energy demand; in both cases the rest is covered by waste heat from combustion engine and steam circuit;
- in the German case the thermal situation is also well balanced, in particular by the small but essential contribution of thermal storage;
- in average, full energetic self-sufficiency of the plant can be achieved over a full year with moderate electrical energy excess exported to the public grid, which in its turn mainly stands for compensating short periods of electricity deficit as well as for providing immediate auxiliary power in case of potential failure of plant devices;
- in economic sense the excess of electricity export to grid against supply from grid compensates the discrepancy of feed-in and import tariffs;
- the simulation as such provides plausible results since, last but not least, annual integrals of both electricity and thermal energy input and output are duly compensated.

Furthermore, from Figures 8.7, 8.9 and 8.12 it can be withdrawn that the initial filling levels of storage (hydrogen and thermal where applicable) get along with similar levels at the end of annual simulation which also proves reasonability of plant operation.

9. Concluding summary and outlook

9.1 Summary

Ordinary sewage conceals an appreciable amount of energy, which can locally be exploited in order to widely cover both electricity and heat demands of a waste water purification plant. Besides prevalent state-of-the-art combustion of biogas from sludge digestion in a small combined heat and power unit, subsequent incineration of digested and solar-thermally dehydrated sludge on site constitutes another less diffused opportunity for further electricity and heat generation; moreover, the large expanse of such plants allows for additional harvest of renewable (wind and solar) energy on site.

For the typical mass streams of two medium-sized exemplary wastewater plant located in Germany and Vietnam the global electric and thermal power balances were derived; based on given annual dependencies of relevant local varying meteorological parameters in hourly resolution – which are rather different for the two chosen examples – the proper ratings of energetic components for such system including hydrogen based energy storage and – in the German case – thermal buffer were identified by use of a meta-heuristic optimization approach. Results from simulative annual operation of the example plant prove reasonable performance under significantly reduced operation cost compared to conventional external electricity supply of the sewage plant; concurrently, the operation is CO_2-neutral and exonerates from disposal of infectious sludge.

9.2 Thesis contributions

In fact, energy harvest in sewage plants is not a new topic; local combustion of biogas from digestion is prevalent at many locations, and exploitation of renewables as well as sludge incineration on the ground of a sewage plant is found incidentally, too. However, from the wastewater community the energetic contribution is often seen as a useful side effect, while in first order the sewage related aspects (e.g., getting rid of infectious sludge by incineration etcetera) are playing the principal role.

In contrast, as a novelty this thesis considers things from a pure energetic point of view by investigating the challenging approach to make a sewage plant utmost energetically independent from outside, and this at reasonable cost compared to conventional energy supply.

Therefore, in the course of this work

- an energetic simulation model of the complete plant was developed, comprising the paths of chemically bound, thermal and electrical power including generation, loads and, where applicable, energy storage;
- a clearly arranged operational surface was proposed which can be used for either the simulation or a real plant;
- a method of reasonable component dimensioning was implemented, which makes use of a state-of-the-art metaheuristic optimization approach;
- appropriate operation strategies were developed and implemented, which could be verified by plant simulation over one year in hourly steps.

9.3 Recommendations for future research

The thesis has proven that the proposed approach is practicable and economic for two examples in climatically very different countries; thus, it can be concluded that it is generally useful and meaningful. However, despite the fact that in this thesis a variety of influences and interdependencies was considered, before practical realization a much more detailed study must be performed, regarding in particular items such as

- fluctuations of the sewage input stream and consequences;
- temporal variations of the electric load (e.g. temporary operation of large pumps), which, if needed, could be smoothed out by a proper load management system;
- meteorological profiles over longer time periods than one year in order to identify possible extraordinary situations or conditions;
- specific local conditions such as ground area available for glass house, photovoltaic and/or wind generation;
- redundancy for cases of failures of system components.

The latter aspect can be intercepted by the public electricity grid if available (as assumed in this thesis, too), which may be given for many locations in practice.

Another challenging task could be the plant design for total energetic independence. In this case, besides redundancy of components, all electric power peaks have to be intercepted, which would additionally necessitate to provide a short time electricity buffer such as an accumulator battery, as well as a sound load management system.

10. References

[1] 'Electricity demand in Germany', Wikipedia

[2] 'So funktioniert eine Kläranlage (*How a sewage plant works*)', http://www.klassewasser.de/content/language1/downloads/schuelerbogen_klaerwerk.pdf ; accessed on Feb. 9, 2015

[3] Sundin, A. M.: 'Disintegration of sludge – A way of optimizing anaerobic digestion', 13th European Biosolids & Organic Resources Conference & Workshop, Lidingö (Sweden), 2008

[4] 'Sewer systems', http://ec.europa.eu/environment/europeangreencapital/wp-content/uploads/2015/06/08_Application-EGC-2017_Water-Management_ESSEN.pdf ; accessed on Oct. 9, 2015

[5] Götzelmann, W., Rölle, R.: 'Klärschlamm und biogene Reststoffe als Energieträger', Fachtagung Energie, Stuttgart (Germany), 2008

[6] 'Aerobic and Anaerobic Digestion and Types of Decomposition', http://munty13.blogspot.de/2014/07/lesson-4-aerobic-and-anaerobic.html ; accessed on Apr. 8, 2016

[7] 'Digesters', Wikipedia

[8] Schreff, D.: 'Überlegungen zum wirtschaftlichen Einsatz der anaeroben Schlammstabilisierung in Kläranlagen', Ingenieurbüro für Wasser, Abwasser und Energie, Irschenberg (Germany), 2015

[9] Frey, W.: 'Stand und Trends bei der Faulgasverwertung auf Kläranlagen', ÖWAV-TU Seminar „Standortbestimmung in der Wassergütewirtschaft", 28.-29. Februar 2012, Wiener Mitteilungen Band 226, Wien (Austria), 2012

[10] Barjenbruch, M.: 'Overview of sludge treatment and disposal', TU Berlin (Germany), Dep. Urban Water Management, 2007

[11] Kügler, I., Öhlinger, A., Walter, B.: 'Dezentrale Klärschlammverbrennung', Umweltbundesamt, Wien (Austria), 2004

[12] Samolada, M. C., Zabaniotou, A. A.: 'Comparative assessment of municipal sewage sludge incineration, gasification and pyrolysis for a sustainable sludge-to-energy management in Greece', Waste Management 34 (2014) 411- 420, ELSEVIER (UK)

[13] 'Wastewater', http://www.eglv.de/en/waterportal/river-basin-management/wastewater-treatment/wastewater.html , accessed on Feb. 9, 2015

[14] 'Values of wastewater', Wikipedia

[15] Rodrigo, M. A., Canizares, P., Lobato, J., Raz, R., Saez, C., Linares, J.-J.: 'Production of electricity from the treatment of urban waste water using a microbial fuel cell', Journal of Power Sources 169 (2007) 198-204, ELSEVIER (UK)

[16] Lenz, G.: 'Training of sewage treatment plant staff', http://www.nb610.dwa-bayern.de/portale/bay-nb-610/bay-nb-610.nsf/C12573C400450D1E/AFDF901AAF9C1371C12574DE0034676F/$FILE/quali_personal.pdf ; accessed on Apr. 5, 2016

[17] Bodik, I., Sedlacek, S., Kubaska, M., Hutnan, M.: 'Biogas production in municipal wastewater treatment plants; current status in EU with a focus on the Slovak Republic', Chem. Biochem, Eng. Q. 25 (3) 335-340 (2011), Slovak University of Technology, Bratislava (Slovak Republic)

[18] 'Chemical Oxygen Demand value', www.atv-dvwk.de ; accessed on Feb. 9, 2015

[19] Haberkern, B., Maier, W., Schneider, U.: 'Steigerung der Energieeffizienz auf kommunalen Kläranlagen', Umweltbundesamt, Stuttgart (Germany), March 2008

[20] Agis, H.: 'Energieoptimierung von Kläranlagen Pilotprojekt'- Detailuntersuchung von 21 Anlagen Endbericht Teil A, AEC Consulting, Wien (Austria), November 2001

[21] Reinholz, J.: 'Energieverbrauch und Energieerzeugung in Thüringer Kläranlagen', Ministerium für Landwirtschaft, Forsten, Umwelt und Naturschutz, Erfurt (Germany), 2011

[22] Haberkern, B.: 'Energiepotenziale auf Kläranlagen', DWA-Fachtagung Energie, Darmstadt (Germany), June 2008

[23] Dicht, N., Bauerfeld, K.: 'Klärschlamm - weltweites Problem oder wertvolle Ressource? ', Expoval-9. BMBF Forum für Nachhaltigkeit, Berlin (Germany), October 2012

[24] Werner, H. J.: 'Wirtschaftlicher Nutzen thermischer Klärschlammverwertung mittels Klärschlammvergasung', German Water Partnership, Berlin (Germany), April 2012

[25] Lindtner, S.: 'Leitfaden für die Erstellung eines Energiekonzeptes kommunaler Kläranlagen /(*Guideline for the development of an energy concept for municipal wastewater treatment*

plants)‘, Kommunalkredit Public Consulting GmbH, Wien (Austria), April 2008, http://www.publicconsulting.at/uploads/energieleitfaden_endversion.pdf ; accessed on Jan. 14, 2015

[26] Ekama, G. A., Sotemann, S. W., Wentzel, M. C.: ‘Biodegradability of activated sludge organics under anaerobic conditions’, *Water Res.* 2007, *41*, 244–252, ELSEVIER (UK)

[27] Rosso, D., Stenstrom, M. K.: ‘The carbon-sequestration potential of municipal wastewater treatment’, *Chemosphere* 2008, *70*, 1468–1475, ELSEVIER (UK)

[28] Stoica, A., Sandberg, M., Holby, O.: ‘Energy use and recovery strategies within wastewater treatment and sludge handling at pulp and paper mills’, *Bioresource Technol.* 2009, *100*, 3497–3505, ELSEVIER (UK)

[29] ‘WÄRTSILÄ’ , http://www.wartsila.com/en/power-plants/highlights ; accessed on Sep. 5, 2014

[30] ‘Dry Substance Ratio’, Wikipedia

[31] Aghbashlo, M., Kianmehr, M.-H, Arabhosseini, A.: ‘Performance analysis of drying of carrot slices in a semi-industrial continuous band dryer’, Journal of Food Engineering, 91 (2009) 99-108, ELSEVIER (UK)

[32] Bogner, R., Faulstich, M., Mocker, M., Quicker, P.: ‘sluge2energy - dezentrale Klärschlammverwertungsanlage zur Erzeugung von thermischer und elektrischer Energie (decentralized sewage sludge exploitation to generate thermal and electrical energy)‘, Hans Huber AG - HUBER Technology, Sulzbach-Rosenberg (Germany), 2005

[33] Eisenmann, ‘Pyrobustor system’, www.eisenmann.de ; accessed on Feb. 27, 2015

[34] ‘Steam turbine’, Predesigned Steam Turbine SST-040, http://www.energy.siemens.com/hq/pool/hq/power-generation/steam-turbines/SST-040/Downloads/Siemens-Industrial-Steam-Turbine-SST-040-EN.pdf ; accessed on Feb. 27, 2014

[35] Mulijadi, E., Sallan, J., Sanz, M., Butterfield, C.: ‘Investigation of Self-Excited Induction Generators for Wind Turbine Applications’, IEEE Industry Applications Society, Annual Meeting, Phoenix-Arizona (USA), October 1999

[36] Druga, M., Nichita, C., Barakat, G., Ceanga, E.: ‘Stand-Alone Wind Power System Operating with a Specific Storage Structure’, International Conference on Renewable Energies and Power Quality (ICREPQ’09), Valencia (Spain), 15th to 17th April, 2009

[37] Zizmann, R.: 'EDZ Trocknungsverfahren', Passavant Geiger GmbH, Limburg (Germany), www.passavant-geiger.de ; accessed on Apr. 15, 2015

[38] Jacobs, U.: 'Machbarkeitsstudie inklusive der technischen Vorplanung zur Klärschlammtrocknung und nachhaltigen Klärschlammentsorgung im Verbandsgebiet des ZVO', EcoSystem/International ESI, Grömitz (Germany), June 2012

[39] Ritterbusch, S.: 'Solare und Abwärmegestützte Klärschlammtrocknung', Technik und Praxisbeispiele, Thermo-System GmbH, Stuttgart (Germany), 2009

[40] Müßig, M.: 'Solare Klärschlammtrocknung auf den Inseln Pellworm, Sylt und Föhr, am Beispiel der Kläranlagen', Abschlussbericht, Ingenieurgesellschaft Steinburg, Itzehoe (Germany), February 2004

[41] Quentmeier, V.: 'Solare Klärschlamm-Trocknung', elementis consult Ingenieur GmbH, Saarbrücken (Germany), 2005

[42] Zizmann, R.: 'Das EDZ-Trocknungsverfahren eröffnet neue Chancen: Vom Nassschlamm zum Brennstoffgranulat. Zur Verwertung in Zementwerken und Kohlekraftwerken. (*The EDC-drying process opens up new opportunities: from the wet sludge to fuel pellets. For recovery in cement plants and coal power plants*)', Bilfinger-Berger Umwelttechnik, Limburg (Germany), June 2006, http://www.stadtentwaesserung-kaiserslautern.de/media/files/SEK/PDF/Fachtagung_2006/Zizmann.pdf ; accessed on Jan. 14, 2015

[43] 'Solar collectors', Wagner & Co, http://uk.wagner-solar.com/ ; accessed on Jan. 14, 2015

[44] 'Heat pump', Bosch Thermotechnik GmbH - Junkers Deutschland, http://www.junkers.com/endkunde/produkte/produktkategorie_10112 ; accessed on Jan. 14, 2015

[45] Akagi, H.: 'Active filters and energy storage systems for power conditioning in Japan', in Proc. 1st Int. Conf. Power Electron. Syst. and Appl., 2004, pp. 80–88 (USA)

[46] Blocquel, A., Janning, J.: 'Analysis of a 300 MW variable speed drive for pump-storage plant applications', 2005 European Conference on Power Electronic and Applications, Dresden (Germany), September 2005

[47] R&D Priorities and Gaps: 'Hydrogen production and storage', IEA – Hydrogen Co-ordination group, OECD/IEA, Paris (France), 2006

[48] Takeichi, N., Senoh, H., 'Hydrid Hydrogen Storage Vessel, a Novel High-pressure Hydrogen Storage Vessel Combined with Hydrogen Storage Material', International Journal of Hydrogen Energy, 2003, 28, pp. 1121-1129, PERGAMON (UK)

[49] 'Small hydro generation', http://www.engineeringtoolbox.com/ ; accessed on Sep. 5, 2014

[50] Venkatesh, G., Elmi, R.-A.: 'Economic-environmental analysis of handling biogas from sewage sludge digesters in WWTPs for energy recovery: Case study of Bekkelaget WWTP in Oslo (Norway)', Energy 58 (2013) 220-235, ELSEVIER (UK)

[51] Kenichi Kuroda Fuji Electric systems Co., Ltd: ' Present and Future of PAFC at Fuji Electric', 4th IPHE Workshop – Stationary Fuel Cells, 1st March 2011, Tokyo (Japan) http://www.iphe.net/docs/Events/Japan_3-11/3%20Kuroda_FujiElectric.pdf ;accessed on Feb. 5, 2015

[52] Roux, N., Jung, D., Pannejon, J., Lemoine, C.:' Modeling of the solar sludge drying process Solia', 20th European Symposium on Computer Aided Process Engineering – ESCAPE20, Naples (Italy), 2010

[53] Cooper, J. R., IAPWS REGIONS: 'Revised Release on the IAPWS Industrial Formulation 1997 for the Thermodynamic Properties of Water and Steam', Lucerne (Switzerland), August 2007

[54] Wang, C., Nehrir, M.-H.: 'Power management of a stand-alone wind/photovoltaic/fuel cell energy system', IEEE Transaction on Energy Conversion, vol., 23. No. 3, (USA), September 2008

[55] 'Power production of a typical wind turbine', Wikipedia

[56] Alireza, K., Somaieh, A. Z.: 'Sizing of rock fragmentation modeling due to bench blasting using adaptive neuro-fuzzy inference system (ANFIS)', International Journal of Mining Science and Technology 23 (2013) 809-813, ELSEVIER (UK)

[57] 'ANFIS and Neuro-Fuzzy Designer', MATLAB ANFIS toolbox, http://de.mathworks.com/help/fuzzy/anfis.html?requestedDomain=www.mathworks.com ; accessed on Apr. 15, 2016

[58] 'IDE visual studio 2013', https://www.visualstudio.com/ ; accessed on Mar. 17, 2015

[59] 'KEPServerEx', https://www.kepware.com/products/kepserverex/documents/kepserverex-manual/ ; accessed on Mar. 7, 2015

[60] 'OPC Foundation', Wikipedia

[61] Nakawiro, W., Erlich, I., Rueda, J. L.: 'A Novel Optimization Algorithm for Optimal Reactive Power Dispatch: A Comparative Study', 2011 4th International Conference on Electric Utility Deregulation and Restructuring and Power Technologies (DRPT), IEEE, Shandong (China)

[62] Rueda, J. L., Cepeda, J. C., Erlich, I.: 'Estimation of Location and Coordinated Tuning of PSS based on Mean-Variance Mapping Optimization', WCCI 2012 IEEE World Congress on Computational Intelligence, June, 10-15, 2012, Brisbane (Australia)

[63] 'Demo MVMO (Mean Variance Mapping Optimization)', https://www.uni-due.de/mvmo/ ; accessed on Feb. 27, 2013

[64] Cepeda, J. C., Rueda, J. L., Erlich, I.: 'Identification of Dynamic Equivalents based on Heuristic Optimization for Smart Grid Applications', WCCI 2012 IEEE World Congress on Computational Intelligence, June, 10-15, 2012, Brisbane (Australia)

[65] Truong, N. H., Krost, G.: 'Metaheuristic Based Device Rating for Energy Harvest in Sewage Plant', Conference 'Intelligent Applications to Power Systems' (ISAP), Porto (Portugal), September 2015

[66] Pollesböck, F.: 'Stoffliche Bilanzierung der Kläranlage Knittelfeld und Umgebung', Bachelor Thesis, University of Leoben (Austria), September 2012

[67] Sedlar, C., Zethner, G., Chovanec, A.: 'Energienutzung von Klärschlamm', Umweltbundesamt, Wien (Austria), ISBN 3-85457-154-2, Dezember 1991

[68] 'CHP - Efficiency', http://www.wartsila.com/en/Home ; accessed on Mar. 4, 2015

[69] Pabsch, H., Wendland, C.: 'Sewage sludge treatment', Project funded by European Union, Institute of Wastewater Management, Hamburg (Germany), 1992

[70] Cho, H. U., Park, S. K., Ha, J. H., Park, J. M.: 'An innovative sewage sludge reduction by using a combined mesophilic anaerobic and thermophilic aerobic process with thermal-alkaline treatment and sludge recirculation', Journal of Environmental Management 129 (2013) 274-282, ELSEVIER (UK)

[71] Koenen, S.: 'Energieanalysen', Tuttahs & Meyer Engineering, Bochum (Germany), 2011

[72] Winkler, M. K. H., Bennenbroek, M. H., Horstink, F. H.: 'The biodrying concept: An innovative technology creating energy from sewage sludge', Bio-resource Technology 147 (2013) 124-129, ELSERIER (UK)

[73] Schreff, D., 'Klärschlammtrocknung: Technologien und aktuelle Konzepte', DWA Bayern – Lehrerfortbildung, München (Germany), 2008

[74] Machbarkeitsstudie: 'Perspektiven der solaren Klärschlammtrocknung im Land Bremen', Bremer Energie-Konsens GmbH, Bremen (Germany), June 2005

[75] Bennamoun, L.: 'Solar drying of wastewater sludge: A review', Renewable and Sustainable Energy Reviews, Algeria 2011, 16 (2012) 1061-1073, ELSEVIER (UK)

[76] Chae, K. J., Kang, J.: 'Estimating the energy independence of a municipal wastewater treatment plant incorporating green energy resources', Energy Conversion and Management 75 (2013) 664-672, ELSEVIER (UK)

[77] 'Small thermal steam power plant', http:// www.siemens.com/energy/steamturbines ; accessed on Feb. 27, 2014

[78] 'Irradiation profiles' and 'Wind speed profiles', http://www.homerenergy.com/software.html ; accessed on Jan. 14, 2015

[79] Khan, M. J., Iqbal, M. T.: 'Dynamic modeling and simulation of a small wind-fuel cell hybrid energy system', Renewable Energy 30 (2005) 421-439, ELSEVIER (UK)

[80] Görgün, H.: 'Dynamic modeling of a proton exchange membrane (PEM) electrolyzer', International Journal of Hydrogen Energy 31 (2006) 29-38, ELSEVIER (UK)

[81] Vatopoulos, K., Andrews, D., Carlsson, J., Papaioannou, I., Zubi, G.: 'Study on the state of play of energy efficiency of heat and electricity production technologies', European Commission – JRC Scientific and Policy reports, Petten (The Netherlands) 2012

[82] Alkaline Electrolyzer : 'High temperature hydrogen production process', http://www.ieahia.org/pdfs/Task25/alkaline-electrolysis.pdf ; accessed on Aug. 28, 2015

[83] Kabus, M.: 'Wirtschaftlichkeitsbetrachtung für den Einsatz von Kraft-Wärme-Kopplungsanlagen mit fossilen Brennstoffen (*Economic evaluation of the use of cogeneration plants using fossil fuels*)',EnergiAgen-NRW, Wuppertal (Germany), February 2013

[84] Theilen, U.: ‚Schlammfaulung auf mittelgroßen Kläranlagen; Wirtschaftlichkeit und Perspektiven', KompetenzZentrum Energie und Umwelt SystemtechnikZeuUS - Technische Hochschule Mittelhessen, Giessen (Germany), 2013

11. APPENDICES

Appendix A2.1: Electrical and thermal energy in wastewater plants [25]

a) Electrical energy indicators

Spez. elektrische Energiebereitsstellung			Normalbereich	
el. Energie aus Faulgas erzeugt	19,7	kWh/EW$_{120}$/a	*10*	*20*
sonstige el. Energie auf ARA erzeugt	0,0	kWh/EW$_{120}$/a	-	-
el. Energie zugekauft	9,3	kWh/EW$_{120}$/a	*10*	*50*
el. Energie ans EVU geliefert	3,5	kWh/EW$_{120}$/a	*0*	*20*
el. Energie bereitgestellt	25,5	kWh/EW$_{120}$/a	*20*	*50*

spez. elektrischer Energieverbrauch			Normalbereich	
Kläranlage gesamt	**25,5**	**kWh/EW$_{120}$/a**	*20*	*50*
1) Zulaufpumpwerk und mechanische Vorreinigung	**4,2**	**kWh/EW$_{120}$/a**	*2,5*	*5,5*
1.1 Zulaufpumpwerk	2,4	kWh/EW$_{120}$/a	*1,5*	*3,5*
1.2 Rechen	0,8	kWh/EW$_{120}$/a	*0,5*	*1*
1.3 Sand- u. Fettfang	1,1	kWh/EW$_{120}$/a	*0,5*	*1*
2) Mechanisch-biologische Abwasserreinigung	**14,9**	**kWh/EW$_{120}$/a**	*14,5*	*33*
2.1 Belüftung	9,9	kWh/EW$_{120}$/a	*11,5*	*22*
2.2 Rührwerk	1,2	kWh/EW$_{120}$/a	*1,5*	*4,5*
2.3 RS-Pumpen	2,5	kWh/EW$_{120}$/a	*1*	*4,5*
2.4 Sonstiges (VKB, NKB,...)	1,2	kWh/EW$_{120}$/a	*0,5*	*2*
3) Schlammbehandlung	**2,8**	**kWh/EW$_{120}$/a**	*2*	*7*
3.1 MÜSE und stat. Eindicker	0,5	kWh/EW$_{120}$/a	*0,5*	*1*
3.2 Faulung	1,9	kWh/EW$_{120}$/a	*1*	*2,5*
3.3 Schlammentwässerung	0,5	kWh/EW$_{120}$/a	*0,5*	*3,5*
4) Infrastruktur	**3,6**	**kWh/EW$_{120}$/a**	*1*	*4,5*
4.1 Heizung	1,0	kWh/EW$_{120}$/a	*0*	*2,5*
4.2 sonstige Infrastruktur	2,6	kWh/EW$_{120}$/a	*1*	*2*

sonstige elektrische Energiekennzahlen			Normalbereich	
Eigenstromabdeckung	77	%	*0*	*100*
WG-Zulaufpumpen	44	%	*30*	*70*
spez. Rührenergie	1,5	W/m³	*1*	*2,5*
belastungsspez. Energieverbrauch von Belüften+Rühren	0,25	kWh/kg$_{CSBBiologie\ zu}$	*0,3*	*0,6*
elektrischer Wirkungsgrad BHKW	36	%	**24**	**38**

Energiekennzahlen für Belüftungsenergie		
Kohlenstoffatmung (OVC) berechnet	2431	kg/d
OVC/CSBzu	0,18	-
denitrifizierte Stickstofffracht (DN)	944	kg/d
Gesamtatmung (OV)	4579	kg/d
erforderliche Belüftungsenergie max	10	kWh/EW$_{120}$/a
erforderliche Belüftungsenergie min	5	kWh/EW$_{120}$/a

b) Thermal energy indicators

spez. thermische Energiebereitsstellung			Normalbereich	
therm. Energie aus Faulgas erzeugt	22,3	kWh/EW/a	*20*	*40*
sonstige therm. Energie auf ARA erzeugt	0,0	kWh/EW/a	-	-
therm. Energie ans EVU geliefert	0,0	kWh/EW/a	-	-
therm. Energie bereitgestellt	**22,3**	**kWh/EW/a**	*0*	*40*

spez. thermischer Energieverbrauch (=Wärmeverbrauch)			Normalbereich	
Kläranlage gesamt	**22,0**	**kWh/EW/a**	*0*	*30*
Schlammaufheizung (Qs)	12,1	kWh/EW/a	*8*	*12*
Transmissionsverluste, Faulbehälterbeheizung (Q_T)	2,8	kWh/EW/a	*0*	*4*
Erzeugungs-, Speicher- und Verteilungsverluste (Q_V)	1,5	kWh/EW/a	*0*	*2*
Wärmemenge für Gebäude ($Q_{Gebäude}$)	0,3	kWh/EW/a	0	2
Wärmemenge für Zuluftgeräte (Q_{Zuluft})	5,2	kWh/EW/a	*0*	*10*

sonstige thermische Energiekennzahlen		Normalbereich	
therm. Wirkungsgrad BHKW	40 %	*50*	*65*

Appendix A7.1: An example of setting parameters for Mean-Variance Mapping Optimization – MVMO (MATLAB code):

```
parameter.MaxEval = 400; % max no. of function evaluations
parameter.mode =1; %Selection strategy for offspring creation
parameter.n_tosave = 5; %Population to be stored in the table
parameter.n_random = 5; %Dimensions/control variables selected for mutation
operation
parameter.n_random_end = 1; %Final dimension change
parameter.n_randomly_freq = 100000; %FE number after which the selected
variables are changed
parameter.fs_factor_start = 1; %Initial scaling factor
parameter.fs_factor_end = 1; %Final scaling factor
parameter.dddd = 1;  %Initial value of the shape factor
parameter.delta_dddd = 1.05;
parameter.n_var = 5; % Total no. of control variables
parameter.ncon_var =  5; % No. of continuous variables
parameter.ndis_var = parameter.n_var-parameter.ncon_var; % no. of discrete
variables
parameter.n_constr = 3; % no. of constraints
% Min and max limits of control variables
min1= [0944  084  39000  0812  15.5 ];
max1= [1300  120  45000  1000  30 ];
parameter.x_min = min1+zeros(1,parameter.n_var);%-2.048*ones(1,30)
parameter.x_max = max1+zeros(1,parameter.n_var);%2.048*ones(1,30)
```

Appendix A8.1: Optimization of German case

Objective function:

$$C_{Total.} = \sum (x_1 + x_2 + x_3 + x_4 + x_5 + x_6 + \Sigma C_{Constant}) ==> \min$$

$$with:$$

$$*x_1 = C_{Wind} \cdot N_{Wind} \Rightarrow N_{Wind} = \frac{x_1}{C_{Wind}}$$

$$*x_2 = C_{elToStorage} \cdot N_{elToStorage} \Rightarrow N_{elToStorage} = \frac{x_2}{C_{elToStorage}}$$

$$*x_3 = C_{elStorage} \cdot E_{elStorage} \Rightarrow E_{elStorage} = \frac{x_3}{C_{elStorage}}$$

$$with\ E_{elStorage} = \{\max(\int(0.95 \cdot 0.6 \cdot P_{elToStorage}(t) - \frac{1}{0.35} \cdot P_{Comb.H_2}(t))dt) - \\ - \min(\int(0.95 \cdot 0.6 \cdot P_{elToStorage}(t) - \frac{1}{0.35} \cdot P_{Comb.H_2}(t))dt)\} \quad (11.1)$$

$$*x_4 = C_{Grid}.N_{Grid} + 0.17 \cdot \int P_{FromGrid}(t)dt - 0.12 \cdot \int P_{ToGrid}(t)dt$$

$$\Rightarrow N_{Grid} = \frac{x_4 - 0.17 \cdot \int P_{FromGrid}(t)dt + 0.12 \cdot \int P_{ToGrid}(t)dt}{C_{Grid}}$$

$$with\ N_{Grid} = \max\{P_{ToGrid}(t), P_{FromGrid}(t)\}$$

$$*x_5 = C_{Comb} \cdot N_{Comb.H_2} \Rightarrow N_{Comb.H_2} = \frac{x_5}{C_{Comb.H_2}}$$

$$*x_6 = C_{thStorage} \cdot E_{thStorage} \Rightarrow E_{thStorage} = \frac{x_6}{C_{thStorage}}$$

$$with\ E_{thStorage} = \{\max(\int(P_{thToStorage}(t) - P_{thFromStorage}(t))dt) - \\ - \min(\int(P_{thToStorage}(t) - P_{thFromStorage}(t))dt)\} \ \leq \text{ Max. MWh}$$

Variables:

- C_i and N_i respectively E_i *(i=1:6)*: capital cost and assigned power respectively energy ratings of particular plant devices;
- Factors 0.95, 0.6 and 0.35: efficiencies in the hydrogen storage path of inverter, electrolyzer and combustion engine, respectively;
- $\Sigma C_{Constant}$: cost of all components having been rated before the optimization such as steam circuit, base power of combustion engine, glass house etcetera; typical values used for the optimization see Table 8.1.

Subjections:

1. El. power balance at any hourly time interval:

$$\begin{aligned}&\{P_{Wind}(t)+P_{elSteam}(t)+P_{SmallHydro}(t)+\\&P_{elCH4}(t)+P_{elH2}(t)+P_{FromGrid}(t)\}\geq\\&\geq\{P_{Load}(t)+P_{elToStorage}(t)+P_{ToGrid}(t)\}\end{aligned} \tag{11.2}$$

where:

- P_{Wind}: varying output of wind generation;
- $P_{elSteam}$: electrical output of the steam process, eventually diminished in case of steam tapping ($0 \leq Tap(t) \leq 40\%$);
- $P_{SmallHydro}$: constant output of the small hydro plant;
- P_{elCH4}: constant partial output of the combustion engine driven generator from methane gas;
- P_{elH2}: varying additive output from supplementary combustion of hydrogen;
- $P_{FromGrid}$: varying grid import power;
- P_{Load}: constant electric load;
- $P_{elToStorage}$: varying el. power fed to the electrolyzer;
- P_{ToGrid}: varying grid export power.

2. Thermal power balance at any hourly time interval:

$$\begin{aligned}&\{P_{thSteam}(t)+P_{thCH4}(t)+\\&+P_{thH2}(t)+P_{Sun}(t)+P_{thFromStorage}(t)\}\geq\\&\geq\{P_{Digester}(t)+P_{GlassHouse}(t)+P_{thToStorage}(t)\}\end{aligned} \tag{11.3}$$

where:

- $P_{thSteam}$: heat power from the steam turbine's condenser plus in case of steam tapping the tapped heat;
- P_{thCH4}: heat power of the combustion engine resulting from constant feed of methane gas;
- P_{thH2}: additional varying heat power of the combustion engine caused by supplementary feed of hydrogen gas;
- P_{Sun}: varying sun power through the glass house;
- $P_{thFromStorage}$: varying output of thermal storage;
- $P_{Digester}$: heat demand of the digester for biogas generation – varying with sludge input temperature;
- $P_{GlassHouse}$: heat demand of the glass house for sludge drying – assumed to be constant;
- $P_{thToStorage}$: varying charge power of the thermal storage.

3. The wind turbine power harvest must cover the power for hydrogen conversion and the power exported to the grid at any time interval:

$$P_{Wind}(t) \geq \{P_{elToStorage}(t) + P_{ToGrid}(t)\} \tag{11.4}$$

where:

- P_{Wind}: varying el. power from wind turbine;
- $P_{elToStorage}$: varying power sent to the electrolyzer;
- P_{ToGrid}: varying power sent to the public grid.

Appendix A8.2: Optimization of Vietnam case

Objective function:

$$
\begin{aligned}
&C_{Total.} = \sum (x_1 + x_2 + x_3 + x_4 + x_5 + x_6 + \Sigma C_{Constant}) ==> \min \\
&with: \\
&*x_1 = C_{Wind} \cdot N_{Wind} \Rightarrow N_{Wind} = \frac{x_1}{C_{Wind}} \\
&*x_2 = C_{PV} . N_{PV} \Rightarrow N_{PV} = \frac{x_2}{C_{PV}} \\
&*x_3 = C_{ToStorage} \cdot N_{ToStorage} \Rightarrow N_{ToStorage} = \frac{x_3}{C_{ToStorage}} \\
&*x_4 = C_{elStorage} \cdot E_{elStorage} \Rightarrow E_{elStorage} = \frac{x_4}{C_{elStorage}} \\
&\quad with\ E_{elStorage} = \{\max(\int (0.95 \cdot 0.6 \cdot P_{elToStorage}(t) - \frac{1}{0.35} \cdot P_{Comb.H_2}(t))dt) - \\
&\qquad\qquad - \min(\int (0.95 \cdot 0.6 \cdot P_{elToStorage}(t) - \frac{1}{0.35} \cdot P_{Comb.H_2}(t))dt)\} \\
&*x_5 = C_{Comb} \cdot N_{Comb.H_2} \Rightarrow N_{Comb.H_2} = \frac{x_5}{C_{Comb}} \\
&*x_6 = C_{Grid} . N_{Grid} + 0.12 \cdot \int P_{FromGrid}(t)dt - 0.09 \cdot \int P_{ToGrid}(t)dt \\
&\qquad \Rightarrow N_{Grid} = \frac{x_6 - 0.12 \cdot \int P_{FromGrid}(t)dt + 0.09 \cdot \int P_{ToGrid}(t)dt}{C_{Grid}} \\
&\qquad with\ N_{Grid} = \max\{P_{ToGrid}(t), P_{FromGrid}(t)\}
\end{aligned}
\tag{11.5}
$$

Variables:

C_i and N_i respectively E_i *(i=1:6)*: capital cost and assigned power respectively energy ratings of particular plant devices;

0.95, 0.6 and 0.35 (for x_4): efficiencies of hydrogen path components;

0.09 and 0.12 (for x_6): grid infeed/supply tariffs (in €/kWh) as given in Table 8.1;

$\Sigma C_{Constant}$: cost of all components having been rated before the optimization such as steam circuit, base power of combustion engine, glass house etcetera; typical values used for the optimization are entered in Table 8.1.

The optimization variables x_1 ... x_6 can also be found in Figure 8.2.

Subjections:

1. El. power balance at any hourly time interval:

$$\{P_{Wind}(t) + P_{PV}(t) + P_{elSteam}(t) + P_{SmallHydro}(t) + P_{elCH4}(t) + P_{elH2}(t) + P_{FromGrid}(t)\} \geq \geq \{P_{Load}(t) + P_{elToStorage}(t) + P_{ToGrid}(t)\} \quad (11.6)$$

where: P_{Wind} is the varying output of wind generation;

P_{PV} is the varying output of photovoltaic;

$P_{elSteam}$ is the constant electrical output of the steam process;

$P_{SmallHydro}$ is the constant output of the small hydro plant (10 kW);

P_{elCH4} is the constant partial output of the combustion engine driven generator from methane gas (306 kW);

P_{elH2} is its varying additive output from supplementary combustion of hydrogen;

$P_{FromGrid}$ is the varying grid import power;

P_{Load} is the constant electric load;

$P_{elToStorage}$ is the varying el. power fed to the electrolyzer;

P_{ToGrid} is the varying grid export power.

2. Thermal power balance at any hourly time interval:

$$\{P_{thSteam}(t) + P_{thCH4}(t) + P_{thH2}(t) + +P_{Sun}(t)\} \geq \{P_{Digester}(t) + P_{GlassHouse}(t)\} \quad (11.7)$$

where: $P_{thSteam}$ is the heat power of the steam turbine's condenser;

P_{thCH4} is the heat power of the combustion engine resulting from constant feed of methane gas (479 kW);

P_{thH2} is the additional varying heat power of the combustion engine caused by supplementary feed of hydrogen gas;

P_{Sun} is the varying sun power through the glass house;

$P_{Digester}$ is the heat demand of the digester for biogas generation varying with seasons;

$P_{GlassHouse}$ is the total heat demand of the glass house for sludge drying – assumed to be constant at 716 kW.

3. The wind turbine and photovoltaic power harvest must cover the power for hydrogen conversion and the power exported to the grid at any time interval:

$$P_{Wind}(t) + P_{PV}(t) \geq P_{elToStorage}(t) + P_{ToGrid}(t) \tag{11.8}$$

where: P_{Wind} is the varying el. power from wind turbine;

P_{PV} is the varying el. power from photovoltaic;

$P_{elToStorage}$ is the varying power sent to the electrolyzer;

P_{ToGrid} is the varying power sent to the public grid.

Curriculum Vitae

Personal data	
Name:	**Truong, Ngoc Hung**
Gender:	**Male**
Date, place of birth:	**April, 20th, 1980 , Tuy Phuoc district, Binh Dinh province, Vietnam**
Nationality:	**Vietnam**
Marital status:	**Married + 2**
School education	
1986 ~ 1991	**Attended the Primary school, Tuy Phuoc district, Binh Dinh province, Vietnam**
1991 ~ 1995	**Attended the Middle school, Tuy Phuoc district, Binh Dinh province, Vietnam**
1995 ~ 1998	**Attended the High school, Tuy Phuoc district, Binh Dinh province, Vietnam**
Study	
1998 ~ 2003	**Undergraduate student, Faculty of electrical and electronic engineering, Ho Chi Minh city University of Technology and Education, Vietnam**
2004 ~ 2006	**Graduate student, Faculty of electrical and electronic engineering, Ho Chi Minh city University of Technology, Vietnam**
Work experience	
2006 ~ 2008	**Lecturer, Faculty of Electricity, Ho Chi Minh city University of Industry, Vietnam**
2008 ~ 2012	**Lecturer, Faculty of Electricity, Quy Nhon Vocational Training College, Quy Nhon city, Binh Dinh province, Vietnam**
2012 ~ Present	**Research assistant, Department of Electrical Engineering, University Duisburg-Essen, Germany**

12. PUBLICATIONS

[1] **Ngoc-Hung Truong,** Gerhard Krost**,** "Intelligent Energy Exploitation from Sewage"; IET Journal of Renewable Power Generation, ISSN 1752-1416, doi:10.1049/iet-rpg.2015.0154; finally accepted for publication: Sept. 23, 2015

[2] **Ngoc-Hung Truong**, Gerhard Krost, "Metaheuristic Based Device Rating for Energy Harvest in Sewage Plant"; Conference "Intelligent Systems Application to Power Systems" (ISAP) 2015, Porto (Portugal), September 2015

ELECTRICAL ENGINEERING